



University of
Stavanger

Faculty of Science and Technology

MASTER'S THESIS

Study program/ Specialization:

Offshore Technology/
Marine and Subsea Technology

Spring semester, 2014.

Open / ~~Restricted access~~

Writer:

Adekunle Peter **Orimolade**

.....
OA Peter Orimolade
(Writer's signature)

Faculty supervisor: Professor. Daniel Karunakaran
(University of Stavanger, Subsea7 Norway)

External supervisor: Professor Daniel Karunakaran

Title of thesis:

STEEL LAZY WAVE RISERS FROM TURRET MOORED FPSO

Credits (ECTS): 30

Key words: Steel Lazy Wave Risers, Turret
Moored FPSO, Harsh Environment,
Deepwater

Pages: 134
+ enclosure: 62
+ 1 CD

Stavanger, June 16, 2014.
Date/year

ABSTRACT

This thesis work is focused on providing a suitable riser configuration for deployment in conjunction with a high motion floater in a remote, deepwater, harsh environment. This is justified by the rising demand for oil and gas, which is driving exploration and production into the deeper waters, and harsher environments.

Steel catenary riser (SCR) is a riser concept that is attractive for deep and ultra-deepwater developments; this is as a result of its capability to withstand the increasing external hydrostatic pressure with increasing water depths, its availability in larger diameters, and its suitability in high temperature and sour service conditions. However, this concept faces limitations for use in conjunction with a Floating Production Storage and Offloading (FPSO) system in deepwater, harsh environments.

An alternative configuration to the SCR is the steel lazy wave riser (SLWR); this configuration allows the FPSO motion to be decoupled from the touchdown point (TDP) of the riser. Some of the areas of interest that is addressed in this thesis work are the extreme and fatigue performance of the SLWR when hanged from a turret moored FPSO in a typical harsh environment.

The design basis was established using typical environmental and design data for offshore West of Shetland, and several analyses were performed to find an optimum configuration for the deepwater, harsh environmental condition. The integrity of the riser was checked in extreme sea state conditions, and detailed analyses were performed to establish the fatigue performance of the riser, considering both wave-induced fatigue and fatigue due to vortex induced vibration (VIV). In addition, detailed sensitivity studies were carried out to establish the extreme response behavior of the SLWR, by varying the main configuration parameters.

Overall, this thesis work showed that the SLWR is a suitable riser configuration for deployment in conjunction with turret moored FPSO in deepwater, harsh environmental conditions. The extreme strength response and wave-induced fatigue performance are satisfactory, however, fatigue damage due to VIV was above the acceptance level, and this will require the introduction of VIV suppression devices along some lengths of the riser.

ACKNOWLEDGEMENT

All glory to the almighty God who has lead and guided my path to this point.

To my late father and mother, your memory and effort linger on; you have raised me to be a better man.

My heartfelt gratitude goes to Professor Ove Tobias Gudmestad of the University of Stavanger, Norway, for his support and guidance in making my dream of a degree in Subsea and Marine Technology realizable, and for introducing me to analyses of offshore structures.

My sincere appreciation to Professor Daniel Karunakaran of Subsea7 Stavanger, Norway, my mentor and thesis supervisor, for the deeper knowledge and understanding impacted in me, in the course of my thesis work, it is indeed a great privilege to have carried out my thesis work under his guidance.

My appreciation goes to Subsea7 Stavanger, for providing me with working space and all the necessary resources that made the thesis work a success.

My appreciation also to the Hydrodynamics and Ocean Technology group, for taking me in as a member of the group, and for all their assistance and guidance, you made my stay fun, and I feel at home away from home.

My appreciation goes to Tommy Andresen, Tomy Nurwanto, and Vasanth Mandapalli for time taken to give me better insights into riser modeling and analyses, and for timely advice and guidance on getting my analyses done the easier and better way. Time will not permit me to mention all names, but it is worth mentioning, that everyone I met in Subsea7 during my thesis period is of immense assistance.

To my beautiful family and friends, to Dawit Berhe my thesis colleague, and to my adorable girlfriend Jovana Milovanovic, your support, guidance and love made this thesis work a success.

To the Norwegian government, thank you for the opportunity for higher quality and free education.

TABLE OF CONTENTS

ABSTRACT.....	ii
ACKNOWLEDGEMENT.....	iii
TABLE OF CONTENTS.....	iv
LIST OF FIGURES.....	viii
LIST OF TABLES.....	ix
ABBREVIATIONS.....	x
CHAPTER 1 INTRODUCTION.....	1
1.1 Background.....	1
1.2 Objective and Scope.....	2
1.2.1 Objectives.....	2
1.2.2 Scope.....	3
1.3 Justification of Thesis.....	3
CHAPTER 2 OVERVIEW OF DEEPWATER FLOATER.....	4
2.1 Introduction.....	4
2.2 Deepwater Floaters.....	5
2.2.1 Tension leg platforms (TLPs).....	5
2.2.2 Spar platforms.....	6
2.2.3 Semisubmersibles (SSs).....	6
2.2.4 Floating production, storage, and offloading (FPSO) systems.....	7
2.3 Criteria for Selection of Deepwater Floater.....	8
2.4 Classification of FPSOs.....	9
2.4.1 Turret moored FPSOs.....	10
2.5 Permanent versus Disconnectable Turret Moored FPSO.....	13
2.6 Selected Floater Concept for Thesis Work.....	13
CHAPTER 3 OVERVIEW OF DEEPWATER RISER CONCEPT.....	14
3.1 Introduction.....	14
3.2 Flexible Risers.....	15
3.3 Rigid (Steel) Risers.....	15
3.4 Configuration of Rigid (Steel) Risers.....	16
3.4.1 Top tensioned risers (TTRs).....	17

3.4.2	Complaint risers	17
3.5	Steel Catenary Risers (SCRs).....	19
3.5.1	Challenges associated with depth.....	19
3.5.2	Challenges associated with harsh environments and large motion host platforms	20
3.6	Steel Lazy Wave Risers (SLWRs).....	21
3.6.1	SLWR static configuration	22
3.7	Factors Influencing Riser Concept Selection for FPSO in Deepwater	26
CHAPTER 4	APPLICABLE DESIGN CODES AND STANDARDS	28
4.1	Introduction	28
4.2	Codes and Standards for Riser Design	28
4.3	Standards for Dynamic Riser Design	29
4.4	Working Stress Design (WSD) and Limit State Design (LSD)	31
4.4.1	Working stress design (WSD) – API approach.....	31
4.4.2	Working stress design (WSD) – DNV approach.....	34
4.4.3	Limit state design (LSD) – DNV approach.....	36
4.5	Design Loads	43
4.6	Safety Classes	43
CHAPTER 5	METHODOLOGY AND DESIGN PREMISE.....	46
5.1	Introduction	46
5.2	General Description	46
5.3	Design standards.....	47
5.4	Data for Design and Analysis.....	47
5.4.1	FPSO data	47
5.4.2	FPSO motion characteristics	47
5.4.3	Accidental and operational design conditions.....	49
5.4.4	Environmental data.....	51
5.4.5	Riser properties.....	53
5.4.6	Design life.....	53
5.4.7	Hydrodynamic data and marine growth.....	55
5.4.8	Buoyancy modules	56
5.4.9	Riser – soil interaction.....	58

5.4.10	Fluid data.....	58
5.4.11	Riser fatigue data	58
5.5	Wall Thickness Sizing.....	59
5.6	Design Cases.....	60
5.7	Acceptance Criteria.....	62
CHAPTER 6	EXTREME RESPONSE AND FATIGUE ANALYSES.....	64
6.1	Introduction	64
6.2	Optimum Static Configuration	64
6.3	Strength Analysis.....	66
6.3.1	Static analysis.....	68
6.3.2	Dynamic analysis.....	69
6.3.3	Discussion of dynamic response results	70
6.3.4	Comparison of response at the critical sections.....	76
6.3.5	Extreme response summary	77
6.4	Fatigue Response Analyses	78
6.4.1	Wave-induced fatigue damage.....	80
6.4.2	Discussion of the SLWR wave-induced fatigue performance	84
6.4.3	Vortex-Induced Vibration (VIV) Fatigue.....	86
6.4.4	Discussion of the SLWR fatigue damage due to VIV	88
CHAPTER 7	SLWR SENSITIVITY STUDIES.....	92
7.1	Introduction	92
7.2	Net Buoyancy Sensitivity Study.....	92
7.2.1	Net buoyancy sensitivity – static results.....	93
7.2.2	Dynamic response (ULS) – net buoyancy sensitivity.....	95
7.2.3	Net buoyancy sensitivity – comparison of sag, hog, and TDP	97
7.3	Sensitivity Study on Height of Sag Bend above Seabed.....	98
7.3.1	Height of sag bend sensitivity– static results.....	99
7.3.2	Dynamic response (ULS) – height of sag bend sensitivity.....	101
7.4	Buoyant Section Length Sensitivity Study.....	104
7.4.1	Buoyant section length sensitivity - static results.....	106
7.4.2	Dynamic response (ULS) – buoyant section length sensitivity	108

7.5	Sensitivity on Hang-off Angle.....	112
7.5.1	Hang-off angle sensitivity - static results	113
7.5.2	Dynamic response (ULS) – hang-off angle sensitivity	114
7.6	Internal Content Sensitivity	117
7.6.1	Empty SLWR - static analysis.....	118
7.6.2	Dynamic response (ULS) – content sensitivity	119
7.7	Sensitivity Studies Summary	122
CHAPTER 8	FABRICATION AND INSTALLATION OF SLWR	123
8.1	Introduction	123
8.2	SLWR Fabrication	123
8.2.1	Welding of SLWRs	123
8.3	SLWR Installation	124
8.3.1	SLWR Hook-Up.....	127
CHAPTER 9	CONCLUSION AND RECOMMENDATIONS.....	128
9.1	Conclusion.....	128
9.2	Recommendation.....	130
REFERENCES	132
APPENDIXES	1
Appendix A	– Wall Thickness Sizing	1
Appendix B	– Brief Description of the Software Programs Used.....	3
Appendix C	– Fatigue Results.....	31
Appendix D	– Detailed Sensitivity Results.....	48

LIST OF FIGURES

Figure 2.1	(a) A Floating System (b) A Fixed System (Odland, 2012b).....	5
Figure 2.2	Illustration of Single Point Mooring – An External Turret (England et al., 2001)	12
Figure 2.3	ÅSGARD A – Internal turret moored FPSO (Odland, 2012a)	12
Figure 3.1	Unbonded Flexible Riser Pipe (Mahoney and Bouvard, 1986)	16
Figure 3.2	Various steel riser configurations used in conjunction with floaters (DNV, 2010a)	18
Figure 3.3	An example of SLWR configuration	23
Figure 3.4	SLWR static configuration parameters	23
Figure 5.1	Overview of the SLWR from a turret moored FPSO.....	48
Figure 5.2	FPSO mean, near, and far offsets, and resulting riser configuration	50
Figure 5.3	Spectral density for the 100-year wave	54
Figure 5.4	Current profile for the 10-year condition	54
Figure 5.5	Illustration of buoyancy modules attached to riser pipes (Balmoral, 2014).	57
Figure 6.1	SLWR static configuration for mean, near, and far FPSO offsets	67
Figure 6.2	Comparison of maximum stresses	73
Figure 6.3	Comparison of minimum tension.....	73
Figure 6.4	Variations of maximum top angle with time.....	75
Figure 6.5	Downward velocity VS minimum tension at the sag bend	75
Figure 6.6	Maximum stresses over the entire arc length, far and near offsets – ULS.....	77
Figure 6.7	S-N curves in seawater with cathodic protection (DNV, 2012).....	79
Figure 6.8	Subdivision of the sea-state scatter diagram into representative blocks	82
Figure 6.9	Calculated SLWR fatigue life considering mean position and one draft	85
Figure 6.10	VIV fatigue damage resulting from combination of in-plane and out-of-plane currents....	90
Figure 7.1	Static configuration: different net buoyancies – mean FPSO position	94
Figure 7.2	Maximum von Mises stresses for different net buoyancies	97
Figure 7.3	von Mises stresses for different net buoyancies – near offset position	99
Figure 7.4	Static configuration: different sag bend heights – mean FPSO position.....	100
Figure 7.5	Maximum effective top tensions for different sag bend heights	102
Figure 7.6	Maximum von Mises stress for different sag bend heights.....	105
Figure 7.7	Static configuration: different buoyant section length – mean FPSO position	107
Figure 7.8	Maximum effective top tension for different buoyant section lengths	111
Figure 7.9	Maximum von Mises stresses for different buoyant section lengths	111
Figure 7.10	Static configuration: different hang-off angles – mean FPSO position	113
Figure 7.11	Maximum effective top tension for different hang-off angles	116
Figure 7.12	Maximum von Mises stress for different hang-off angles	116
Figure 7.13	SLWR configuration – empty riser condition in mean offset position	118
Figure 8.1	Mechanized PGTAW and grinding of weld cap to improve fatigue performance	125
Figure 8.2	Seven Borealis (Subsea 7, Norway).....	125
Figure 8.3	Typical SCR flex joint (Oilstates, 2014).....	127

LIST OF TABLES

Table 2.1	Evaluation of the Floater Concepts	9
Table 2.2	A Comparison of Spread and Turret Moored FPSOs (England et al., 2001).....	11
Table 4.1	Various Standards and Riser Design Requirements (Kavanagh et.al, 2003).....	30
Table 4.2	Single Usage Factor for Combined Loading.....	36
Table 4.3	Design Fatigue Factors, DFF (DNV, 2010a)	43
Table 4.4	Riser Loads	44
Table 4.5	Safety Class Classification/Description	45
Table 5.1	FPSO Main Data	48
Table 5.2	FPSO Intact and Accidental Offsets	50
Table 5.3	Typical Wave and Current Data for the West of Shetland.....	52
Table 5.4	Riser Properties	55
Table 5.5	Hydrodynamic Coefficients	56
Table 5.6	Buoyancy Module Properties.....	57
Table 5.7	Wave Direction Annual Probability.....	59
Table 5.8	Minimum Wall Thickness.....	61
Table 5.9	Load Case Matrix.....	61
Table 6.1	Partial Safety Factors for ULS and ALS Code Check	65
Table 6.2	Static Results – Functional Loads.....	69
Table 6.3	Strength Response Summary Results – Set A.....	71
Table 6.4	Strength Response Summary Results – Set B.....	72
Table 6.5	Representative Sea-States and Lumped Probability of Occurrence.....	83
Table 6.6	Fatigue Life in Years at Critical Locations	85
Table 6.7	Current Profile Probability of Occurrence	89
Table 6.8	Minimum VIV Fatigue Life in Years.....	90
Table 7.1	Net Buoyancy Sensitivity Parameter	93
Table 7.2	Net Buoyancy Sensitivity – Summary Static Results	95
Table 7.3	Net Buoyancy Sensitivity – Summary Dynamic Response (ULS).....	96
Table 7.4	Height of Sag Bend above Seabed – Sensitivity Parameter.....	100
Table 7.5	Height of Sag Bend above Seabed – Summary Static Results.....	102
Table 7.6	Height of Sag Bend above Seabed – Summary Dynamic Response (ULS)	103
Table 7.7	Buoyant Section Length Sensitivity Parameter.....	107
Table 7.8	Buoyant Section Length Sensitivity – Summary Static Results	108
Table 7.9	Buoyant Section Length Sensitivity – Summary Dynamic Response (ULS)	109
Table 7.10	Hang-off Angle Sensitivity – Static Analysis Results	114
Table 7.11	Hang-off Angle Sensitivity – Summary Dynamic Response (ULS).....	115
Table 7.12	Static Results – Empty SLWR	120
Table 7.13	Content Sensitivity – Summary Dynamic Response (ULS)	121

ABBREVIATIONS

ALS	Accidental Limit State
API	American Petroleum Institute
ASME	American Society of Mechanical Engineers
BSR	Buoyancy Supported Riser
CAPEX	Capital Expenditure
DDCV	Deep Draft Caisson
DDSS	Deep Draft Semisubmersible
DNV	Det Norske Veritas
DSAW	Double Submerged Arc Welded
ERW	Electric Resistance Welded
FLS	Fatigue Limit State
FPDSO	Floating Production, Drilling, Storage, and Offloading
FPS	Floating Production System
FPSO	Floating Production Storage and Offloading
FSO	Floating Storage and Offloading
GOM	Gulf of Mexico
IOR	Improved Oil Recovery
JONSWAP	Joint North Sea Wave Project
LF	Low Frequency
LRFD	Load and Resistance Factor Design
LSD	Limit State Design
NPV	Net Present Value

OPEX	Operating Expenditure
PET	Pipeline Engineering Tool
RAOs	Respond Amplitude Operators
RISKEX	Risk Expenditure
SCF	Stress Concentration Factor
SCR	Steel Catenary Riser
SDO	Standard Developing Organization
SLS	Serviceability Limit State
SS	Semisubmersible
SLWR	Steel Lazy Wave Riser
TDP	Touchdown Point
TLP	Tension Leg Platform
UK	United Kingdom
ULS	Ultimate Limit State
VIV	Vortex Induced Vibration
WF	Wave Frequency
WoS	West of Shetland
WSD	Working Stress Design

CHAPTER 1 INTRODUCTION

1.1 Background

The Floating Production, Storage and Offloading (FPSO) systems have found applications in shallow, deep, and ultra-deep waters, for oil and gas exploration and production. The choice of mooring for a FPSO system is influenced by a number of factors including environmental conditions, method of offloading, rate of production, and storage capacity. In harsh environmental conditions, turret moored FPSO is a preferred alternative in order to allow the FPSO to weathervane, thereby adapting its orientation to the current environmental conditions.

A major challenge in selecting a reliable riser concept for FPSO in deep and ultra-deep water applications is reducing the impact of the FPSO's severe motion characteristics, in particular the heave and pitch motions in harsh environmental conditions.

Among the various riser concepts for deep and ultra-deep water applications, the steel catenary riser (SCR) has been a preferred choice (Phifer et al., 1994). In comparison to flexible riser, SCR is a simple and cost effective alternative in greater water depth. Also, as water depth increases, hydrostatic pressure increases; in SCR the problem posed by increased pressure can be overcome by increasing the wall thickness. In addition, SCR is applicable in high temperature and sour service conditions.

However, SCR is highly sensitive to FPSO heave motion, and in harsh environmental conditions a large dynamic response may be imposed on the SCR, also the fatigue response in such conditions is deemed poor. This problem can be solved by improving on the configuration of the SCR. A more compliant configuration can improve the fatigue life of the SCR, and make it better suitable for application with a FPSO in harsh environmental conditions.

A steel lazy wave riser (SLWR) is a more compliant configuration of the SCR; its configuration differs from the SCR because buoyancy elements are added along some length of the riser (Karunakaran and Olufsen, 1996). The addition of buoyancy elements has the tendency to decouple the FPSO motions from the touchdown point (TDP) area of the riser, and thereby

improve the riser extreme response behavior and the fatigue performance at the TDP (Senra et al., 2011). Addition of buoyancy elements can also reduce the riser payload acting at the connection point; this may be advantageous for design conditions limited by vessel payload.

Although a number of FPSOs have been successfully deployed in conjunction with different riser systems, in deep and ultra-deep waters, however, none has been deployed in remote, deepwater, harsh environments, therefore the need to carry out more qualifying works on the applicability of the concept in conjunction with SLWR. This need is necessitated by the increasing demand for energy worldwide which is driving exploration and production of oil and gas into deeper, remote, and harsh environments.

1.2 Objective and Scope

1.2.1 Objectives

The main objectives of this thesis work are the establishment of a SLWR configuration that is suitable for deployment with a turret moored FPSO, and an assessment of the dynamic responses and fatigue performance of the SLWR in extreme sea states.

The thesis work will also cover an assessment and selection of floaters for deep and ultra-deepwater field developments, an assessment and selection of riser concepts, factors affecting selection of riser concept for use in conjunction with FPSOs, and the applicable design codes and standards for dynamic risers.

The design basis will be established using a typical deepwater, harsh environmental design data and conditions. The established design basis will provide the necessary input for modeling and analysis of the steel lazy wave riser from the turret moored FPSO. It will also provide necessary information regarding the acceptance criteria of the design.

The modeled steel lazy wave riser from turret moored FPSO will be analyzed under extreme sea state conditions to establish the extreme response behavior, also the SLWR fatigue performance will be established using typical North Sea fatigue wave and current data.

Finally, detailed sensitivity will be performed to establish how various configuration parameters of the SLWR will affect the extreme behavior, and how these parameters can be used to optimize

the SLWR configuration.

The thesis work aim to contribute to the body of knowledge by establishing the behavior of a SLWR from a turret moored FPSO in a deepwater, remote, harsh environment, and the technical feasibility of deployment of such a concept.

1.2.2 Scope

This thesis work covers discussion of various floaters and riser concepts that are used in deep and ultra-deepwater field developments, deepwater in this thesis is referred to as water depth exceeding 600 meters (NORSOK, 2004), and ultra-deepwater is water depth exceeding 1830 meters (API, 2006). The work will also cover modeling and analysis of a steel lazy wave riser from turret moored FPSO. The focus of the analysis will be the riser integrity in extreme sea state conditions and its fatigue performance.

Design of floaters is beyond the scope of work. Also, an establishment of capital expenditure (CAPEX) or other related costs of the SLWR and turret moored FPSO are beyond the scope of work.

Modeling of VIV suppression devices such as strakes is not taken into consideration in the current work, also, the SLWR installation analysis has not been considered due to time constraints.

1.3 Justification of Thesis

The justification for this thesis work is the need to carry out further qualifying works on the technical feasibility of the deployment of SLWR in remote, deepwater, harsh environments. This is because the concept has not been deployed in such conditions, and current demand for oil and gas is driving future exploration and production to oil fields in deeper waters, with harsh environmental conditions.

CHAPTER 2 OVERVIEW OF DEEPWATER FLOATER

2.1 Introduction

Floating systems have found increased application in deep and ultra-deepwater oil and gas production; this is because they are more competitive and suitable for deepwater developments compared to fixed platforms. The distinguishing feature between floating systems and fixed systems is that floaters are held up by buoyancy of displaced water, an example is as shown in Figure 2.1(a), while for fixed systems; the main structure has a supporting structure that extends to the seabed as illustrated in Figure 2.1(b). For fixed structures therefore, the cost and weight increases exponentially with increasing water depth, while for floating structures, the cost and weight increases linearly (Hamilton and Perrett, 1986).

Selection of floater for deep and ultra-deepwater field development is dependent on a number of technical requirements and site specific limitations, including environmental conditions, water depth, riser concept, subsea layout, flow assurance, export system, location of market, and existing infrastructure (Hansen, 2011). Selection of a suitable floater concept is also influenced by cost constraints, which are required to ensure the project profitability, including capital expenditure (CAPEX), operating expenditure (OPEX), and risk expenditure (RISKEX).

In harsh environmental conditions, up to 500 meters water depth, a number of floater systems have been successfully deployed, also in benign deepwater environments such as offshore West Africa and Brazil, a number of deepwater floaters have been successfully deployed; for these environmental conditions and water depths, the floater system is therefore considered a mature technology. However, for deep and ultra-deepwater fields in harsh environments such as offshore West of Shetland and offshore Norway, the technology is unproven as no such field is yet in production (Meling, 2013).

Considering the many technical and cost related issues that need to be considered in selecting deepwater field development concept, especially for field developments in harsh environments, it is pertinent to carry out an assessment of deepwater floaters and their applicability for field developments in harsh environments.

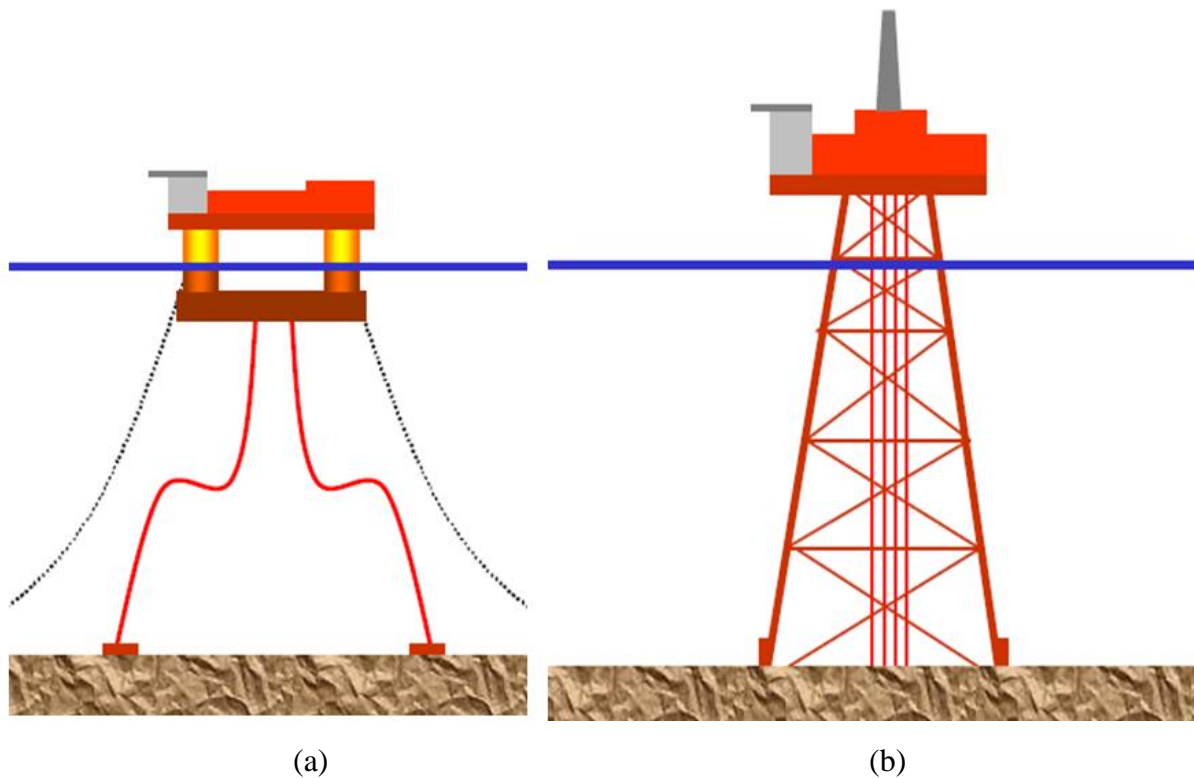


Figure 2.1 (a) A Floating System (b) A Fixed System (Odland, 2012b)

2.2 Deepwater Floaters

Floaters come in various sizes and shapes, and vary in scope of applicability. Floaters for deepwater application include the following:

- Tension Leg Platform (TLP)
- Spar Platform or Deep-Draft Caisson (DDCV)
- Semisubmersible (SS)
- Deep-Draft Semisubmersible (DDSS)
- Floating Production, Storage, and Offloading (FPSO)
- Floating Production, Drilling, Storage, and Offloading (FPDSO)

2.2.1 Tension leg platforms (TLPs)

TLPs have been deployed and are in operation today in water depth up to 1500m in benign environments, and in water depths up to 350m in harsh environments(Odland, 2012b). Similar to

other floaters, TLPs are subjected to six (6) degrees of freedom motion; however, the heave motion of a TLP is constrained by vertical tethers connecting the TLP to the seabed. The vertical tethers can be designed such that their periods in heave, pitch, and roll are below the wave periods at a specific field, and thereby limiting also the pitch and roll motions. As a result of its limited heave motion, the concept is well suited for dry tree applications. There also exist mini-TLPs that are used with wet tree wells.

TLPs respond to payloads significantly as a result of tensioning effects of tethers, and are therefore not used to provide storage (Paik and Thayamballi, 2007). They are used where pipeline infrastructure can be provided, or in combination with floating, storage and offloading systems (FSOs).

Installation of TLP, particularly, installation of the tethers, is usually carried out in calm weather, and is therefore dependent on weather window (Olufsen et al., 2003). This poses significant challenge in harsh environmental conditions, combined with greater water depth.

2.2.2 Spar platforms

Spars or deep-draft caissons (DDCV) have been installed in deep and ultra-deep water depths, with a current record of up to 2500m water depth in the Gulf of Mexico (GOM) (Odland, 2012c). The deep-draft hull of the spar produces favorable motion characteristics, the center of gravity is lower than the center of buoyancy, giving it a robust stability; in addition, spar platform has a moon-pool that provides protection and an attractive configuration for operations in deep waters. Spars provide suitable platform for dry trees, and may include wet trees.

They are less sensitive to payloads on the topsides, and may or may not contain a storage facility, however, when they contain storage facility, the storage capabilities is limited.

In harsh environments, wave's peak periods may be higher, requiring a redesign of the spar with longer natural periods in heave. Of significant concern, when considering spar for deeper water application in harsh environments is strength of mooring system, and fatigue performance.

2.2.3 Semisubmersibles (SSs)

The oil and gas exploration and production industry have deployed SS platforms in water depths above 2000m in relatively benign environments in the GOM, and in water depths up to 300m in

harsh environments offshore Norway. SSs have natural periods above the natural wave periods range, except when considering extreme sea states (Gudmestad, 2013), making them an attractive choice for operations in benign deepwater environment.

SSs respond significantly to changes in weight, limiting their flexibility for oil storage and deck load (DNV, 2010b). They can be deployed in deepwater fields, where pipeline infrastructure exists or installation of new ones is both technically feasible and economical, and for fields where other storage and export means of produced oil is feasible.

A semisubmersible platform has a draft of about 25 meters; however, to improve suitability for application in certain environmental conditions, the draft may be increased to achieve better motion characteristics (Gudmestad, 2013). Direct offloading may be required in harsh environment to make this concept feasible, this however require further works (Meling, 2013).

2.2.4 Floating production, storage, and offloading (FPSO) systems

FPSOs have been successfully deployed in shallow waters in harsh environments, and in deep and ultra-deep waters in benign environments (Olufsen et al., 2003). In harsh environments, FPSOs currently operate in water depths up to 500m, and in water depth over 2500m in benign environment (Duggal et al., 2009, Meling, 2013).

FPSOs have large superstructures, and the ability to passively or actively weather-vane. These make wind forces dominant in comparison to current forces. In the horizontal plane, FPSOs respond significantly to low frequency, and may be very sensitive to surge excitations as a result of their low viscous hull damping (DNV, 2010b), the level of sensitivity is however reduced as water depth increases.

The concept is attractive in frontier field developments where there are no pipeline infrastructures, or where installation of pipelines may be technically challenging or economically not viable. They also find application in hostile environments, in remote locations, and where oil reserves may be too small to require installation of a platform. However, for application in deep and ultra-deep water in harsh environments, the FPSO will require improved riser concept, turret-swivel system, and mooring.

2.3 Criteria for Selection of Deepwater Floater

Several parameters including wet or dry trees, local storage requirement, method of offloading, topside size limitation, and suitable riser concept, need to be properly considered, when decision is to be made regarding floater concept. Another important consideration during selection process is the net present value (NPV).

According to Odland (2012b), the following criteria may be considered in addition to NPV to take care of risks and challenges for each case being considered, including:

- HSE related issues: health, safety, and environment
- Technology maturity: new, proven, prior experience
- Flexibilities and constraints with respect to operation: production, manning, logistics
- Resource utilization: reservoir management, IOR
- Assessment of value chain: existing infrastructure, new infrastructure, strategic interests

A summary of the evaluation of the four floater concepts discussed is shown in Table 2.1; the Table shows that these technologies are relatively matured for deepwater applications; however, certain criteria need to be further developed for their suitability in harsh environments.

Among the floater concepts FPSO is by far the most commonly used (Paik and Thayamballi, 2007). The technology has been deployed in ultra-deepwater, and allows for large storage of oil. The challenges of FPSO for deep and ultra-deepwater applications include (Odland, 2012a):

- Turret and swivel design
- Riser system design
- Mooring system
- Offloading system
- Motion characteristics related to riser and mooring systems
- Green water and slamming design

Table 2.1 Evaluation of the Floater Concepts

Deepwater Floater	TLP	Spar (DDCV)	Semisubmersible	FPSO
Pros	Proven technology	Proven technology, Possibility for storage	Proven technology, Good motion characteristics	Proven technology, Large storage capability Proven direct loading
Cons	No storage capability. Requires separate storage and loading buoy or ship	Motion and air gap problems. Direct loading requires further work	Limited storage capability Direct loading requires further work	High sensitivity to motions, turret limitations

2.4 Classification of FPSOs

With advancement in technology and increase in innovative concepts to overcome the challenges associated with exploration and production in harsh environments, FPSOs have evolved from being built from oil tankers to purpose-built, including circular shape FPSO. The current work is focused on ship-shaped FPSO; this may be purpose-built or converted.

The ship-shaped FPSO can be classified based on the station keeping concept used; the two main classes are, spread-moored FPSOs, and weather-vaning FPSOs. Spread moored FPSOs are suitable for use in benign environments and in locations dominated by one wind or wave direction, however, for harsh environments, weather-vaning capability is essential (Odland, 2012a).

Spread moored FPSOs require less CAPEX as they do not require turret and swivel. The turret is a cylindrical-shaped structure, which allows the FPSO to rotate in the direction of wind and waves. Selecting between the two concepts requires consideration for riser design; coupled or uncoupled, and the impact they will have on the FPSO mooring (Saint-Marcoux and Legras, 2014). A summary of the comparison of the two classes is presented in Table 2.2.

2.4.1 Turret moored FPSOs

Turret moored FPSOs are FPSOs with weather-vaning capabilities, the mooring system is referred to as single point mooring system because the mooring lines are connected to a single point, that is, to the turret as shown in Figure 2.2.

In addition to allowing the FPSO to weather-vane, the turret serves as a connecting point between the topside and the subsea systems. For instance, the riser system is connected to the FPSO through the turret. The turret is used with a swivel stack, which allows fluid transfer from the seabed to the topside and vice-versa. Depending on the area of application, turrets can be permanently connected or disconnectable.

Also, depending on the top-side layout, the turret can be an “internal turret” or an “external turret”, and for purpose-built ship shaped FPSOs, internal turrets are more used, while for ship shaped FPSOs made from tankers, external turrets are more practical (Odland, 2012a). It is also noted that internal turret are used in harsh environments, while for relatively benign environments, external turrets can be used (2b1st, 2012).

Typically, the turret mooring system comprises of the following components:

- Anchor lines and a column for anchor lines on the turret for station keeping
- Bearing arrangement and a vessel support structure
- A system for fluid transfer

One advantage of the internal turret compared to external turret is easier transfer of mooring forces into the hull. The internal turret system can also accommodate more risers compared to external turret, and may be preferred for large number of wells. Figure 2.3 is an illustration of a typical internal turret moored FPSO.

Table 2.2 A Comparison of Spread and Turret Moored FPSOs (England et al., 2001)

	Spread Moored FPSO	Turret Moored FPSO
Vessel Orientation	Fixed orientation	Weather-vaning capability
Environment	Mild to moderate	Mild to harsh
Riser Number and Arrangement	Can be designed for flexibility, additional tie-ins	Moderate expansion capability
Riser Systems	Adapts to various riser systems	Location of turret requires robust riser design
Station-keeping Performance	Large number of anchor legs, offsets variable	Number of anchor legs, offsets minimized
Vessel Motions	Dependent on relative vessel/environment directionality	Weather-vaning capability reduces motions
Vessel Arrangement	Components spread on deck	Turret provides compact load and fluid transfer system
Offloading Performance	Dependent on vessel/environment orientation	Vessel typically aligned with mean environment

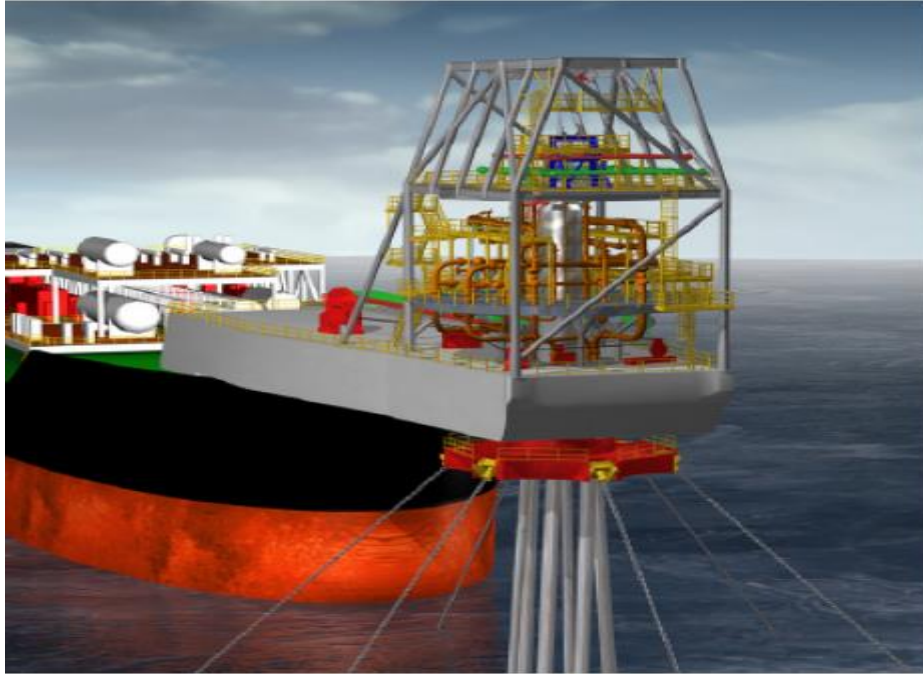


Figure 2.2 Illustration of Single Point Mooring – An External Turret (England et al., 2001)



Figure 2.3 ÅSGARD A – Internal turret moored FPSO (Odland, 2012a)

2.5 Permanent versus Disconnectable Turret Moored FPSO

The environmental condition at the location of the field development is one of the main factors influencing the decision between permanent and disconnectable turret. In areas that are subjected to cyclone occurrence, drifting iceberg, or where extreme sea states can regularly prevent production (Saint-Marcoux and Legras, 2014), the disconnectable option may be preferred, because in the event of an approaching iceberg or possibility of a cyclone, the FPSO can release its mooring and riser systems and move away from the location.

For areas where cyclone, iceberg, and related occurrences that are dangerous to stability and safety of the FPSO are not a challenge, permanent turret may be used. The permanent option is used on most of the FPSOs currently operating in the North Sea (2b1st, 2012), and is used with internal turret mooring system.

2.6 Selected Floater Concept for Thesis Work

The preferred floater concept for this thesis work is the FPSO system. The justification for choosing the FPSO concept is based on focus on a field development in remote, harsh environment, where pipelines infrastructure may not be feasible, technically or otherwise, and where their maintenance, inspection, and repair may be difficult.

The FPSO option is a turret moored type, to allow the FPSO to weathervane to the direction with least resistance to hydrodynamic loads from currents, waves, and wind, in other words, the FPSO will lay at head seas to the prevailing environmental conditions. The turret type is the permanent internal turret option; this is because the area of interest is a remote, deepwater, harsh environment where cyclones and iceberg are not of significant concerns.

CHAPTER 3 OVERVIEW OF DEEPWATER RISER CONCEPT

3.1 Introduction

Risers are a form of pipelines that serve as a link between facilities on seabed and topside facilities. They are of significant importance in all the different phases of oil and gas exploration and production. Selection of appropriate riser concept and design of riser are crucial to ensuring safety and product availability, from drilling to oil and gas production and export.

Based on the purpose of use and application area, functions of risers include (DNV, 2010a):

- Provision of fluid transport to the well and from the well, support auxiliary lines, guide tools, and drilling string; it also serve as a running and retrieving string for the BOP.
- Transfer of processed fluids from the floater to the structure and vice-versa; they are also used to transfer processed fluid between platforms or floaters.
- Transportation of fluids produced from the reservoir.
- Convey fluids to the producing reservoir from the topside.

A riser system comprises of three essential elements, these are the riser or conduit, top interface, and bottom interface (API, 1998). Risers are of two main types; flexible risers and rigid (steel) risers. They find application as production/injection, import/export, drilling, and workover/completion risers. Both riser types have also found applications in shallow and deeper waters, however, in recent times; rigid risers are becoming more attractive for ultra-deepwater applications. A hybrid riser is another type of riser; this is actually a combination of flexible and rigid risers.

Selection of riser concept is influenced by a number of factors including floater type, environmental conditions, and depth of water. This Chapter is focused on assessment of riser types and configurations for deepwater applications, and factors influencing riser concept for deep and ultra-deep waters applications.

3.2 Flexible Risers

Flexible risers are flexible pipes with several layers. They are able to take large motions, and are characterized by low bending moment and high axial stiffness (DNV, 2009), this is as a result of the presence of sealing materials with low stiffness, and helical armoring with high stiffness. Flexible risers can be bonded or unbonded, but the unbonded type is mostly used in riser applications, this is as shown in Figure 3.1, the different layers provide different functions, for instance, sealing is provided by the inner steel carcass, and pressure containment is provided by the zeta spiral layer (Mahoney and Bouvard, 1986).

Flexible risers can accommodate both horizontal and vertical movement, and have therefore found great applications in conjunction with floating production systems (FPSs).

They have found applications in conjunction with FPSs in shallow waters as well as in deep waters, however, with increasing water depths, they become less desirable both from technical and economic point of view, and therefore the need for improvements or more suitable alternatives.

The challenges for deployment of flexible risers in deep and ultra-deep waters include, increase in top tension load, and increase in external hydrostatic pressure (collapse pressure). The collapse pressure requirements limit flexible risers' maximum diameter and this may also not be desirable if the deepwater field has wells with high productivity.

3.3 Rigid (Steel) Risers

Rigid risers are metallic pipes made from materials such as low carbon steel, Titanium, or Aluminum alloys. Most of the rigid risers in the industry today are the low carbon steel riser type, referred to as steel risers. They come in different grades including X60, X65, and X70, and may differ in thickness. Steel risers materials are well known, they are available in large diameters, and the material cost is low (Phifer et al., 1994, Huang and Hatton, 1996).

In recent times, steel risers are becoming more attractive for oil and gas developments in deep and ultra-deep waters, particularly, in deepwater fields with high productivity wells. This is as a result of their availability in larger diameters, and their technical, and economical feasibilities.

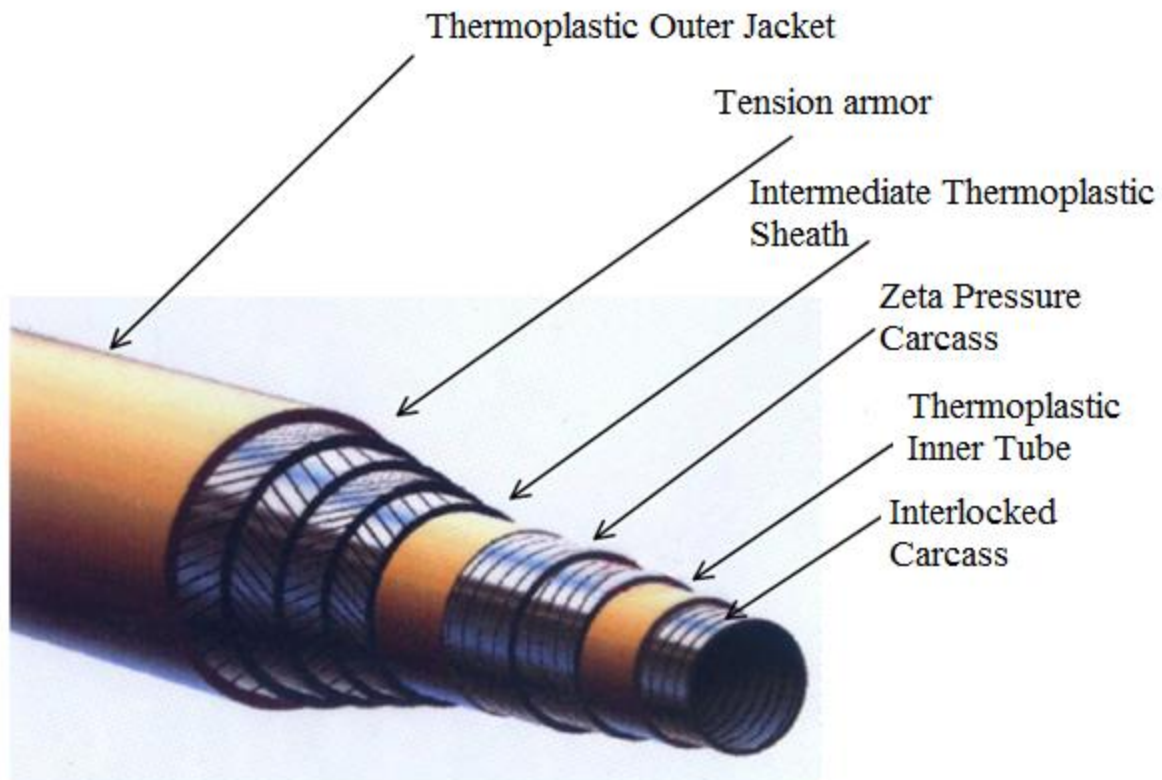


Figure 3.1 Unbonded Flexible Riser Pipe (Mahoney and Bouvard, 1986)

Steel risers can be effectively suspended in greater water depths due to their high axial strength (Huang and Hatton, 1996), in addition, they find applications under high pressures and temperatures (Bai and Bai, 2005), and can accommodate different fluid compositions than is possible with flexible risers.

Similar to flexible risers, steel risers can be configured to have a catenary shape, in order to make the riser compliant. The following is a discussion of the possible configurations for steel riser pipes.

3.4 Configuration of Rigid (Steel) Risers

With advances in technology and the need to explore oil and gas fields in deeper waters, in remote, harsh environments, the applicable numbers of rigid risers' configurations have increased. According to DNV (2010a), the configurations can be categorized into two main groups, namely, top tensioned and compliant risers. This classification is based on the dynamic

behavior of floater. There also exist a third category known as hybrid riser; this combines the properties of tensioned and compliant risers in an efficient way. Some examples of different steel riser configurations used in conjunction with floaters is shown in Figure 3.2.

3.4.1 Top tensioned risers (TTRs)

Traditionally, rigid risers employ top-tensioned configuration, these are vertical risers with top tension support and a system that compensate for relative motion between riser and floater. TTRs are constrained in such a way that the riser follows the horizontal floater motion at different locations. They rely on a top tensioner in excess of their apparent weight for stability, making them suitable for use on floaters with limited heave motions.

They found application with use in conjunction with floaters such as TLPs, Spars, SS, and DDSS (DNV, 2010a). However, for floaters with large offsets and dynamic motions, like the ship-shaped FPSO, this configuration becomes technically impractical, and requires a configuration that allows the riser to absorb the vessel motions.

3.4.2 Compliant risers

The main characteristic of compliant risers is related to their configurations, which enable them to absorb floater motions as a result of change in geometry, without the introduction of heave compensating systems. For conventional water depths, the required flexibility can be achieved by arranging unbonded flexible pipes in one of the compliant riser configurations, including free hanging or catenary, lazy wave, steep wave, lazy S, and steep S (DNV, 2010a).

For deepwater applications, rigid steel risers can be configured in the compliant riser configurations form. The catenary concept has gained popularity in recent years, in use in conjunction with various types of floaters. The lazy wave concept has been used for example, in conjunction with an FPSO offshore Brazil, and more works are ongoing to establish its applicability in deepwater, harsh environments.

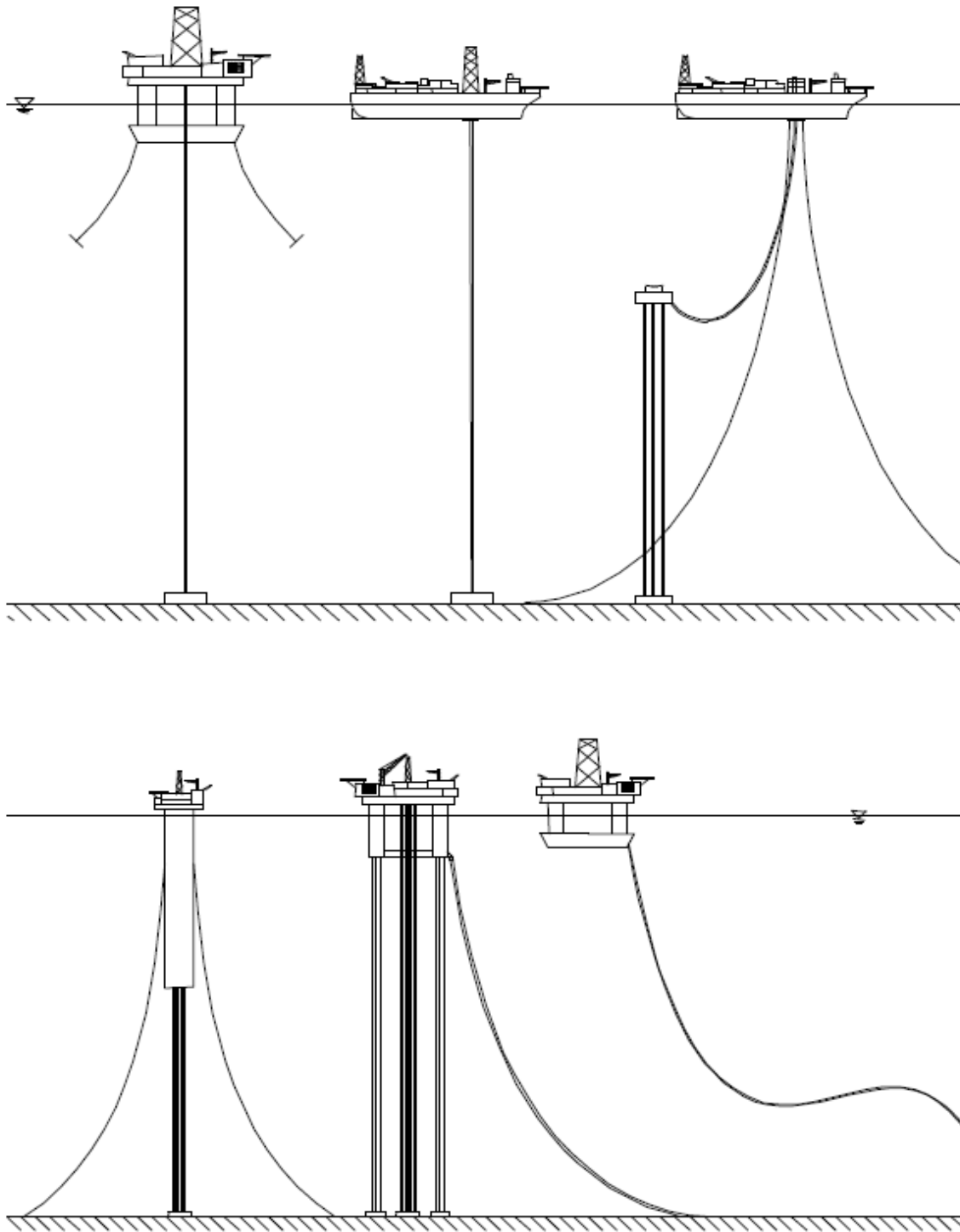


Figure 3.2 Various steel riser configurations used in conjunction with floaters (DNV, 2010a)

3.5 Steel Catenary Risers (SCRs)

According to Karunakaran et al. (2013), the SCRs concept has been an attractive solution for deepwater field developments in recent times. SCRs widespread acceptability for deployment in deep and ultra-deep waters is attributed to their simplicity in conception, ease of construction, ease of installation, and simple pipeline-riser interface (Song and Stanton, 2007).

They have been used in conjunction with different types of deepwater floaters, including FPSO system, Spar, TLP, and SS, in many fields across the world, for instance in the GOM, offshore Brazil and offshore West Africa.

3.5.1 Challenges associated with depth

In deep and ultra-deepwater, the increased water depth poses a big challenge, as external hydrostatic pressure on the riser pipe increases with water depth. Designing risers for these water depths therefore bring additional challenges as a result of extreme loads, which vary as the riser descends through the water column (Petromin, 2012). The main challenges in deep and ultra-deep water riser design are increasing top tensions due to riser pipe larger diameters and deeper water.

The effects of water depth on riser can be summarized as (Howells and Hatton, 1997):

- Increased length and weight
- Increased thickness to resist hydrostatic loading
- Increased spread
- Increased cost

The increased length is the most apparent influence of increased water depth on riser system arrangements; the increase in weight may be disproportional to depth as the resistance to collapse from hydrostatic pressure can dictate riser wall thickness (Howells and Hatton, 1997). Another effect of increase water depth is change in riser spread. For instance, SCRs have a typical radial spread of 1 to 1.5 times the water depth, and in a 1500m water depth, this could result in a spread between diametrically opposed risers of 3000m to 4500m (Howells and Hatton, 1997), and this may be a key factor affecting riser system selection, production system arrangement and positioning.

The challenges associated with the design of deepwater SCRs tied back to a floater include (Song and Stanton, 2007):

- Hang-off system limit
- Riser top payload (weight budget) limit
- Hang off angle limit
- Cathode protection design limit; and
- Thermal insulation design limit

Hang-off system limit: A hang-off system is required to terminate a SCR to a floater. Hand-off system selection is influenced by its functional requirements in terms of required angular deflection, the SCR size, and the expected top tension. The challenge is in selecting an appropriate hang-off system that can accommodate the most stringent variations in riser performance characteristics.

Weight budget limit: There is always a weight budget limit imposed on SCR to be tied back to a floater, depending on the sensitivity of the floater to riser top payload. The challenge is in selecting a SCR solution within the weight budget limit and that is technically feasible. Examples of SCRs with different weight include pipe-in-pipe SCR, and single wall SCR with constant thermal insulation coating.

Hang off angle limit: For a SCR tied back to a floater, the hang-off angle is provided from the preliminary host platform design, and this angle is fixed. The challenge is that the given angle may introduce strength fatigue, and there is a potential interference with other risers.

Thermal insulation design limit: Thermal insulation is limited by weight budget, riser interference, and riser strength.

3.5.2 Challenges associated with harsh environments and large motion host platforms

In addition to the challenges associated with increase water depths, the use of SCRs in harsh environmental conditions, or use in conjunction with deepwater floaters with large motions characteristics poses further challenges. The main challenge is fatigue near the hang-off position and the TDP (Karunakaran et al., 2013).

Floater motions contribute to the stresses that the riser experience along its length, and riser's material and configuration influences how well the riser system is able to accommodate motions of the floater (Carter and Ronalds, 1998).

SCRs are very sensitive to dynamics, and more so when they are light in water. When they are used in conjunction with ship-shaped FPSOs, one of the main challenges is how to accommodate the high motion response of FPSOs. This requires modifications to the SCRs configuration, in order to improve fatigue performance of the SCRs.

Some of the configurations that have an improved compliancy and have improved SCRs response include, steel lazy wave riser (SLWR) configuration, weight-distributed SCR, and buoyancy supported riser (BSR - an uncoupled riser type). It is beyond the scope of this thesis work to discuss the details of the applicability and limitations of all these configurations. The thesis is focused on SLWR, its deployment in conjunction with a turret moored FPSO in remote, deepwater, harsh environments.

3.6 Steel Lazy Wave Risers (SLWRs)

The SLWR is a SCR with buoyancy modules added along some length of the riser to decouple the floater dynamic motions from the TDP of the riser, and to reduce the top payload. The lazy wave configuration approaches the seabed in a horizontal manner and is therefore suitable for similar applications with the SCRs, where the riser-pipe is required to extend along the seafloor to form part of a pipeline.

Some of the pros and cons of this concept when used in conjunction with a FPSO system are as summarized below (Andrade et al., 2010, Senra et al., 2011, Song and Uppu, 2012):

Pros:

- Motion of FPSO is to a large extent absorbed by the buoyancy modules
- Technically feasible
- A relatively simple concept
- Possible to transfer experience from SCR
- May be economically effective

Cons:

- Need to further investigate SLWR termination system with turret
- Landing point from turret is further away due to large horizontal span
- Need to further qualify buoyancy modules
- New turret bearing capacity requirement

3.6.1 SLWR static configuration

The SLWR configuration is divided into three main sections, including upper and lower catenary sections, and middle buoyant section. There is also a bottom section, which is the horizontal part on the seafloor. An example of the configuration is as shown in Figure 3.3, with highlights of the different sections, as well as the TDP and the hang-off position. Figure 3.4 shows some of the parameters for determining the static shape of a typical lazy wave riser, including:

- H = horizontal component of the tension on the SLWR
- S = length of SLWR to the seafloor
- y = water depth
- W = submerged weight per unit length of the riser
- L = horizontal length from the point where tension is applied to the TDP
- $l_i (i = 1,6)$ = each segment length
- $x_i (i = 1,6)$ = horizontal segment length
- θ = departure angle

Using the basic parameters defined above, and the geometry in Figure 3.4, the shape of the SLWR can be defined using the following equations, as derived from the basic catenary equation for a free hanging chain.

For a free hanging chain, the relationship among the parameters is given by:

$$y = \frac{H}{W_i} \left(\cosh \left(\frac{W_i}{H} \right) - 1 \right)$$

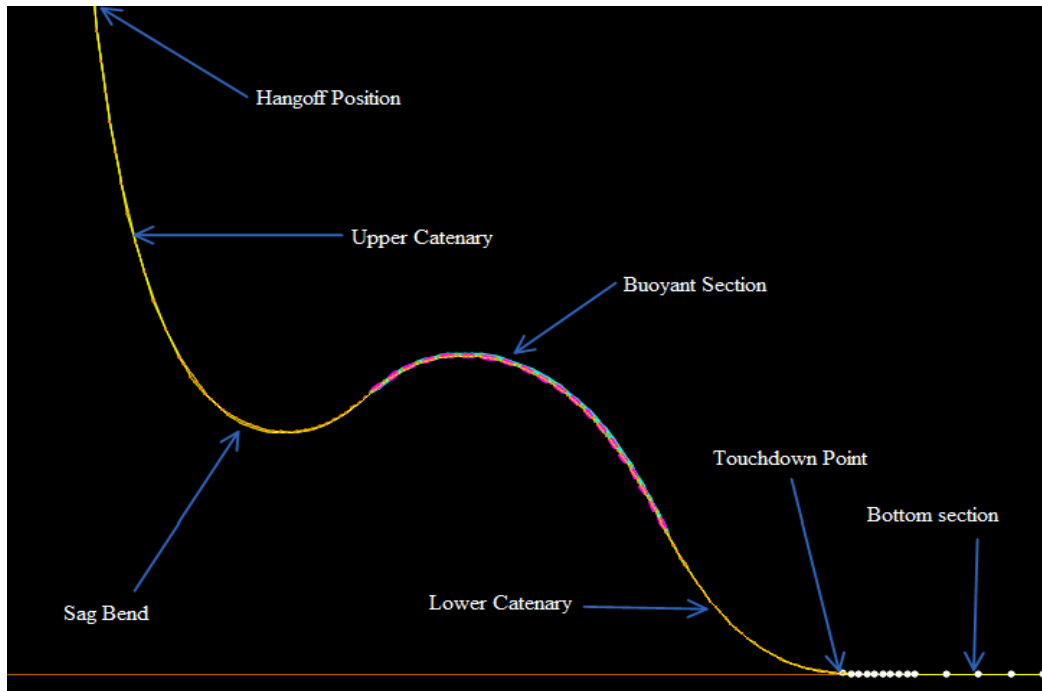


Figure 3.3 An example of SLWR configuration

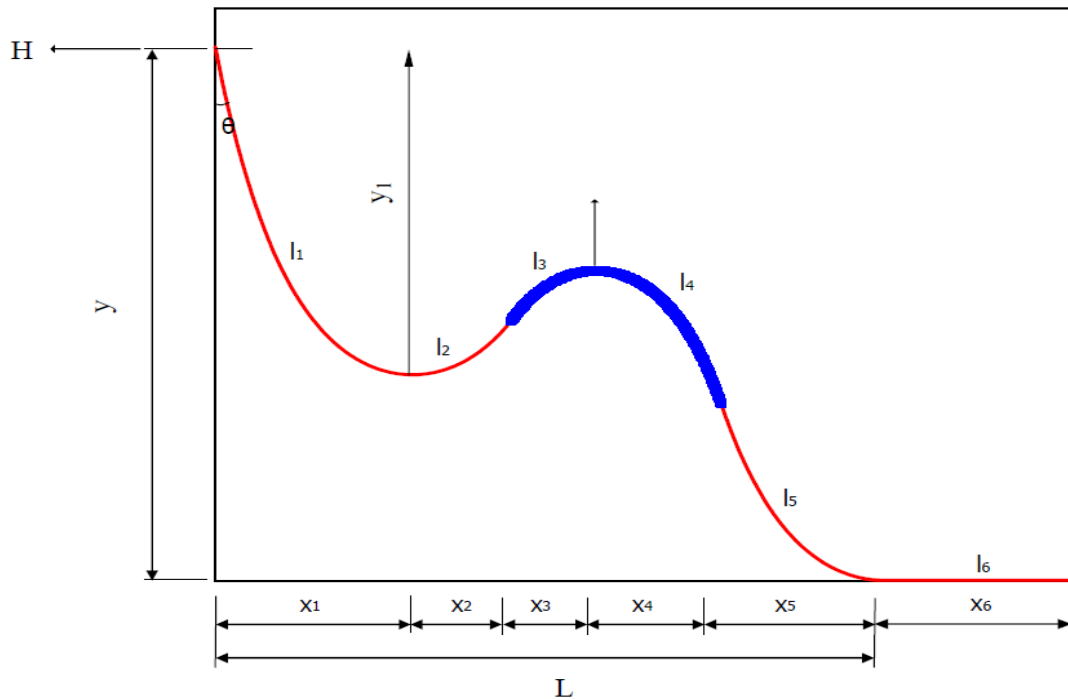


Figure 3.4 SLWR static configuration parameters

From which the total length of riser to the seafloor is:

$$S = \frac{H}{W_i} \sinh\left(\frac{W_i}{H} x\right)$$

$\frac{H}{W_i}$ – represents the curvature radii at the sag bend, arch bend, and TDP

For the lazy wave configuration, we consider the different sections, and segment lengths, the resulting equation for each section length are given by:

For the upper catenary section, total length of riser as seen from geometry is s_1 :

$$s_1 = l_1 + l_2$$

$$s_1 = \frac{H}{W_1} \sinh\left(\frac{W_1}{H} x_1\right) + \frac{H}{W_2} \sinh\left(\frac{W_2}{H} x_3\right)$$

For the middle buoyant section, total length of riser as seen from geometry is s_2 :

$$s_2 = l_3 + l_4$$

$$s_2 = \frac{H}{W_2} \sinh\left(\frac{W_2}{H} x_3\right) + \frac{H}{W_2} \sinh\left(\frac{W_3}{H} x_5\right)$$

For the lower catenary section, total length of riser as seen from geometry is s_3 :

$$s_3 = l_5$$

$$s_3 = \frac{H}{W_3} \sinh\left(\frac{W_3}{H} x_5\right)$$

For the bottom section, s_4 :

$$s_4 = l_6 = x_6$$

Therefore, the total SLWR length required to the TDP is:

$$S = s_1 + s_2 + s_3$$

And the total riser length required, including section on the seafloor is:

$$S = s_1 + s_2 + s_3 + s_4$$

Where:

W_1 = submerged weight per unit length of the upper catenary

W_2 = submerged weight per unit length of the buoyant section

W_3 = submerged weight per unit length of the lower catenary

Giving the mass in water for the riser pipes, where:

m_1 = mass per unit length of the upper catenary

m_2 = mass per unit length of the buoyant section

m_3 = mass per unit length of the lower catenary, and

F = net upward force of buoyancy

Then:

$$W_1 = m_1 g$$

$$W_2 = F - m_2 g$$

$$W_3 = m_3 g$$

and:

$$\text{Buoyancy ratio} = 1 + \frac{W_2}{W_1}$$

As a result of the effect of the net upward force of buoyancy of the buoyancy modules, that is lifting on segments l_2 and l_5 of the riser pipe as shown in Figure 3.4, the total weight of the riser pipe is reduced, and it equals to segment l_1 weight.

The dynamic analysis of SLWR depends on the initial static equilibrium position, it is therefore of significant importance during design, to have the appropriate static configuration. During design, the variable parameters can be re-defined in order to achieve an optimum configuration, these include the departure angle, θ , the length of the buoyancy section, s_2 , and the water depth for riser pipe equivalent weight, y_1 .

3.7 Factors Influencing Riser Concept Selection for FPSO in Deepwater

To summarize this chapter, it is important to highlight some of the many factors to be considered when considering selection of riser concept for use in conjunction with an FPSO in deepwater. Some of the main factors to be considered include (Song and Uppu, 2012):

- FPSO motion characteristics
- Depth of water
- Dimensions of riser
- Metocean data
- Schedule
- Cost
- Ease of Installation
- Thermal performance requirement
- Location and method of riser termination
- Field layout

FPSO Motion: The severe motion characteristics of FPSO require a riser concept that can absorb the motion in order to improve fatigue performance at the TDP of the riser system.

Depth of water: Increasing water depth will result in an increase in required riser length, and therefore an increase in riser weight, resulting in increase in top tension. Increase in top tension may limit the availability of suitable installation vessels. Other considerations associated with water depth include increase in external hydrostatic pressure, and increase in riser spread.

Dimensions of riser: The dimensions of importance are riser diameter and wall thickness. Large diameter requirement favors steel risers due to their availability in larger diameters compared to flexible risers. Also, at greater water depth, the increasing external hydrostatic pressure may require an increase in wall thickness.

Metocean data: The Metocean data provide information about the environmental conditions, in harsh environments, characterized by high waves and currents, FPSOs response increases significantly, this is a challenge requiring proper consideration during riser concept selection.

Schedule: Weather conditions may limit the available time for riser installation, this may require a riser concept that is easy to fabricate and install.

Cost: With an increase in water depth, the required riser length increases, and so is the cost of the riser material, in addition, cost of installation, inspection, and maintenance may increase when considering harsh environments. High CAPEX may limit the economic feasibility of a concept, and require proper consideration.

Ease of Installation: installation of riser in deepwater is a challenging task, and more so when considering harsh environments. In an environment with limited weather window, successful installation of the riser system within the weather window may be crucial to the overall success of the project. For SLWR, the geometry and load distribution may be affected by the attached buoyancy modules, this is more so when the riser is to be installed empty (Andrade et al., 2010).

Thermal performance requirement: There is need to balance the minimum thermal performance requirement and the global riser response.

Location and method of riser termination: It is important to select an appropriate termination location on the FPSO, select appropriate termination angle, and use a suitable method, in order for the riser system to be able to accommodate the most stringent variations in riser performance characteristics.

Field layout: there is need to avoid risers' interference or clashing, this may require large clearance between the risers, and may limit the number of risers that may be deployed from the FPSO.

CHAPTER 4 APPLICABLE DESIGN CODES AND STANDARDS

4.1 Introduction

In the oil and gas industry, standards are important for the technical definition of offshore structures' designs and installations. The standards could be national, regional, international or from industry standard developing organizations (SDO). Considering that the oil and gas industry is becoming increasingly complex and globalized the use of good standards for all relevant areas make offshore/onshore oil and gas activities easier (OGP, 2010). According to OGP (2010), the use of recognized or referenced standards appears to be voluntary in most cases, in the sense that other technical solutions, methods or procedures can be opted for, provided a documented proof of compliance with the requirements of the regulations itself or standards referenced is made available.

The following are different types of standards, and their definitions according to API:

- Specifications: these are documents that facilitate communications between purchasers and manufacturers
- Recommended Practices: these are documents that communicate proven industry practices
- Standards: documents that combine elements of both specifications and recommended practices
- Codes: they are documents intended for adoption by regulatory agencies or authorities having jurisdiction
- Bulletins and Technical Reports: these are documents that convey technical information on a specific subject or topic.

4.2 Codes and Standards for Riser Design

The following are the most applied codes and standards for riser design, especially for deep waters riser design (Kavanagh et al., 2003).

- API-RP-2RD – Design of Risers for Floating Production Systems (FPSs) and Tension

Leg Platforms (TLPs)

- API-RP-1111 – Design, Construction, Operation, and Maintenance of Offshore Hydrocarbon Pipelines (Limit State Design)
- ASME-B31.4 – Pipeline Transportation Systems for Liquid Hydrocarbons and Other Liquids, Chapter 9 – ‘Offshore Liquid Pipeline Systems’
- ASME-B31.8 - Gas Transmission and Distribution Piping Systems, Chapter 8 - "Offshore Gas Transmission", and
- DNV-OS-F201 - Dynamic Risers. Offshore Standard

The design requirements govern by these standards include failure mode by:

- hoop stress
- collapse
- propagation buckling
- longitudinal stress, and
- combined stress

An overview of which of the highlighted standards provide specific requirements to address specific failure mode is shown in Table 4.1.

4.3 Standards for Dynamic Riser Design

Both API-RP-2RD and DNV-OS-F201 are dynamic riser standards, while API-RP-1111 is a pipeline standard and includes dynamic pipeline risers.

These standards can be distinguished based on two fundamental design approaches, working stress design (WSD), and limit state design (LSD). API-RP-2RD provides design requirements based on the WSD, API-RP-1111 provides design requirements based on the LSD, while DNV-OS-F201 specifies design requirements that allow for both LSD and WSD.

However, this section is focused on API-RP-2RD and DNV-OS-F201, both of which are dynamic riser standards, their applications, strengths and weaknesses.

Table 4.1 Various Standards and Riser Design Requirements (Kavanagh et.al, 2003)

Failure Mode		Standard				
		API-RP- 2RD	API-RP- 1111	ASME- B31.4	ASME- B31.8	DNV-OS- F201
Hoop Stress	Design	-	Yes	Yes	Yes	Yes
	Hydrotest	-	Yes	-	-	-
Collapse	External pressure & bending	Yes	Yes	-	-	Yes
	External pressure	-	Yes	-	-	Yes
Propagation Buckling		Yes	Yes	Implicit	Implicit	Yes
Longitudinal Stress		Yes	Yes	Yes	Yes	Yes
Combined Stress		Yes	Yes	Yes	Yes	Yes

The dash denotes ‘no specific requirements to address that failure mode’

The term “optimized” in riser design can be described as “a fit for purpose design solution in all anticipated scenarios with minimal life cycle cost” (Katla et al., 2001), and in order to achieve optimized cost a rational design criteria and analyses procedures is required. In WSD format structural safety is taken care of by using a single safety factor, one of the limitations of this format is that a single safety factor leads to a safety level that is strongly dependent on the load conditions. For applications to well-known concepts, the WSD is considered acceptable, but for new concepts the WSD cannot be said to be neither optimal nor appropriate. However, the DNV-OS-F201 which allows for both LSD and WSD is considered a contribution towards optimal design.

While API (RP-2RD and RP1111) implicitly assumes displacement controlled riser configuration with a secondary bending stress for ultimate limit state (ULS) design checks, DNV-OS-F201 reasonably assumes that important riser locations, that is, top and TDP, are load

controlled unless otherwise argued and documented (DNV, 2010a).

Among its main benefits as described in (DNV, 2010a), the DNV-OS-F201 gives provision of the state-of-the-art limit state functions in load and resistance factor design (LRFD) format with reliability-based calibration of partial safety factors. As an alternative, the standard also allows a simple conservative WSD format. The standard is applicable even in new concepts with no limitations regarding floater type, water depth, riser application and configuration.

Some of the limitations with the API-RP-2RD include (Stanton et al., 2010):

- Lack of a specific hoop stress check, therefore designers have to depend on the requirements of supporting standards like ASME-B31.4 and 31.8, and API-RP-1111 for pipeline design, for initial wall thickness sizing.
- Use of working stress design approach for combined loads, specifying the allowable von Mises stress limits in terms of the utilization of material yield stress, instead of allowable loads that relate to specified limit states.
- Joint criteria for the design of pipe and pipe components, making it cumbersome to apply specific criteria to the pipe part of the riser

4.4 Working Stress Design (WSD) and Limit State Design (LSD)

4.4.1 Working stress design (WSD) – API approach

WSD is a design approach governed by specified allowable stresses which shall not be exceeded (API, 1998). In WSD, uncertainties associated with the loads and resistances can be accounted for by specifying a single factor of safety, applied to nominal yield strength.

The WSD format for plain pipe is expressed as follows (API, 1998):

$$(\sigma_p)_e < C_f \sigma_a$$

Where:

σ_p = primary membrane stress = average value across the thickness of a solid section
excluding the effects of discontinuities and stress
concentrations

$(\sigma_p)_e$ = equivalent von Mises stress, where the principal stress consists of primary membrane stresses

σ_a = $C_a \sigma_y$ = basic allowable combined stress (or resistance)

C_a = 2/3 = allowable stress factor

σ_y = material minimum yield strength

C_f = design case factor

The applicable design case factors based on different load categories are (API, 1998):

C_f = 1.0 (operating)

= 1.2 (extreme)

= 1.5 (survival)

❖ Determination of allowable stresses

A pipe with axisymmetric geometry is referred to as plain pipe. For plain round pipe, both transverse shear and torsion are negligible; the three principal stress components of primary membrane stress are therefore in the axial, hoop and radial directions. These are combined to form equivalent von Mises stress defined as follows:

$$(\sigma_p)_e = \frac{1}{\sqrt{2}} \left(\sqrt{(\sigma_1 - \sigma_2)^2 + (\sigma_2 - \sigma_3)^2 + (\sigma_3 - \sigma_1)^2} \right)$$

Where:

$\sigma_1, \sigma_2, \sigma_3$ = Principal stresses in the axial, hoop, and radial directions

And:

$$(\sigma_p)_e < C_f \sigma_a$$

The allowable stress is therefore:

$$\sigma_a > \frac{(\sigma_p)_e}{C_f}$$

❖ Allowable deflections

Allowable deflections may need to be specified to prevent unacceptable high bending stresses. The purpose of setting allowable deflection is to prevent high bending stresses or large riser curvatures. Also, deflections shall be controlled to prevent clashing between multiple risers.

❖ Determination of allowable external design pressure (collapse pressure)

The maximum allowable hydrostatic external pressure is taken into consideration during design, this is necessary to ensure that the pipe material used for the riser will not collapse under hydrostatic pressure. This is particularly so in deep water applications, where the external hydrostatic pressure is high.

API (1998) specified that the net allowable external design pressure be less than the predicted collapse pressure, multiplied by the design factor. The relationship among these parameters is given by:

$$P_a \leq D_f P_c$$

Where:

P_a = net allowable external design pressure

P_c = predicted collapse pressure

D_f = design factor

= 0.75 for seamless or Electric Resistance Welded (ERW) API pipe

= 0.60 for double submerged arc welded (DSAW) internally cold expanded API pipe

❖ Collapse propagation design criteria

Collapse may be initiated by accidental means at a lower pressure than the specified allowable external pressure, and form a propagating buckle that travel along the pipe until the external pressure drops below this propagating pressure or the buckle is arrested.

The design criterion to limit the extent of a propagation failure is defined in API (1998) as follows:

$$P_d < D_p P_p$$

Where:

P_d = design pressure differential

P_p = predicted propagation pressure

D_p = design factor = 0.72

API (1998) noted that where the pipe design is sufficient to meet the propagation criterion, the collapse criterion is met as well.

❖ Fatigue/service life criterion

The API standard also gives a criterion for fatigue. This is described in relation to the service life of the riser. The criterion is given by:

$$\sum_i SF_i D_i < 1.0$$

Where:

D_i = the fatigue damage ratio for each phase of loading

SF_i = associated safety factor

In relation to service life, for locations that can and will be inspected or where safety and pollution are low, API recommends that the designed fatigue life be at least 3 times the service life ($SF = 3$). For locations that cannot be inspected or where safety and pollution risk are significant, this should be 10 times the service life ($SF = 10$).

4.4.2 Working stress design (WSD) – DNV approach

As mentioned in section 4.3, DNV-OS-F201 specifies requirements allowing for both LSD and WSD. According to the standard, this WSD is an easy alternative to the LSD, and is applicable for combined loading checks, when working on pipes with diameter to wall thickness ratio of less than 30. The result so obtained is a conservative of the LSD approach.

Unlike the LSD approach, where several combinations of design load effects are used, the WSD

approach uses a single usage factor for combined loading check.

The WSD design format according to DNV (2010a) is given by:

$$g(S, R_k, \eta, t) \leq 1$$

Where:

S = total load effect

R_k = resistance

η = usage factor

$g()$ = generalized load effect

The usage factor for different combined loading conditions according to DNV (2010a) is shown in Table 4.2.

❖ Combined Load Criteria

The following shall be satisfied for pipe members that are subjected to a combination of effective tension, bending moment, and net internal overpressure (DNV, 2010a):

$$\left\{ \left(\frac{|M_d|}{M_k} \cdot \sqrt{1 - \left(\frac{p_{ld} - p_e}{p_b(t_2)} \right)^2} \right) + \left(\frac{T_{ed}}{T_k} \right)^2 \right\} + \left(\frac{p_{ld} - p_e}{p_b(t_2)} \right)^2 \leq \eta^2$$

And for pipe members subjected to a combination of effective tension, bending moment, and net external overpressure, the following shall be satisfied (DNV, 2010a):

$$\left\{ \left(\frac{|M_d|}{M_k} + \left(\frac{T_{ed}}{T_k} \right)^2 \right) \right\}^2 + \left(\frac{p_e - p_{min}}{p_c(t_2)} \right)^2 \leq \eta^4$$

Table 4.2 Single Usage Factor for Combined Loading

Safety Class		
Low	Normal	High
0.83	0.79	0.75

Where:

M_d = design bending moment

$$= \gamma_F \cdot M_F + \gamma_E \cdot M_E + \gamma_A M_A$$

M_F, M_E, M_A = bending moment from functional, environmental, accidental loads respectively

$\gamma_F, \gamma_E, \gamma_A$ = load effect factor for functional, environmental, accidental respectively

$$\gamma_F = \gamma_E = \gamma_A = 1 \text{ (WSD)}$$

M_k = the (plastic) bending moment resistance

$$= f_y \cdot \alpha_c \cdot (D - t_2)^2 \cdot t_2$$

α_c = parameter accounting for strain hardening and wall thinning.

T_{ed} = design effective tension

$$= \gamma_F \cdot T_{eF} + \gamma_E \cdot T_{eE} + \gamma_A T_{eA}$$

T_{eF}, T_{eE}, T_{eA} = effective tension from functional, environmental, accidental loads respectively

T_k = plastic axial force resistance

$$= f_y \alpha_c \pi (D - t_2) \cdot t_2$$

p_e = local external pressure

p_{ld} = local internal pressure

$p_b(t_2)$ = burst resistance

$p_c(t_2)$ = hoop buckling capacity

4.4.3 Limit state design (LSD) - DNV approach

The limit state with regard to riser design is defined as the “state beyond which the riser or part of the riser no longer satisfies the requirements laid down to its performance or operation” (DNV, 2010a). DNV-OS-F201 provides riser design checks with special emphasis on ultimate limit state (ULS), fatigue limit state (FLS), serviceability limit state (SLS), and accidental limit

state (ALS). The aim is to design for the actual modes of failure and the safety margin is ensured by a combination of material requirements, and testing (DNV, 2010a).

❖ Serviceability Limit State (SLS)

SLS requires that the riser must be able to remain in service and be in normal operating conditions. Therefore, the riser pipe shall be designed against the following failure modes (DNV, 2010a):

- Clearance
- Excessive angular response
- Excessive top displacement
- Mechanical function

SLS for the global riser behavior for instance are associated with limitations with regard to deflections, displacements and rotation of the global riser or ovalisation of the riser pipe. For example, for a typical production riser with a surface tree, the riser is a part of the well control system and may not be disconnected; in addition:

- During riser installation, a weather limitation shall be set to avoid riser interference
- Out-of-roundness tolerance of the pipe shall be set to avoid premature local buckling.

This shall be limited to 3% (DNV, 2010), that is:

$$f_o = \frac{D_{\max} - D_{\min}}{D_o} \leq 0.03$$

- Other SLSs include determination of limit to the degradation of riser coatings and attachments or for allowances due to wear and erosion

❖ Ultimate Limit State (ULS)

ULS requires that the riser must remain in designed form and be free from rupture; operability of the riser is however not necessarily a requirement. For operating condition it corresponds to the

maximum resistance to applied loads with an annual probability of exceedence of 10^{-2} (DNV, 2010a).

According to this limit state, the riser pipe shall be designed against the following failure modes (DNV, 2010a):

- Busting
- Hoop buckling (collapse)
- Propagation buckling
- Gross plastic deformation and buckling
- Gross plastic deformation, local buckling, and hoop buckling
- Unstable fracture
- Liquid tightness, and
- Global buckling

Bursting criterion

Bursting occurs due to internal overpressure only. The top-end of a content filled riser is the most critical area for bursting; this is because the external hydrostatic pressure is minimal compared to the internal fluid pressure at this location.

According to DNV (2010a), it is required that pipe members under internal overpressure satisfy the following design criterion at all cross sections:

$$p_{li} - p_e \leq \frac{p_b(t_1)}{\gamma_m \cdot \gamma_{SC}}$$

Where:

p_{li} = local incidental pressure

$$= p_{ld} + 0.1 * p_d$$

p_{ld} = local internal design pressure

$$= p_d + \rho_i g h$$

p_d = design pressure

ρ_i = density of the internal fluid

g = acceleration due to gravity

h = height difference between the actual location and the internal pressure reference point

p_e = external pressure

p_b = burst resistance, and

$$p_b(t) = \frac{2}{\sqrt{3}} \cdot \frac{2 \cdot t}{D-t} \cdot \min\left(f_y; \frac{f_u}{1.15}\right)$$

t = dummy variable, to be substituted by t_1 or t_2

t_1 = minimum required wall thickness for a straight pipe without allowances and tolerance

$$= \frac{D}{\frac{4}{\sqrt{3}} \gamma_m \cdot \gamma_{SC} (p_{li} - p_e)^{+1} \cdot \min\left(f_y; \frac{f_u}{1.15}\right)}$$

γ_m = material resistance factor

γ_{SC} = safety class resistance factor

D = nominal pipe outer diameter

f_y = yield strength of pipe

f_u = tensile strength of pipe

Hoop buckling (collapse) criterion

Hoop buckling occurs due to external overpressure only. External overpressure increases with water depth; therefore the lower-end of the riser is the most critical area for collapse failure.

According to DNV (2010a), it is required that pipe members under external overpressure satisfy the following design criterion:

$$p_e - p_{\min} \leq \frac{p_c(t_1)}{\gamma_m \cdot \gamma_{SC}}$$

Where:

p_{\min} = local minimum internal pressure; taken as the most unfavorable internal pressure plus static head of the internal fluid

= zero; for installation

= p_e for installation with water-filled pipe

$p_c(t)$ = resistance for external pressure (hoop buckling), and

$$(p_c(t) - p_{el}(t)) \cdot (p_c^2(t) - p_p^2(t)) = p_c(t) \cdot p_{el}(t) \cdot p_p(t) \cdot f_o \cdot \left(\frac{D}{t}\right)$$

$p_{el}(t)$ = elastic collapse pressure (instability) of a pipe

$$= \frac{2 \cdot E \cdot \left(\frac{t}{D}\right)^3}{1 - \nu^2}$$

$p_p(t)$ = plastic collapse pressure

$$= 2 \frac{t}{D} \cdot f_y \cdot \alpha_{fab}$$

α_{fab} = fabrication factor

f_o = the initial ovality

$$= \frac{D_{max} - D_{min}}{D}$$

E = Young's modulus of pipe material

Propagating buckling criterion

Hoop buckling may still be initiated at a lower pressure by accidental means, and the local buckle due to accidental means may propagate to other areas of the pipe and consequently lead to collapse if not controlled.

According to DNV (2010a), the following criterion shall be satisfied to ensure local buckle do not propagate:

$$p_e - p_{min} \leq \frac{P_{pr}}{\gamma_c \cdot \gamma_m \cdot \gamma_{SC}}$$

Where:

γ_c = 1.0 if no buckle propagation is allowed once initiated
 = 0.9 if the buckle is allowed to travel a short distance

p_{pr} = resistance against buckling propagation

$$= 35 \cdot f_y \cdot \alpha_{fab} \cdot \left(\frac{t_2}{D}\right)^{2.5}$$

Where:

$$t_2 = t_{\text{nom}} - t_{\text{corr}}$$

$$t_{\text{norm}} = \text{nominal thickness}$$

$$t_{\text{norm}} = t_1 + t_{\text{corr}} + t_{\text{fab}}$$

If the riser pipe design is sufficient to meet the propagation criterion, the hoop buckling criterion is also met.

The propagating buckling criterion usually results in significantly thicker wall thickness requirement compared to other criteria, and therefore, the design may be too conservative if this criterion must be satisfied. In practice, the other criteria are used, and buckle arrestors are provided in the critical region where propagation may occur, saving significant amount of riser weight and cost.

Combination loading criteria

For pipe members under combined load effects of effective tension, bending moment, and net internal overpressure, in addition to burst and hoop buckling criterion, the pipe members shall be designed to meet the following design criterion (DNV, 2010a):

$$\{\gamma_{\text{sc}} \cdot \gamma_{\text{m}}\} \left\{ \left(\frac{|M_{\text{d}}|}{M_{\text{k}}} \cdot \sqrt{1 - \left(\frac{p_{\text{ld}} - p_{\text{e}}}{p_{\text{b}}(t_2)} \right)^2} \right) + \left(\frac{T_{\text{ed}}}{T_{\text{k}}} \right)^2 \right\} + \left(\frac{p_{\text{ld}} - p_{\text{e}}}{p_{\text{b}}(t_2)} \right)^2 \leq 1$$

The equivalent criterion for pipe members subjected to combined load effect of effective tension, bending moment, and net external overpressure is:

$$\{\gamma_{\text{sc}} \cdot \gamma_{\text{m}}\}^2 \left\{ \left(\frac{|M_{\text{d}}|}{M_{\text{k}}} \right) + \left(\frac{T_{\text{ed}}}{T_{\text{k}}} \right)^2 \right\}^2 + \{\gamma_{\text{sc}} \cdot \gamma_{\text{m}}\}^2 \left(\frac{p_{\text{e}} - p_{\text{min}}}{p_{\text{c}}(t_2)} \right)^2 \leq 1$$

❖ Accidental Limit State (ALS)

This is a ULS due to accidental loads. Accidental loads in this report refers to loads acting on the riser system, as a result of a “sudden, unintended and undesirable event”, with an annual probability of occurrence less than 10^{-2} (DNV, 2010a). Accidental loads can result from abnormal conditions, incorrect operation or technical failure.

The applicable design checks according to (DNV, 2010a) include:

- Resistance against direct accidental load
- Ultimate resistance and consequence assessment due to exceedence of a SLS introduced to define operational limitations;
- Post-accidental resistance against environmental loads

DNV-OS-F201 provide provision for simplified design check with respect to accidental loads

❖ **Fatigue Limit State (FLS)**

This is a ULS from accumulated excessive fatigue crack growth or damage under cyclic loading causing degradation of the riser system. It is required for the riser system to have adequate safety against fatigue within its service life (DNV, 2010a). According to the standard, fatigue can be checked using the following methods:

- Methods based on S-N curves
- Methods based on fatigue crack propagation calculations

The fatigue criterion according to the S-N curves methods is given by (DNV, 2010a):

$$D_{\text{fat}} \cdot \text{DFF} \leq 1.0$$

Where:

D_{fat} = accumulated fatigue damage

DFF = design fatigue factor; the factors are shown in Table 4.3 based on safety classes

The fatigue criterion according to the crack propagation calculations methods is given by (DNV, 2010a):

$$\frac{N_{\text{tot}}}{N_{\text{cg}}} \cdot \text{DFF} \leq 1.0$$

Where:

N_{tot} = total number of applied stress cycles during service or in-service inspection

N_{cg} = number of stress cycles necessary to increase the defect from the initial to the critical defect size

The design factors in Table 4.3 also apply.

Table 4.3 Design Fatigue Factors, DFF (DNV, 2010a)

Safety Class		
Low	Normal	High
3.0	6.0	10.0

4.5 Design Loads

Risers are subjected to different types of loads, through installation and beyond, these loads can be grouped into three main categories including functional loads, environmental loads, and installation loads (Guo et al., 2005).

Functional loads are loads resulting from the physical presence of the riser system and as a result of handling and operation of the riser system, excluding pressure loads (DNV, 2010a). Environmental loads are loads resulting from interaction with ocean environment. Accidental loads are loads resulting from unplanned occurrences.

Table 4.4 shows some of the load types in each category described above (API, 1998; DNV, 2010a).

4.6 Safety Classes

The safety class is a concept adopted to classify the criticality of the riser system. The structural safety requirement of the riser system is dependent on the consequences of a failure. These consequences are grouped into:

- risk to life
- environmental pollution, and
- Political and economic consequences.

Based on these requirements, three safety classes are introduced; they are low, normal and high.

Table 4.4 Riser Loads

Functional/Pressure	Environmental	Accidental
Weight of riser	Wave loads	Small dropped objects
Weight of coatings, attachments, and tubing	Current loads	Vessel impact
Internal pressure due to contents	Vessel motions	Normal handling impact
External hydrostatic pressure	Seismic loads	Tensioner failure
Nominal top tension	Ice loads	Flow-induced impact between risers
Buoyancy	Wind loads	Partial loss of station keeping capability
Vessel constraints		Fires and explosions
Weight of marine growth		
Thermal		
Installation		
Inertia		

The selection of a safety class for riser design depends on the following (DNV, 2010a):

- the fluid category of the riser content
- the riser location class, and
- whether the riser is in its operating phase or in a temporary phase

The use of DNV-OS-F201 for riser design ensures the application of safety class methodology linking acceptance criteria to consequence of failure. A description of the classification of safety classes according to DNV (2010a) is shown in Table 4.5.

Based on the foregoing analysis and descriptions, the principal reference standard for this thesis work is DNV-OS-F201.

Table 4.5 Safety Class Classification/Description

Safety class	Description
Low	This applies to situations where failure implies low risk of human injury and minor environmental and economic consequences.
Normal	This applies to conditions where failure implies risk of human injury, significant environmental pollution or very high economic or political consequences
High	This applies to operating conditions where failure implies high risk of human injury, significant environmental pollution or very high economic or political consequences.

CHAPTER 5 METHODOLOGY AND DESIGN PREMISE

5.1 Introduction

The methodology and design data used in establishing the SLWR configuration and behavior in harsh environmental conditions are presented in this chapter. In addition, the methodology and design data used to determine the fatigue performance for both wave-induced and VIV fatigue damage are also presented.

The design premise with respect to this thesis work is a documentation of specific data and conditions that are required for the design and in-place extreme strength analyses, and fatigue response analyses of the SLWR from a turret moored FPSO. The design premise therefore, is the basis for modeling, analyses and verification of results of the behavior of the SLWR in a harsh environment. The SLWR system will be designed to satisfy both functional and environmental requirements that are detailed in the premise.

5.2 General Description

The area selected for this study is offshore West of Shetland (WoS) in the United Kingdom (UK) part of the North Sea. The environmental condition in this area is very harsh, and the field under consideration is in the remote and deepwater part of the WoS. The water depth at the location is 1,100 meters, and can be classified as deepwater as described in NORSOK (2004).

The selected platform concept is a turret moored FPSO, considering that the field is in a remote location, with no nearby infrastructures, and that the platform will be installed in harsh environmental conditions. The selected turret moored FPSO and its associated RAO data is for a typical FPSO platform for operations in this part of the North Sea. The turret type considered is the permanent type as there is no significant challenge of hurricane or ice-drift.

Consideration is given mainly to production risers in this study; due to their challenging characteristics from both strength and fatigue perspectives. ORCAFLEX has been selected as the main software program for modeling and analysis of the SLWR and further analysis may be carried out using other similar software as required.

A general overview of the riser layout, attached to the turret section of an FPSO is shown in Figure 5.1.

5.3 Design standards

The SLWR is designed in accordance with the guidance in DNV-OS-F201, 2010. In addition, the following standards are also used in establishing other required design criteria:

- Fatigue Strength Design of Offshore Steel Structures – DNV-RP-C203, 2010
- Riser Fatigue – DNV-RP-F204, 2010
- Riser Collision – DNV-RP-F205, 2004
- Design of Risers for Floating Production Systems (FPSs) and Tension-Leg Platforms (TLPs) – API-RP-2RD, 1998
- Specification for Line Pipe – API SPECIFICATION 5L, 2012
- Submarine Pipeline Systems – DNV-OS-F101, 2010
- Action and Action Effects – NORSOK N-003, 2007

5.4 Data for Design and Analysis

5.4.1 FPSO data

The dimensions of the turret moored FPSO used in this thesis work are presented in Table 5.1. The FPSO local coordinate system is defined in ORCAFLEX as follows:

- Origin – located at the FPSO amidships
- X-axis – longitudinal axis positive to FPSO bow (Vessel heading) or direction of surge
- Y-axis – transversal axis or direction of sway
- Z-axis – vertical axis or direction of heave

5.4.2 FPSO motion characteristics

It is important to accurately characterize the FPSO motions to ensure a reliable riser design, including (DNV, 2010a):

- FPSO static offsets
- Wave frequency motions (WF); and
- Low frequency motions (LF)

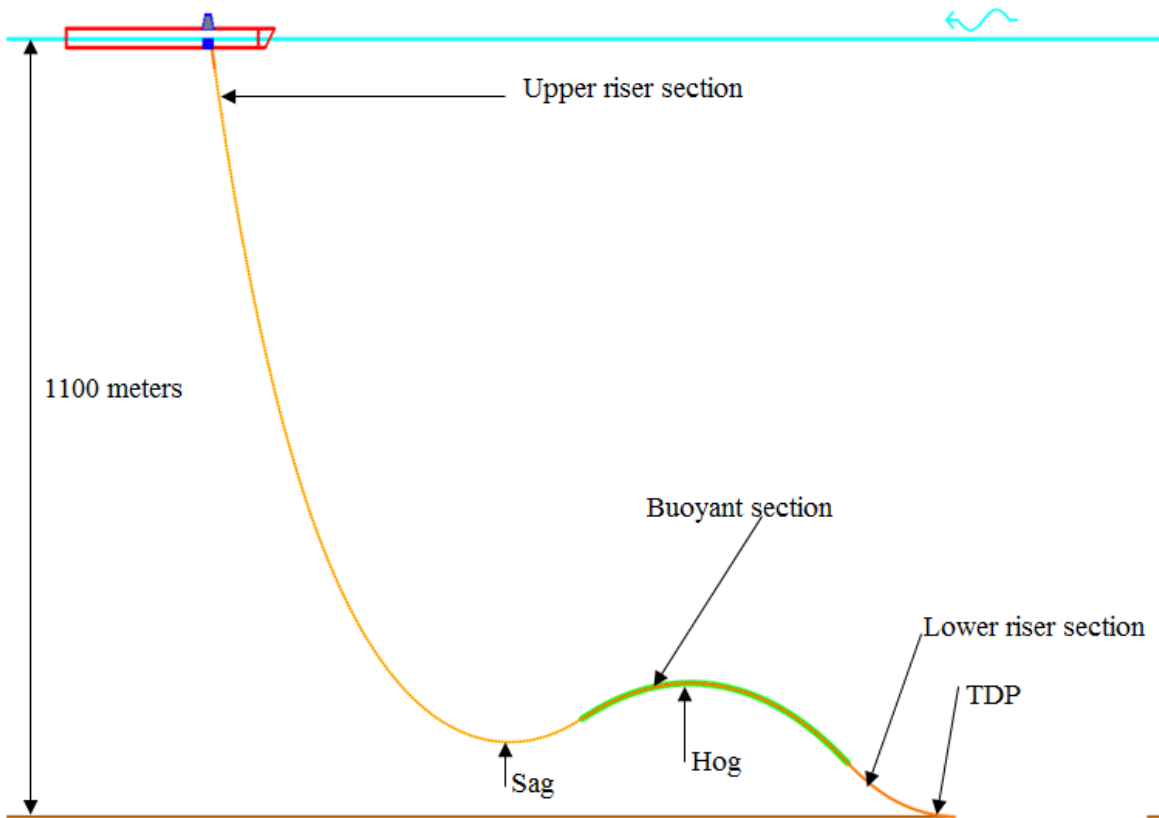


Figure 5.1 Overview of the SLWR from a turret moored FPSO

Table 5.1 FPSO Main Data

FPSO Parameter	Unit	Value
Length	m	295
Breadth	m	46
Height	m	27
Turret diameter	m	12
Turret location forward of amidships	m	55

FPSO Static Offsets: these are as a result of motions induced by mean environmental loads from waves, current, and wind. In this study, static offset is considered for mean (nominal), near, and far positions of the FPSO.

The near offset position refers to the FPSO displacement along the riser's plane, towards the riser connection point on the seabed. The far offset position refers to the FPSO displacement along the riser's plane, away from the riser's connection point on the seabed. An illustration of these offset positions and the resulting SLWR configuration is shown in Figure 5.2.

Wave Frequency Motions (WF): these are the first order motions of the FPSO as a result of wave actions. WF motions are described by Response Amplitude Operators (RAOs).

The RAO data used in this study defined the turret moored FPSO harmonic motions in six degrees of freedom, both translational and rotational. The RAO origin is at the center of gravity of the FPSO. This RAO data is however confidential and is therefore not presented in this thesis report.

Low Frequency Motions (LF): these are FPSO motions as a result of second order wave effects and wind gust loading, with periods ranging from 30 to 300 seconds (DNV, 2010a).

5.4.3 Accidental and operational design conditions

For the strength analysis, both operational and accidental conditions are considered. Intact mooring is an operational condition, and maximum FPSO offset under this condition, in the far and near positions is 10% of the water depth.

One broken mooring line is considered as accidental condition in this study, the maximum FPSO offset under this condition, in the far and near positions is 12 % of water depth.

For this study, a turret mooring system with catenary mooring legs has been considered, and the offsets are in compliance with API-RP-2SK (API, 2005) requirement. A summary of the FPSO offsets for intact and accidental mooring conditions is presented in Table 5.2.

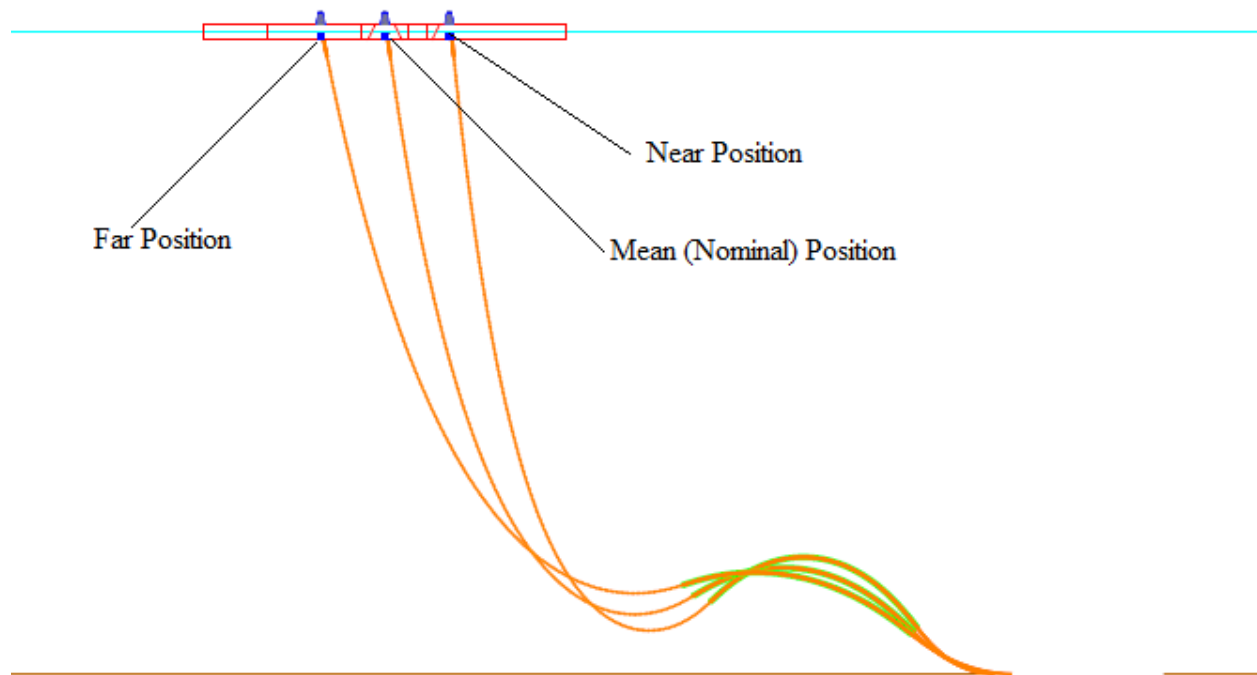


Figure 5.2 FPSO mean, near, and far offsets, and resulting riser configuration

Table 5.2 FPSO Intact and Accidental Offsets

Mooring condition	FPSO Offset (% of water depth)	FPSO Offset (± m)
Intact	10	110
Accidental	12	132

5.4.4 Environmental data

The environmental conditions in the WoS area are extremely dynamic. The area is exposed to extreme winds, and wind speeds vary, reaching a peak in winter periods. The area is also affected by long periods of swells, and calm sea state conditions are very rare all through the year. These conditions generate an extreme wave regime, and are more significant between December and January.

In this study, ULS design is driven by a combination of the extreme sea-state of 100-year wave with 10-year current. The wave and current data used for the study are for a typical WoS location and are presented in Table 5.3. Irregular wave theory was used in modeling the extreme sea-state, following the JONSWAP (Joint North Sea Wave Project) spectrum.

The JONSWAP spectrum is a modification of Pierson-Moskowitz spectrum for a sea-state that is developing in limited fetch situation, and is given by (DNV, 2007):

$$S_J(\omega) = A_\gamma S_{PM}(\omega) \gamma^{\exp\left(-0.5\left(\frac{\omega-\omega_p}{\sigma\omega_p}\right)^2\right)}$$

Where:

$S_{PM}(\omega)$ = Pierson-Moskowitz spectrum

γ = non-dimensional peak shape parameter

σ = spectral width parameter

$$\sigma = \sigma_a \text{ for } \omega \leq \omega_p$$

$$\sigma = \sigma_b \text{ for } \omega > \omega_p$$

A_γ = $1 - 0.287 \ln(\gamma)$ (a normalizing factor)

For $\gamma = 1$, the JONSWAP spectrum is equal to the Pierson-Moskowitz spectrum, given by:

$$S_{PM}(\omega) = \frac{5}{16} \cdot H_s^2 \omega_p^4 \cdot \omega^{-5} \exp\left(-\frac{5}{4} \left(\frac{\omega}{\omega_p}\right)^{-4}\right)$$

Where:

$$\omega_p = \frac{2\pi}{T_p} \text{ (angular spectral peak frequency)}$$

Table 5.3 Typical Wave and Current Data for the West of Shetland

Parameter	100-Year	10-Year
Omni Directional Wave		
H_s (m)	17.7	14.9
T_p (s)	18.6	17.3
Water Depth (m)		
Omni Directional Current Speed (m/s)		
At surface	1.67	1.47
- 70	1.31	1.16
- 110	1.05	0.93
- 150	0.83	0.74
- 325	0.54	0.48
- 490	0.39	0.34
- 650	0.23	0.23
- 1200	0.23	0.23

According to DNV, 2007, γ is governed by:

$$\gamma = 5 \quad \text{for} \quad \frac{T_p}{\sqrt{H_s}} \leq 3.6$$

$$\gamma = \exp\left(5.75 - 1.15 \cdot \frac{T_p}{\sqrt{H_s}}\right) \quad \text{for} \quad 3.6 < \frac{T_p}{\sqrt{H_s}} < 5$$

$$\gamma = 1 \quad \text{for} \quad 5 \leq \frac{T_p}{\sqrt{H_s}}$$

Based on the γ conditions described above, for the 100-year wave condition in this study, the following condition holds:

$$3.6 < \frac{T_p}{\sqrt{H_s}} < 5$$

Therefore:

$$\gamma = \exp\left(5.75 - 1.15 \cdot \frac{T_p}{\sqrt{H_s}}\right) = 1.946$$

Similarly, for the 10-year wave condition

$$\gamma = 1.815$$

The resulting spectral energy density for the 100-year wave is shown in Figure 5.3, and a pictorial view of the associated 10-year current is shown in Figure 5.4.

The seawater density is 1025 kg/m^3 and the seabed is assumed to be flat, which can either be horizontal or sloping.

5.4.5 Riser properties

The parameters of the production riser pipe used for design and analysis of the SLWR in this thesis work are presented in Table 5.4.

A flex joint is considered as the interface between the riser and the upper termination point. This is used to relieve stress at the riser hang-off location. For extreme sea-state strength analysis, the SLWR upper end is assumed pinned to the turret section of the FPSO, and is modeled with zero rotational stiffness. This is because, under extreme loading conditions, riser response is not influenced by flex joint stiffness (Karunakaran and Meling, 2006).

For fatigue analysis, flex joint rotational stiffness contributes to riser fatigue response, particularly in the cross section of the riser around the flex joint. To account for this response a flex joint rotational stiffness as defined in Table 5.4 is used.

5.4.6 Design life

The design life of the production riser is considered to be 25 years. Using safety class high, a safety factor of 10 will be used on wave-induced fatigue life, and the minimum required fatigue life for the SLWR will be 250 years. For vortex induced vibration (VIV) fatigue analysis, the required minimum fatigue life for the SLWR is 20 times the design life, that is, 500 years.

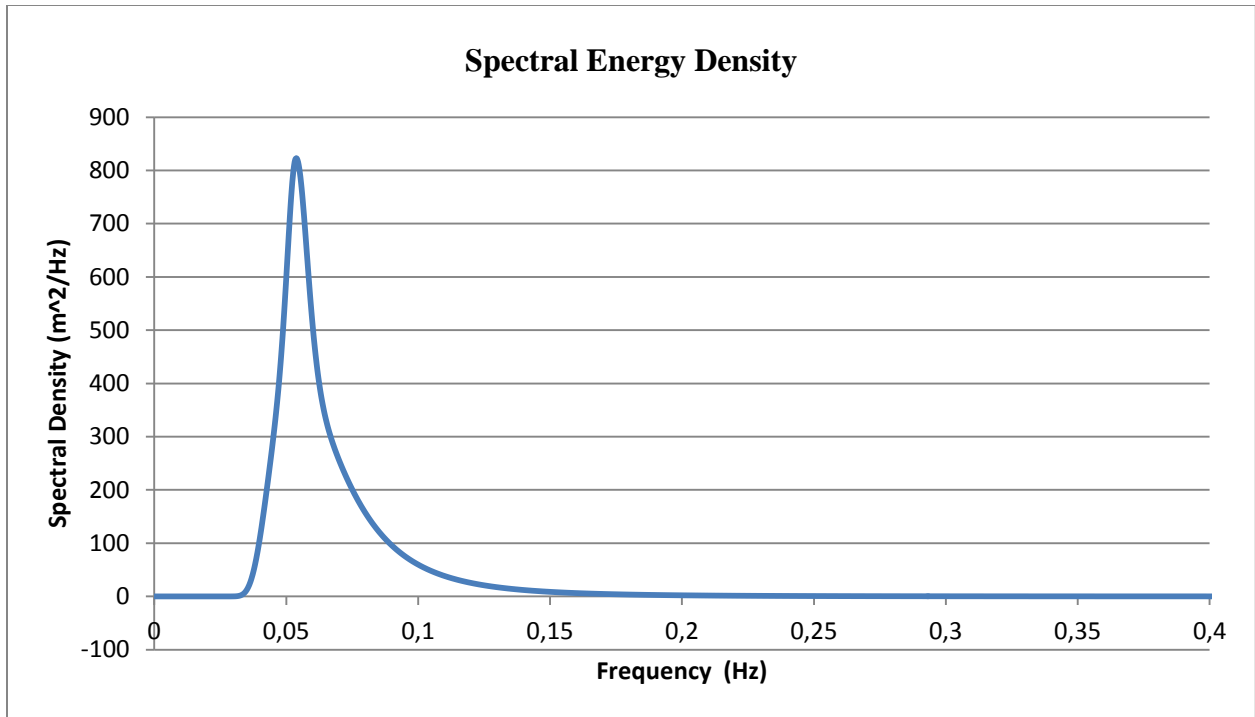


Figure 5.3 Spectral density for the 100-year wave

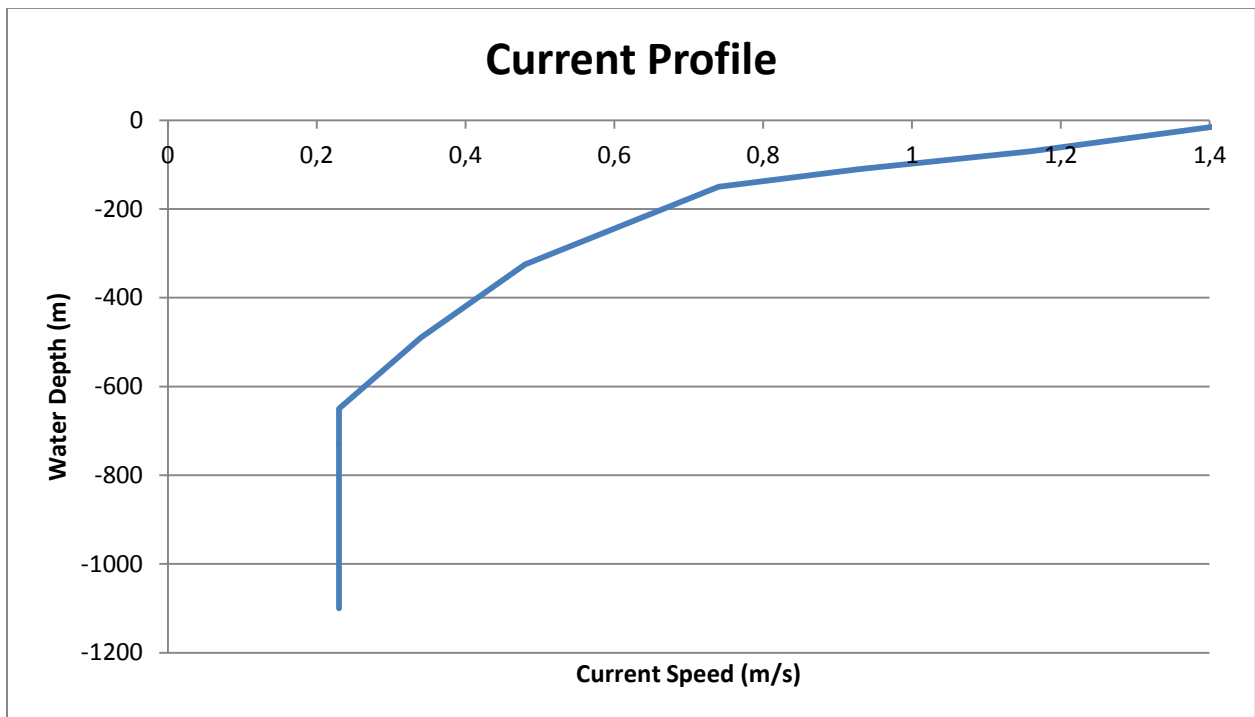


Figure 5.4 Current profile for the 10-year condition

Table 5.4 Riser Properties

Riser Parameter	Value
Internal diameter (in/mm)	10/254
Wall thickness (mm)	25
Specified minimum yield strength (SMYS) (MPa)	448.2
Specified minimum tensile strength (SMTS) (MPa)	530.9
Design pressure (MPa)	34.5
Elastic modulus (MPa)	207,000
Poisson ration	0.3
Steel density (kg/m^3)	7,850
Steel grade	API X65
Internal fluid density (kg/m^3)	800
External coating thickness (mm)	75
Coating density (kg/m^3)	700
Flex joint rotational stiffness (kN.m/deg)	50

5.4.7 Hydrodynamic data and marine growth

Morison equation can be used to express hydrodynamic loading on the SLWR, as a function of the relative fluid velocities and accelerations. Both drag and added mass coefficients vary with variations in Reynolds number, Keulegan-Carpenter number, and the surface roughness of a structure (Sarpkaya, 1976, Sarpkaya, 1977). However, constant value of drag coefficient can be conservatively used over the depth.

According to the reference standard (DNV-OS-F201), a drag coefficient between 0.7 and 1.0 and inertia coefficient of 2.0 can be used for cylindrical bare pipes. For rough cylinders, it can be taken as 1.05 (NORSOK, 2007), for instance to account for presence of marine growth.

In this thesis work, the hydrodynamic coefficient data used for the SLWR is presented in Table 5.5, the conservative approach is adopted, and therefore the value is assumed constant over the entire depth.

Table 5.5 Hydrodynamic Coefficients

Hydrodynamic Data	Value
Normal drag coefficient	1.0
Axial drag coefficient	0.0
Normal added mass coefficient	1.0
Axial added mass coefficient	0.0

The presence of marine growth may result in an increase in added mass and tangential drag coefficients, thereby influencing the SLWR response. Marine growth is however not modeled separately in this thesis work, and the possibility of having marine growth is assumed taken care of by the hydrodynamic coefficient data used.

In the analysis, mass coefficient, C_m , is taken as added mass coefficient, C_a , plus one, that is:

$$C_m = C_a + 1$$

5.4.8 Buoyancy modules

Buoyancy modules are required at certain lengths of the riser to achieve the required lazy wave configuration. Distributed buoyancy is considered in this study, this buoyancy type is provided by placing individual modules at specified uniform intervals known as pitch, along certain riser arc length.

The distributed buoyancy modules is modeled in this study as having smeared properties, that is, buoyancy is provided through a riser arc length with equivalent distributed properties of the combined riser section and attached buoyancy modules. To achieve the lazy wave configuration, a negative net buoyancy force must be ensured.

The main properties of the buoyancy modules used in this study, and its hydrodynamic properties, are presented in Table 5.6. Also, an illustration of typical distributed buoyancy modules on a riser is shown in Figure 5.5.

Table 5.6 Buoyancy Module Properties

Buoyancy Module Parameter	Value
Material Density (kg/m^3)	395
Outer diameter (mm)	758
Inner diameter (mm)	254
Pitch (m)	12
Normal drag coefficient	1.38
Axial drag coefficient	0.126
Normal added mass coefficient	1.0
Axial added mass coefficient	0.346

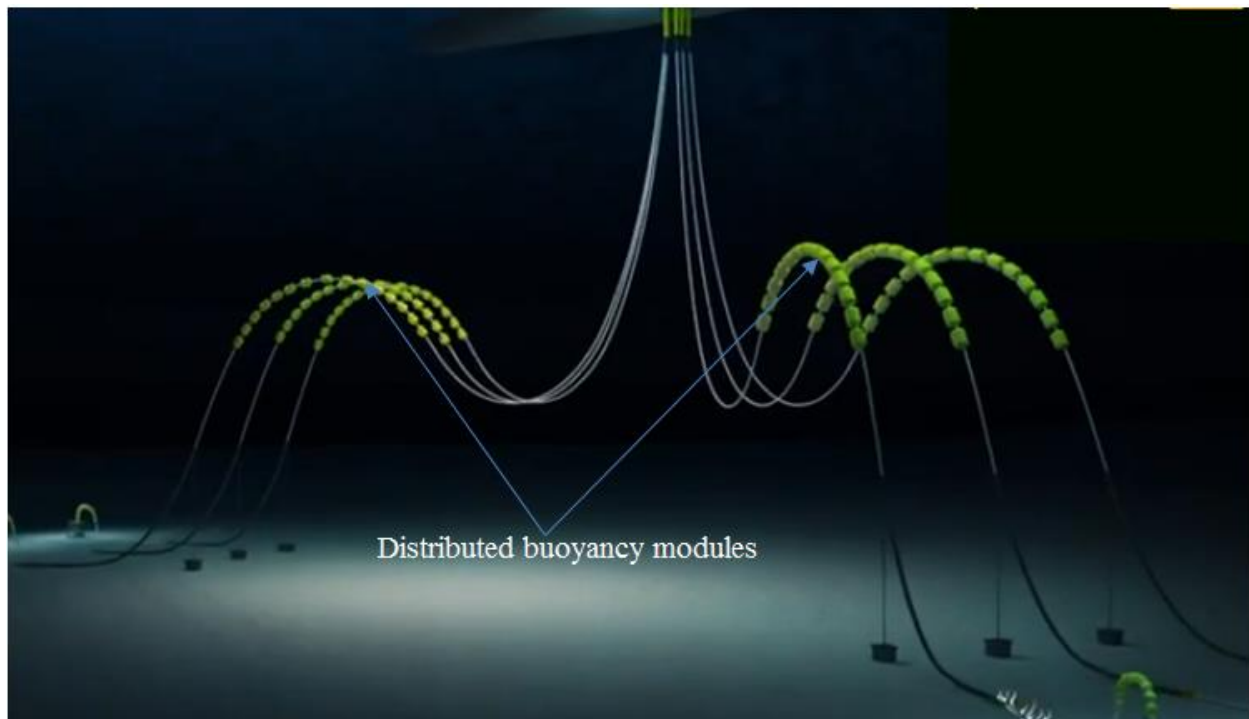


Figure 5.5 Illustration of buoyancy modules attached to riser pipes (Balmoral, 2014).

5.4.9 Riser – soil interaction

Complex interactions exist between riser pipe movements, its penetration into the seabed, and soil resistance, when the riser is subjected to oscillatory motion (Bai and Bai, 2005). This interactions leads to an out-of-plane motions of the riser at the TDP area, and will affect the riser fatigue life.

It is therefore important to properly describe the riser-soil interactions to accurately capture the riser's fatigue performance.

The riser-soil interaction parameters used in this thesis work are as follows:

- Axial friction coefficient – 0.3
- Lateral friction coefficient – 0.5
- Horizontal lateral/axial soil stiffness – 200 kN/m²
- Vertical soil stiffness – 50 kN/m²

5.4.10 Fluid data

The main internal fluid under consideration in this thesis work is a production fluid with density of 800 kg/m³, and the corresponding design internal pressure is 34.5 MPa. In addition, sensitivity will be carried out considering the case when the SLWR is empty. Water filled is however not considered as a result of lack of associated environmental data.

5.4.11 Riser fatigue data

Long-term wave induced fatigue analysis is performed in this thesis work; the data used is taken from a typical North Sea Metocean data. The wave scatter diagram is defined by significant wave height, (H_s), and spectral peak period, T_p , covering a period of 100 years, based on 3 hours sea state. The H_s covers a range of 0 to 16 meters, while the T_p covers a range of 0 to 25 seconds. The wave scatter diagram is confidential and is not presented in this thesis work.

A total of 12 wave directions are considered for the wave induced fatigue analysis, based on the Metocean data. The annual probability for each wave direction based on ORCAFLEX global axes is presented in Table 5.7; this is used to determine the fatigue damage contribution from each wave direction.

Table 5.7 Wave Direction Annual Probability

Wave Direction (⁰)	Annual Probability (%)
0	12.61
30	19.98
60	14.0
90	4.61
120	2.64
150	1.41
180	1.16
210	2.72
240	10.5
270	11.89
300	8.68
330	9.8
Total	100

Similarly, long-term vortex induced vibration (VIV) is performed, with data taken from typical North Sea current profile for fatigue analysis. A total of 14 unidirectional current profiles are used, the analysis is performed with the current in-plane and out-of-plane of the SLWR, with 50% probability of occurrence each. The current profile data is confidential and is not presented in this thesis work.

5.5 Wall Thickness Sizing

This is an important step in riser design; the minimum wall thickness used must be able to withstand internal overpressure, external hydrostatic pressure, and combined loading. The minimum wall thickness used in this study is estimated based on pressure containment, collapse,

and combined loading criteria in accordance with DNV-OS-F201.

Pipeline Engineering Tool (PET) software, a product of DNV, is used to determine the minimum required wall thickness, the software is based on DNV-OS-F101. The formula used in determining the wall thickness is the same as in DNV-OS-F201 discussed in section 4.4.3.

A summary of the results is presented in Table 5.8, from the results; buckle propagation gives the highest minimum wall thickness requirement. However, consideration is usually not given to buckle propagation criteria to avoid excessive wall thickness sizing, and since buckling can be controlled by installing buckle arrestors.

Based on the assessment, a relatively thick wall thickness of 25 mm is used in this study. The details of the parameters used in calculating the wall thickness and detailed results are presented in Appendix A.

5.6 Design Cases

The various load cases considered in the present study for static and dynamic strength analysis are presented in Table 5.9. The far and near offset position are as defined in section 5.4.3 and Table 5.2.

A combination of FPSO heading of 0^0 with wave and current heading of 180^0 results in the far offset position, while a combination of FPSO heading of 180^0 with wave and current heading of 0^0 results in the near offset position.

Sensitivity studies will be carried out on the SLWR configuration, by considering the following in extreme sea-state:

- Variation of net buoyancy force
- Variation of the SLWR sag-bend height from seabed
- Variation of the SLWR hang-off angle
- Variation of buoyant section length, L_2

Sensitivity studies will be carried out on the SLWR behavior, by considering the case when the riser is empty.

Table 5.8 Minimum Wall Thickness

Burst (Operation) (mm)	Burst (System test) (mm)	Collapse (mm)	Propagation buckling (mm)
19.82	17.97	16.12	23.43

Table 5.9 Load Case Matrix

Load Case	Stage/Limit State	Load Type	Wave	Current	Offset
1	Static	Functional	-	-	Mean
2	Dynamic – ULS	Functional +Environment	100-year	10-year	Near
3	Dynamic – ULS	Functional +Environment	100-year	10-year	Far
4	Dynamic – ULS	Functional +Environment	10-year	100-year	Near
5	Dynamic – ULS	Functional +Environment	10-year	100-year	Far
6	Dynamic – ALS	Functional +Environment	100-year	10-year	Near
7	Dynamic –ALS	Functional +Environment	100-year	10-year	Far
8	Dynamic – ALS	Functional +Environment	10-year	100-year	Near
9	Dynamic –ALS	Functional +Environment	10-year	100-year	Far

For the strength analysis, the following SLWR response characteristics will be observed and discussed:

- Top section:
 - ✚ Maximum top angle
 - ✚ Minimum top angle
 - ✚ Maximum effective tension
- Sag bend, Hog bend, and TDP:
 - ✚ Maximum Effective Tension
 - ✚ Minimum Effective Tension
 - ✚ Maximum Bending Moment
 - ✚ Maximum von Mises Stress
 - ✚ Maximum Utilization (LRFD)

5.7 Acceptance Criteria

As a minimum, the following acceptance criteria are adhered to in this thesis work:

- The SLWR strength performance shall fulfill DNV-OS-F201 combined loading criteria for:
 - ✚ Bending moment, effective tension, and net internal pressure
 - ✚ Bending moment, effective tension, and net external pressure
- In accordance with DNV-OS-F201, LRFD design format, the utilization factor shall be less than unity, for both static and dynamic response.
 - ✚ The LRFD design format is governed by generalized load effect or utilization function, this is given by:

$$g(t) = g(M_d(t), T_{ed}(t), \Delta p, \mathbf{R}_k, \Lambda) \leq 1$$

Where:

- M_d : Bending moment
- T_{ed} : Effective tension
- Δp : Local differential pressure
- \mathbf{R}_k : Vector of cross-sectional capacities

Λ : Vector of safety factors

$g(t) < 1 \rightarrow$ safe design

$g(t) > 1 \rightarrow$ failure

- The allowable maximum static stress for this study is 298 MPa, corresponding to 2/3 of SMYS. For ULS design, the maximum allowable stress is 358 MPa, this is based on a design factor of 0.8. For ALS design, the maximum allowable stress is 448 MPa, and is based on a design factor of 1.0. The allowable maximum stress is in accordance with API-RP-2RD.
- Excessive compression (negative minimum tension) is undesirable and shall be avoided or be minimal.
- Fatigue due to combined loading from WF and LF motions shall be at least 10 times the SLWR design life.
- Fatigue as a result of VIV shall be at least 20 times the SLWR design life.

CHAPTER 6 EXTREME RESPONSE AND FATIGUE ANALYSES

6.1 Introduction

The primary software program used for modeling and analysis is ORCAFLEX. For analysis of fatigue damage as a result of VIV, the model was replicated in another software program, RIFLEX, and VIVANA software tool was used to analyze the VIV fatigue response. A brief description of the main aspects of these software programs is presented in Appendix B.

The approach adopted in modeling and analyses can be summarized as follows:

- Determination of an optimum static configuration for the SLWR, including the riser's:
 - ✚ Upper section length, L_1
 - ✚ Buoyant section length, L_2
 - ✚ Lower section length, L_3
 - ✚ Optimum net buoyancy force
- Static analysis
- Dynamic analysis
 - ✚ Strength analysis in extreme sea-states under combined actions of waves and currents as described in Table 5.9
- LRFD code checks
- Wave induced fatigue analysis using a typical North Sea scatter diagram
- VIV fatigue analysis using typical North Sea fatigue current profile

The combinations of partial safety factors used in checking ULS and ALS conditions according to the LRFD design format are presented in Table 6.1.

6.2 Optimum Static Configuration

According to DNV (2010a), the sag and hog bend area, and the TDP zone are critical locations on lazy wave risers. High static bending stresses at the sag and the hog bends are design issue for lazy wave configurations (Karunakaran and Olufsen, 1996). In addition, the riser top section may be subjected to high stresses and low fatigue performance in extreme state (Senra et al., 2011).

Table 6.1 Partial Safety Factors for ULS and ALS Code Check

	ULS	ALS
Functional, γ_F	1.1	1.0
Environmental, γ_E	1.3	1.0
Reduced Functional, γ_{RF}	0.91	-
Reduced Environmental, γ_{RE}	0.77	-

It is therefore a design objective in this thesis work to ensure low static bending stresses in these zones, by ensuring low curvatures at the sag and the hog bends.

To achieve an ideal configuration, the following factors were considered:

- Optimized number of buoyancy elements, to ensure “low lazy wave configuration”, this will in essence also reduce costs of a project.
- Sufficient height between the sag bend and the hog bend (wave zone), the hog bend height is chosen such that interference problems with other lines can be avoided. This consideration is important due to high current velocities in the WoS.
- Sufficient clearance height between the sag bend and the seabed, to avoid clashing between them, when the SLWR is in the near position. This consideration is important considering when the riser is filled with denser fluid, for instance, flooded with water.

With the considerations above, a combination of the following parameters gives an ideal static configuration, and forms the base case configuration for further studies and analyses:

- Total riser length: 2100 meters
 - ✚ Upper section length, L_1 : 1239 m
 - ✚ Buoyant section length, L_2 : 420 m
 - ✚ Lower section length, L_3 : 441 m
- Hang-off angle: 8 degrees
- Net upward buoyancy: 700 N/m

- Upper termination point (UTP): 5 meters from the turret center, and 12 meters below water surface
- Horizontal span: 1380 meters (UTP to connection point on seabed)
- Horizontal distance to TDP: 1116 meters from UTP
- Sag-bend height above seabed: 100 m
- Height between sag and hog bend: 80 m (at mean offset)

The resulting static configuration is shown in Figure 6.1, for intact mooring in the mean, the near, and the far positions. This configuration gives a minimum sag bend height from the seabed to be 76 meters in the near position, and minimum height of 36 meters between sag bend and hog bend in the far position for intact mooring. These clearance heights are considered safe for the case study in this thesis work.

6.3 Strength Analysis

The objective here is to confirm the integrity of the SLWR from turret moored FPSO, in the extreme sea-state conditions in the near and far FPSO offset positions. This objective is achieved by comparing the results under the different load combinations as described in Table 5.9, with the allowable criteria, and the LRFD design criterion.

The extreme response calculation is based on irregular time-domain analysis. The JONSWAP spectrum described in section 5.4.4 was used to model the irregular waves. The main analysis was performed using a number of 3-hour storm simulations for the extreme sea state response, by randomly selecting different user defined seed components for a given wave train.

Since each set of wave train from the randomly selected seed components, generates different sea-state realization, 10 random seed components were therefore used for the base case study, that is, we have 10 different realizations of the sea-state. For each wave train, the significant wave height is covered at least once.

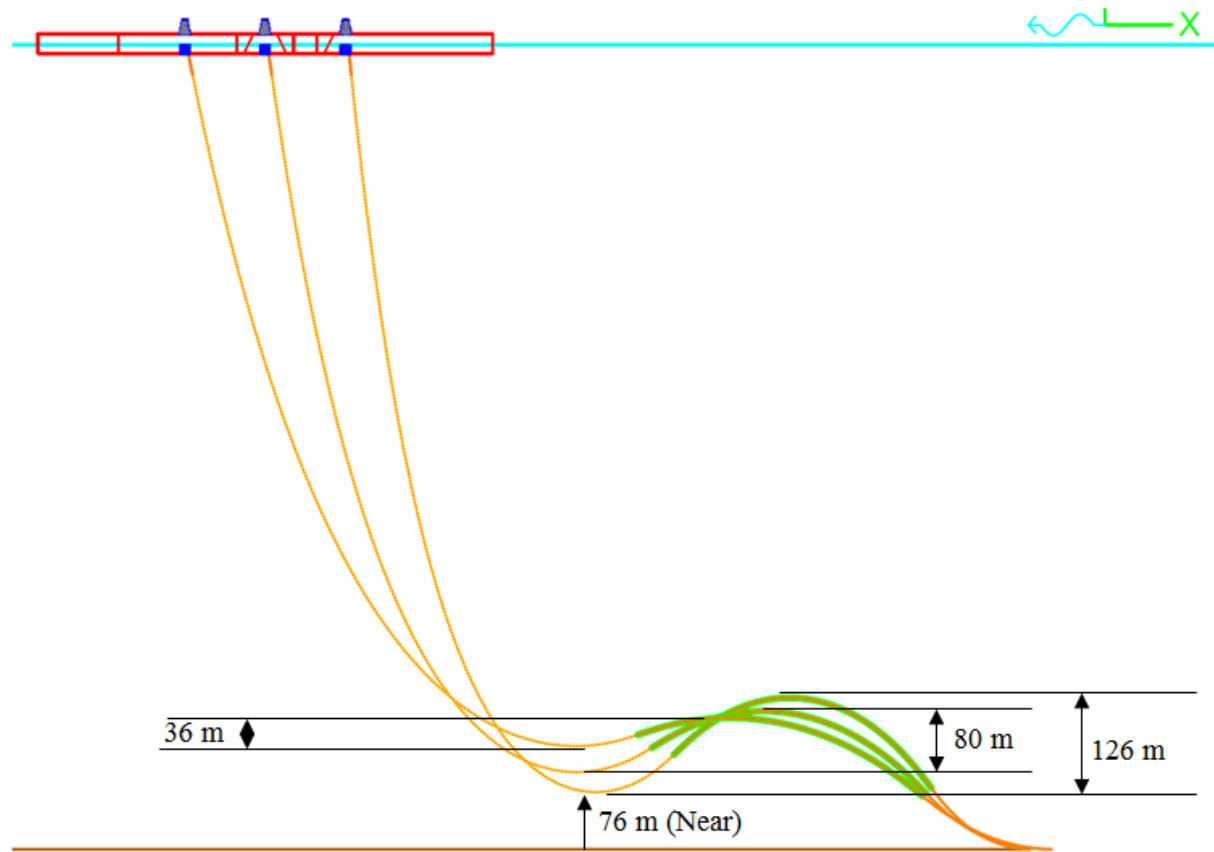


Figure 6.1 SLWR static configuration for mean, near, and far FPSO offsets

The SLWR responses from the different sea-state realizations are different. To ensure therefore that the extreme value distribution for the storm condition under consideration is properly accounted for, the average value of the responses from the 10 realizations is considered as the extreme response value for the base case study.

The purpose of the long simulation time and consideration of 10 realizations in this study is to ensure the extreme response analyses is performed in accordance with DNV-OS-F201, for adequate statistical confidence.

A simplified approach was employed in the sensitivity study; the analysis was performed for a shorter duration, following recommended standard industrial procedure. In this approach, a total simulation time of 135 seconds was considered, while still capturing the worst response of the

SLWR. This is achieved by identifying the simulation periods at which the worst response occurred. The following procedure is then applied:

- Set the simulation time origin to 5-wave periods less than the identified period that give worst response
- Perform dynamics analysis such that;
 - ✚ Wave build-up stage is set to 10 seconds
 - ✚ Main analysis is run for minimum of 7-wave periods, 5 periods before the identified worst response period, and 2 periods after

The simplified procedure above save time spent on simulation, and if care is taken in identifying the period which give worst response, the exact extreme response will be obtained compared to when full 3-hour simulation is performed. It is noted that the worst response does not always occur when we have peak sea-state, therefore running at least one full 3-hour simulation is recommended to identify worst response time interval.

Also taken into consideration during the analysis is that, for a given FPSO heading and offset; waves and current are conservatively assumed to be acting in the same direction, and at the bow of the FPSO. This consideration is to account for the worst 3-hour design storm combination. Analyses were performed with the FPSO in the mean, far, and near positions, and the characteristic response is taken as the worst response identified from these analyses.

6.3.1 Static analysis

The static analysis gives a static equilibrium configuration of the SLWR. In this analysis, consideration is given to functional loads and mean vessel offset, no environmental load is considered. The functional loads considered are as described in section 4.5 and Table 4.4. A summary of the results of the static analysis, for the critical sections of the SLWR is presented in Table 6.2.

Table 6.2 Static Results – Functional Loads

FPSO Mean Position			
Hang-off Angle ($^{\circ}$)	8		
Effective Top Tension (kN)	1224		
Critical Locations			
	Sag Bend	Hog Bend	TDP
Effective Tension (kN)	169	169	169
Bending Moment (kN.m)	275	182	92
von Mises Stresses (MPa)	251	219	194
DNV Utilization (LRFD)	0.52	0.44	0.38

Discussion of Static Analysis Results:

The following is a general description of the SLWR response under functional loadings in the mean offset position:

- The effective tensions at the sag-bend, the hog-bend, and the TDP are equal. This showed that the forces at the sag and hog bends are horizontal, and equal the horizontal force acting at the TDP.
- The static stresses at the three critical locations are fairly low, especially at the TDP area, and are below the allowable limit.
- The maximum utilization value is 52 percent, and is observed at the sag bend area.

It should be noted that, the DNV utilization is determined using only functional load partial factor of safety; this is in accordance with DNV-OS-F201.

6.3.2 Dynamic analysis

A time domain dynamic analysis was carried out considering ULS and ALS design. The riser integrity was checked against the load combinations described in Table 5.9 for each design category.

The extreme analysis was carried out as described in section 6.3, for waves and current in plane with the SLWR configuration, that is, 0 and 180 degrees. This is because this combination is more critical when considering extreme strength response compared to waves and current out of plane with the riser configuration.

A summary of the dynamic analysis responses is presented in Tables 6.3 for ULS and ALS design, when considering a load combination of 100-year wave with 10-year current, this will be referred to as load combination set A.

The SLWR response summary, when considering a combination of 10-year wave with 100-year current is presented in Table 6.4 and this will be referred to as load combination set B.

Although, the analysis was performed for the entire riser length, the summary results is given in Tables 6.3 and 6.4 for the critical sections of the SLWR, and the worst stresses and utilization at the sag bend area, the hog bend area, and the TDP area are presented.

6.3.3 Discussion of dynamic response results

A comparison of the responses from the combination of 100-year wave with 10-year current, and 10-year wave with 100-year current, showed that 100-year wave with 10-year current give worse response behavior.

The observations include:

- Maximum stresses occurred when the SLWR is subjected to combination of 100-year wave with 10-year current, as shown in Figure 6.2
- Residual compression (negative effective tension) is observed along the SLWR arc length in the case of 100-year wave with 10-year current, but no residual compression in the case of 10-year wave with 100-year current, as shown in Figure 6.3

The 100-year wave with 10-year current is therefore selected as the governing load combination for further studies and discussions in this thesis work.

Table 6.3 Strength Response Summary Results – Set A

100-year wave + 10-year current	FPSO Position			
	Intact		Accidental	
	Near	Far	Near	Far
Max. Top Angle	18.7	14.6	16.6	15.9
Min. Top Angle	4.8	0.1	3.8	0.1
Max. Effective Top Tension (kN)	1854	1958	1850	1986
Sag Bend				
Max. Effective Tension (kN)	248	658	232	749
Max. Compression (kN)	50	86	46	95
Max. Bending Moment (kN.m)	425	332	445	338
Max. von Mises Stresses (MPa)	335	272	348	274
Max. DNV Utilization (LRFD)	0.77	0.65	0.73	0.56
Hog Bend				
Max. Effective Tension (kN)	159	594	146	680
Max. Compression (kN)	-	36	-	64
Max. Bending Moment (kN.m)	308	315	326	345
Max. von Mises Stresses (MPa)	264	272	271	278
Max. DNV Utilization (LRFD)	0.60	0.67	0.56	0.57
TDP				
Max. Effective Tension (kN)	111	576	97	657
Max. Compression (kN)	-	-	-	-
Max. Bending Moment (kN.m)	400	283	412	286
Max. von Mises Stresses (MPa)	314	252	322	252
Max. DNV Utilization (LRFD)	0.73	0.56	0.68	0.50

Table 6.4 Strength Response Summary Results – Set B

10-year wave + 100-year current	FPSO Position			
	Intact		Accidental	
	Near	Far	Near	Far
Max. Top Angle	18.9	12.2	18.7	13.2
Min. Top Angle	6.2	0.05	5.8	0.2
Max. Effective Top Tension (kN)	1756	1972	1750	2009
Sag Bend				
Max. Effective Tension (kN)	231	636	216	711
Max. Compression (kN)	-	-	-	-
Max. Bending Moment (kN.m)	420	247	442	241
Max. von Mises Stresses (MPa)	330	240	344	238
Max. DNV Utilization (LRFD)	0.75	0.47	0.72	0.45
Hog Bend				
Max. Effective Tension (kN)	153	563	141	642
Max. Compression (kN)	-	-	-	-
Max. Bending Moment (kN.m)	302	225	320	223
Max. von Mises Stresses (MPa)	261	232	268	232
Max. DNV Utilization (LRFD)	0.52	0.48	0.56	0.42
TDP				
Max. Effective Tension (kN)	103	531	95	614
Max. Compression (kN)	-	-	-	-
Max. Bending Moment (kN.m)	381	228	395	225
Max. von Mises Stresses (MPa)	303	232	311	231
Max. DNV Utilization (LRFD)	0.69	0.47	0.66	0.42

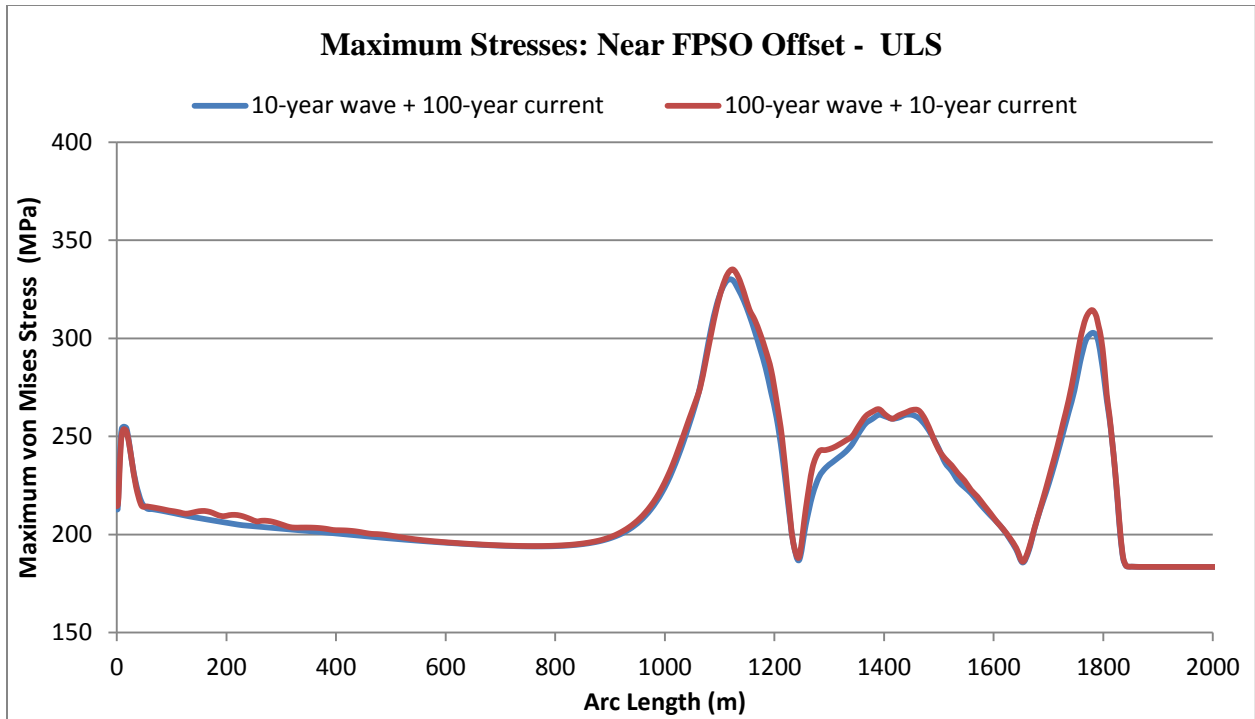


Figure 6.2 Comparison of maximum stresses

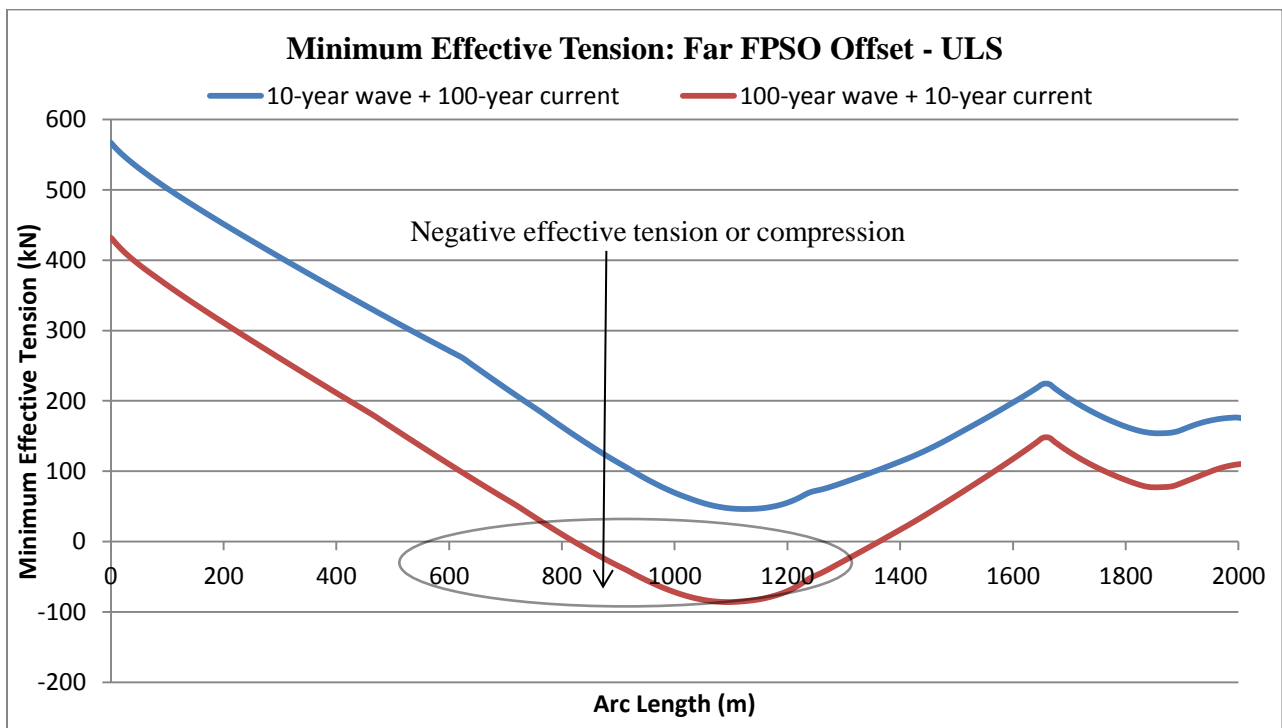


Figure 6.3 Comparison of minimum tension

In general, the following are observed from the SLWR response when subjected to extreme sea-state condition:

- The SLWR top angle changes as the riser system responds to extreme sea-state conditions. The maximum change in top angle is observed in the near offset position. The variations in the maximum top angle can be said to be in the range of -8.0° to $+10^\circ$, this is shown in Figure 6.4.
- The maximum effective top tension at the connection point to the turret is 1958 kN, for ULS design, this maximum value is observed in the far offset position.
- Residual compression is observed at the sag bend and hog bend in extreme sea-state conditions. This is as a result of high FPSO downwards velocity heave motion of about 3.6 m/s. A time-history plot of the downward velocity and minimum tension at the sag bend area is shown in Figure 6.5, for far offset position.
- The maximum compression for ULS design is 86 kN, and occurs in far FPSO offset position. Although compression is not desirable, the observed compression is minimal, and will not result into riser buckle; therefore, the observed compression is acceptable in this study.
- For ULS design, the maximum stress for this configuration is 335 MPa, and this value is below the allowable maximum stress.
- The difference between the static stress and dynamic stress is 20 MPa for the mean offset position, and 34 MPa for the near position. This shows that the contribution from environmental actions from waves and current is minimal, and static stresses therefore dominate.
- The maximum stress occurred at the sag bend area. This is observed in the near offset position.

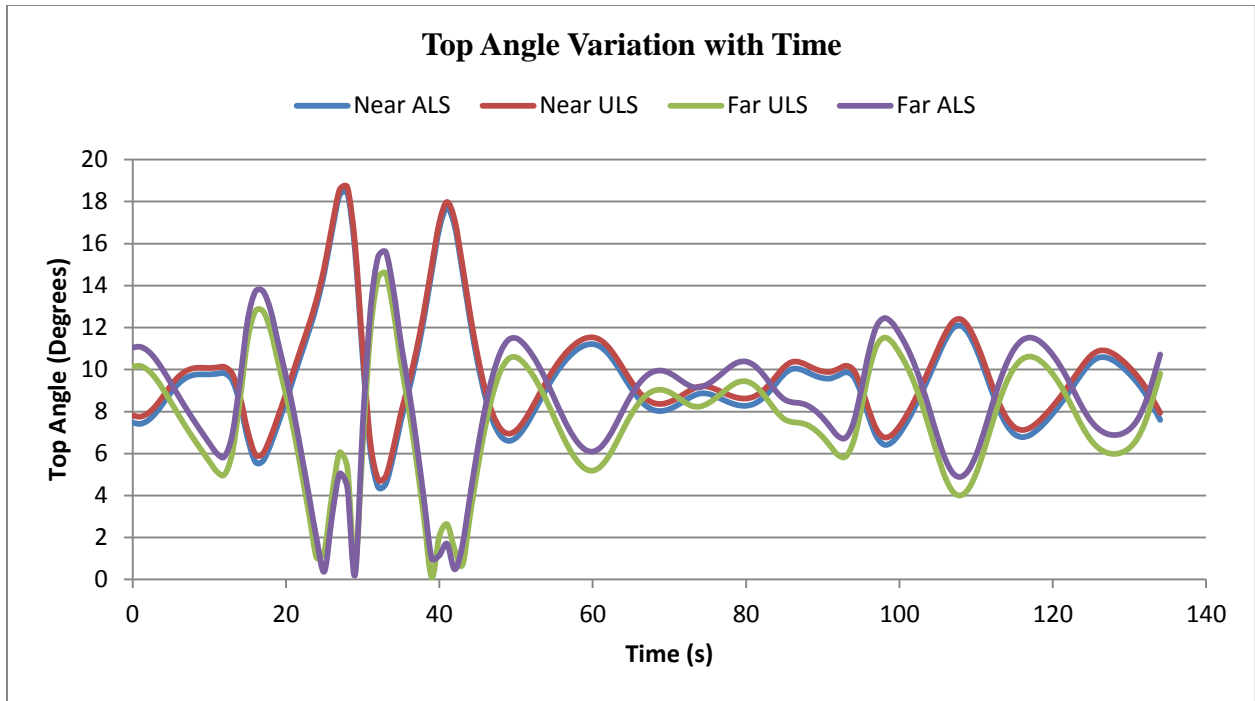


Figure 6.4 Variations of maximum top angle with time

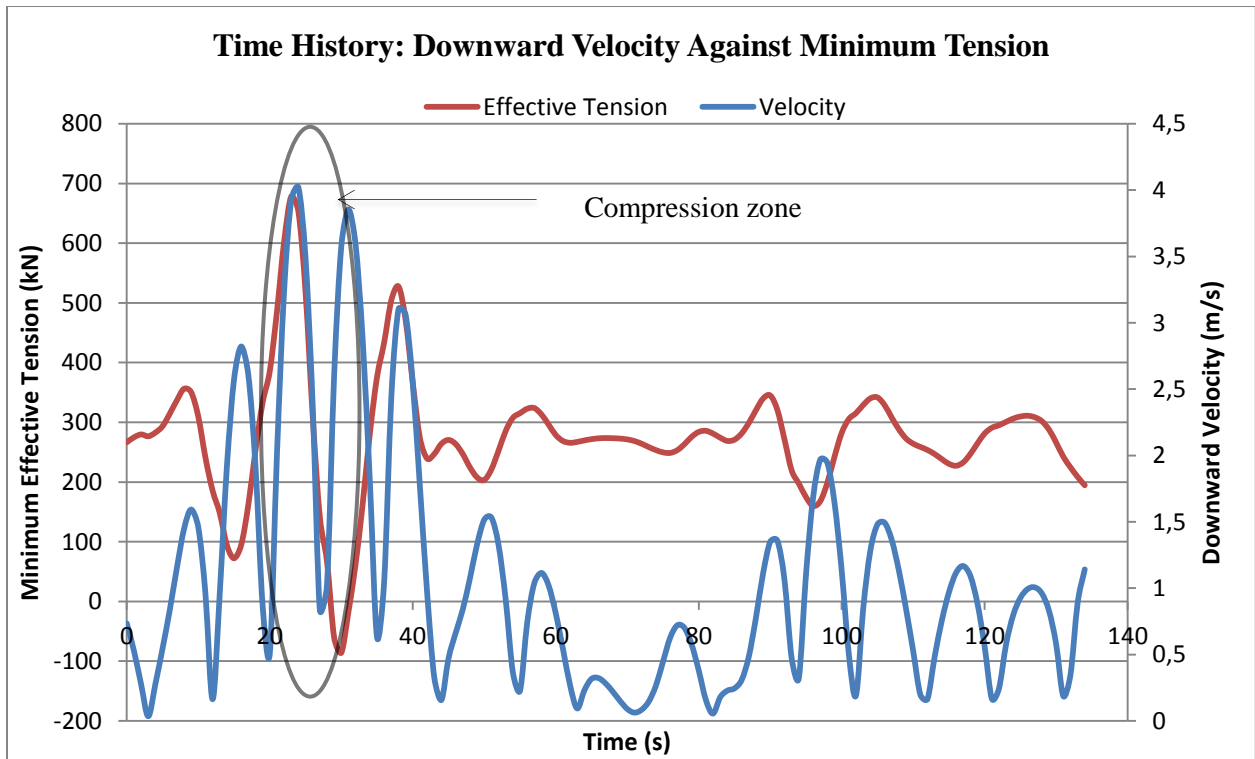


Figure 6.5 Downward velocity VS minimum tension at the sag bend

- The maximum LRFD utilization is 77 percent for ULS design. This is also observed at the sag bend, and in the near FPSO offset position. The utilization is below unity, and we therefore have a safe design.
- In summary, the above observations showed that the extreme response of a production riser for deployment in deepwater, harsh environment is within the allowable and safe design criteria, when adopting the steel lazy wave configuration.

It should be noted that, the utilization in this case is determined using both functional and environmental partial factors of safety. This may be determined manually by separating the static and dynamic stresses, and applying their respective partial safety factor as presented in Table 6.2.

More efficient LRFD calculations can be performed in ORCAFLEX version 9.7, this was used in the LRFD code checks in this thesis, and a general description of the approach is presented in Appendix B.

6.3.4 Comparison of response at the critical sections

Considering the load combination governing this design, it can be seen from Table 6.3 that the SLWR respond differently at the sag bend and TDP compared to the hog bend. The maximum stresses at these critical sections of the SLWR are shown in Figure 6.6.

The following observations are made from the Figure:

- The maximum stresses at the sag bend and the TDP are at a peak when the FPSO is in the near offset position. However, the maximum stress at the hog bend is at its peak when the FPSO is in the far offset position.
- The maximum stresses at the sag bend and TDP are higher than the stress at the hog bend considering this base case configuration. This is an indication that the sag bend and TDP are more critical to extreme response in the design.
- The maximum stress at the top section also occurs in the far offset position.

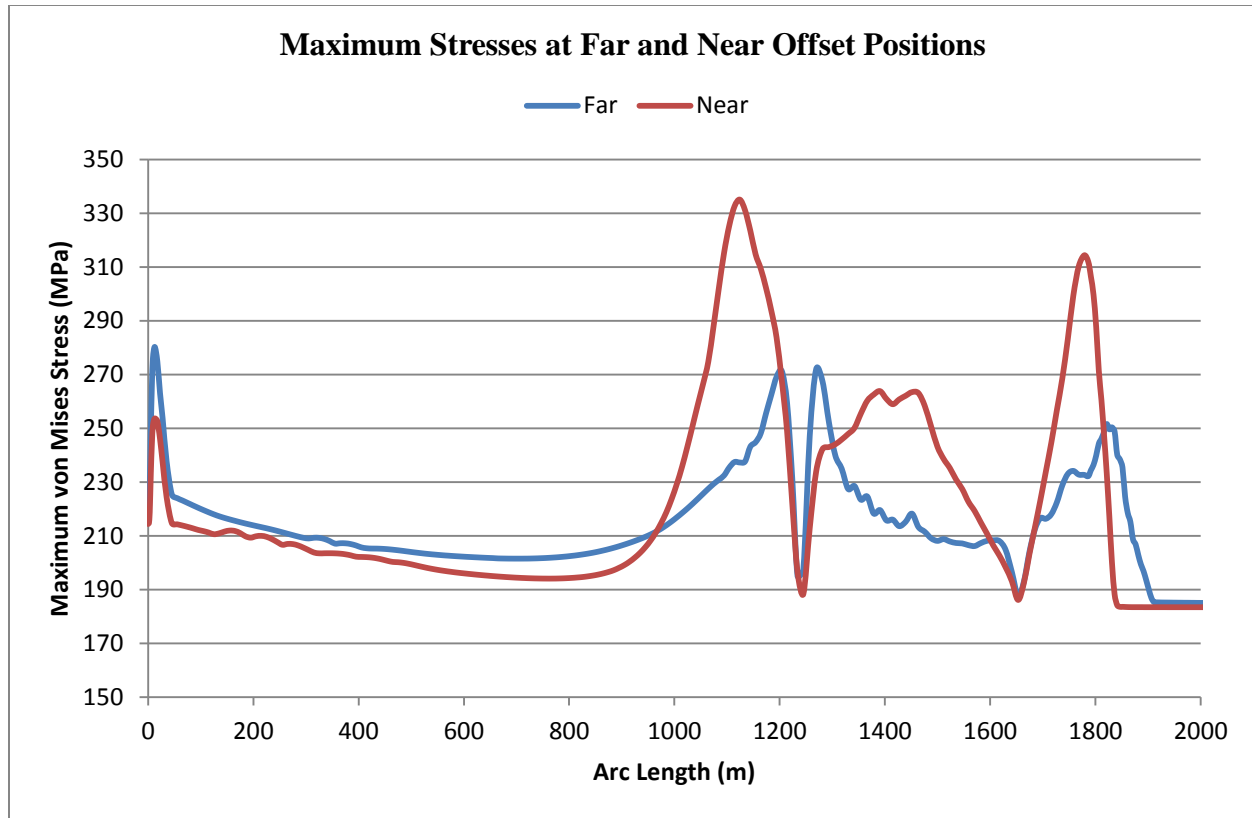


Figure 6.6 Maximum stresses over the entire arc length, far and near offsets – ULS

6.3.5 Extreme response summary

From the discussions in section 6.3.3, it can be summarized that the SLWR meet the design criteria as defined in the acceptance criteria.

The maximum static and dynamic stresses are observed at the sag bend area, and this occurred when the FPSO is in the near offset position.

Although residual compression is observed, the compression is of no significant concern, and the SLWR will not buckle under the condition.

Since both ULS and ALS design criteria are satisfactory, fatigue response analysis will now be performed to establish the fatigue behavior of the SLWR, and check against FLS design criteria, this precludes the final recommendation on the integrity of the SLWR from turret moored FPSO, for the harsh environment under consideration.

6.4 Fatigue Response Analyses

One of the major objectives of this thesis work is the establishment of the fatigue response of the SLWR in deepwater, harsh environment.

According to DNV (2010a), the following contributions to riser fatigue damage are to be taken into consideration during riser design:

- Wave-induced stress cycles
- Low-frequency stress cycles; and
- Vortex-induced stress cycles

The analysis methodology employed for wave-induced fatigue damage is nonlinear time domain (NDT) using irregular wave model. For vortex-induced fatigue damage, a combination of frequency domain procedure and nonlinear time domain is employed, using fatigue current profile. The NDT is a numerical integration on a step by step basis of small increments of dynamic equilibrium equations (DNV, 2010a).

The S-N curve methodology is used in estimating the fatigue response of the SLWR in this study. For a given stress range, the curve defines the number of cycles to failure as shown in Figure 6.7, the Figure shows different S-N curves in seawater with cathodic protection. To analyze welds in the SLWR, consideration is given to C2 and D curves in this study, the basis for this is established in previous work by Karunakaran et al. (2013). The C2-curve is more tolerant compared to D-curve and is expected to give lower fatigue damage or higher fatigue life for the same riser section.

The S-N curve is governed by the following expression (DNV, 2010a):

$$\log N = \log \bar{a} - m \log S$$

$$S = S_o \cdot \text{SCF} \left(\frac{t_3}{t_{\text{ref}}} \right)^k$$

Where:

N – number of stress cycles to failure

S – stress range

\bar{a} , m – empirical constants

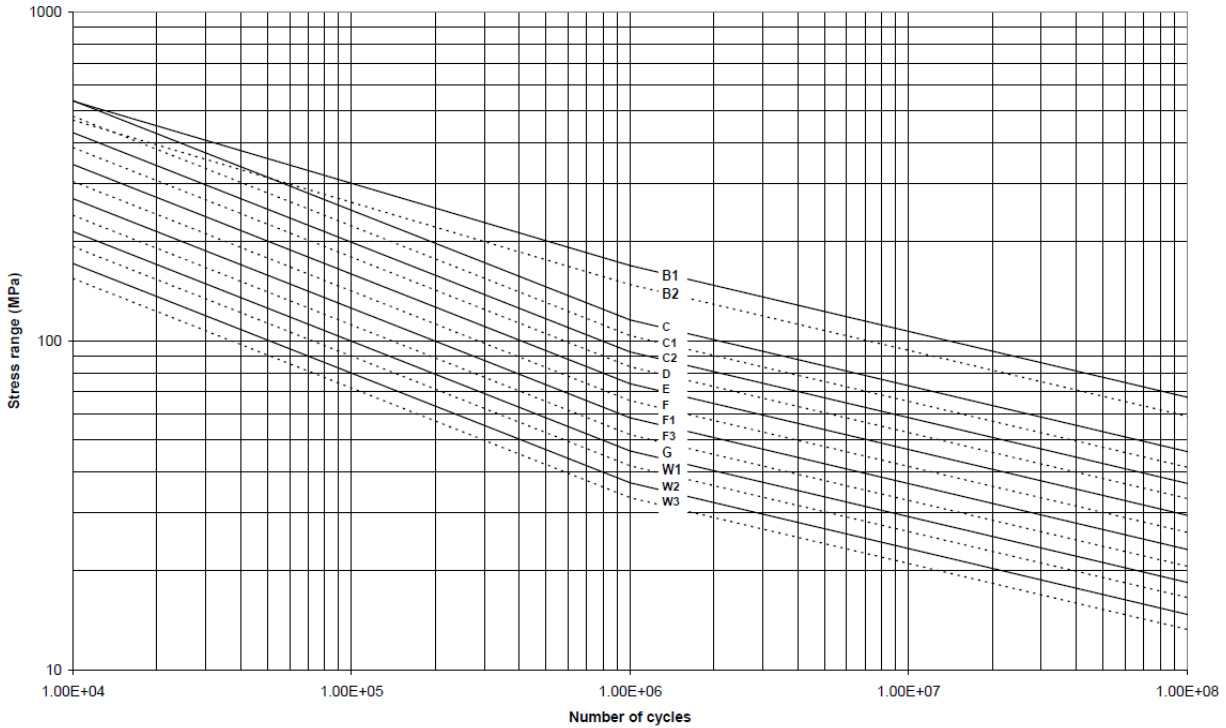


Figure 6.7 S-N curves in seawater with cathodic protection (DNV, 2012)

S_o – nominal stress range

SCF – stress concentration factor

$\left(\frac{t_3}{t_{ref}}\right)^k$ – thickness correction factor; applicable to pipes with $t_3 > t_{ref}$

t_3 – pipe wall thickness

t_{ref} – reference wall thickness = 25mm

Stress concentration factor (SCF) is used to account for uncertainties, for instance, magnification of stress resulting from imperfections in geometry between adjacent joints.

The SCF can be obtained by finite element analyses or by a closed form expression. For welded riser joints, the following closed form expression applies (DNV, 2010a):

$$SCF = 1 + \frac{3e}{t_3} \exp\left(-\left(\frac{D}{t_3}\right)^{-0.5}\right)$$

Where:

e – representative eccentricity due to imperfections in geometry

Based on the expression above, an estimated value of 1.2 is used for both curves that are considered in the fatigue damage calculations.

In this thesis work, fatigue damage is calculated using Palmgren-Miner accumulation law, defined by (Bai and Bai, 2005):

$$D_{\text{fat}} = \sum_{i=1}^{M_c} \frac{n_i}{N_i} \leq \eta$$

Where:

D_{fat} = accumulated fatigue damage

n_i = number of stress cycles with stress range in block i

N_i = number of cycles to failure at the i -th stress range defined by S-N curve

η = allowable damage ratio, taken as 0.1

An endurance limit, otherwise known as cut-off stress range can also be specified. No significant fatigue damage occurs below this stress range, and according to Bai and Bai (2005), the endurance limit is at $2 * 10^8$ cycles for joints with adequate cathodic protection in seawater, and stress ranges smaller than this can be ignored in accumulated fatigue damage calculations.

6.4.1 Wave-induced fatigue damage

Wave induced fatigue response is primarily driven by vessel motion, and is therefore sensitive to vessel design and the hang-off location on the FPSO. The mean offset of the FPSO and SLWR system is considered in the fatigue damage calculations in this study. Wave induced fatigue damage from a total of 12 wave directions at an interval of 30^0 as described in section 5.4.11, are considered in this thesis work. This resulted into a total of 216 load cases for wave induced fatigue damage calculations.

The following procedure as described in DNV (2010a) is adopted in the wave-induced fatigue damage calculations.

- Subdivision of the sea-state scatter diagram into representative blocks.

In this study, the sea-state scatter diagram was divided into 18 representative blocks as shown in Figure 6.8.

- Selection of a single sea-state representing all the sea-states located within each block, with the probability of occurrence of all sea-states within the block lumped to the representative sea-state.

The representative sea-state in each block in this thesis work is represented with a red asterisk as shown in Figure 6.8. The lumped probability of occurrence is presented in Table 6.5; this is a percentage of all the occurrences in each block over the total occurrences.

- Computation of fatigue damage for each of the representative sea-state within the blocks.

This was computed in ORCAFLEX, using deterministic random wave fatigue analysis with the rain-flow cycle counting technique.

The simulation time for each of the load cases is 1-hour; this duration was selected to accurately capture the fatigue damage.

Damage is calculated at 16 equally spaced points, around the circumference of the riser pipe at each weld along the arc length of the riser, and at the outer fiber of the riser pipe; the worst damage from the 16 points is conservatively selected as the damage at that particular joint.

- Calculation of the weighted fatigue damage accumulation covering all the sea-states based on:

$$D_L = \sum_{i=1}^{N_s} D_i P_i$$

Where:

D_L = long – term fatigue damage

N_S = number of discrete sea – states in the wave scatter diagram

P_i = sea – state probability

D_i = short time fatigue damage

The weighted fatigue damage accumulation covering the 18 sea-states is then computed as the summation of the products of the worst damage and the sea-state probability, as described by the formula.

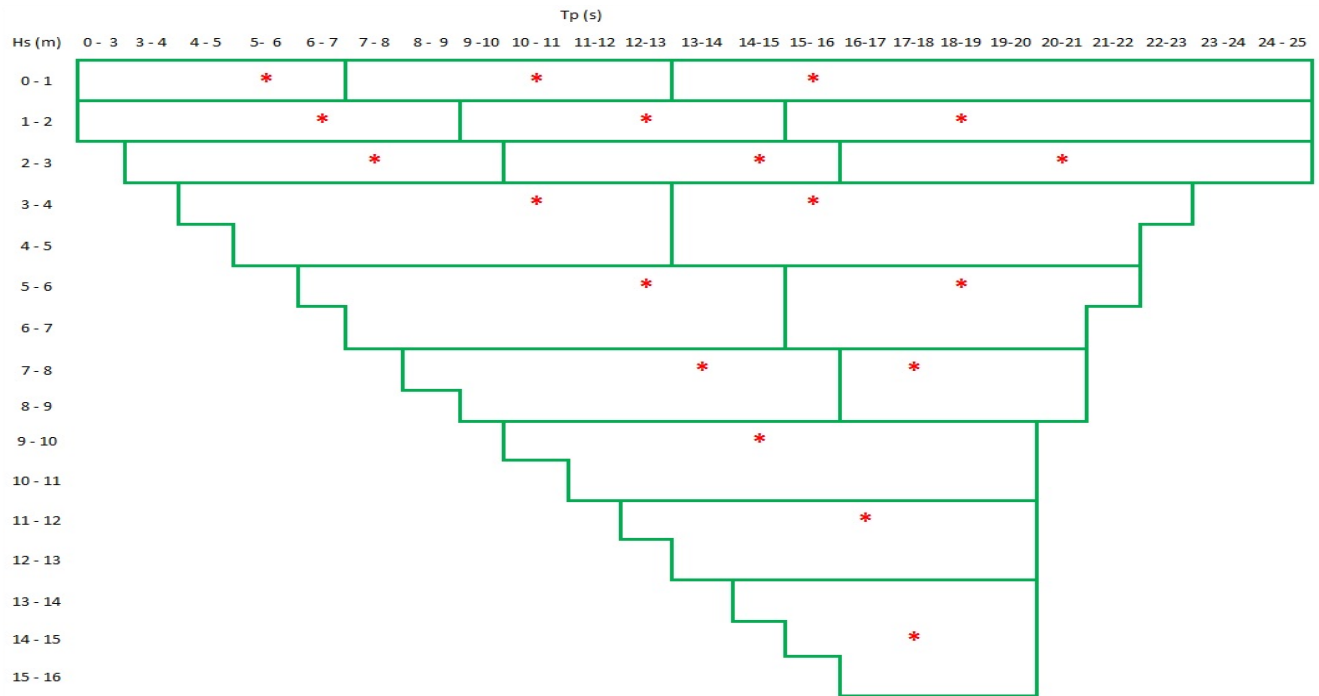


Figure 6.8 Subdivision of the sea-state scatter diagram into representative blocks

Table 6.5 Representative Sea-States and Lumped Probability of Occurrence

S/N	Sea-State			Lumped Probability (%)
	Hs (m)	Tp (m)	Gamma	
1	0.5	5.5	1.00	2.83
2	0.5	10.5	1.00	3.52
3	0.5	15.5	1.00	0.14
4	1.5	6.5	1.00	18.53
5	1.5	12.5	1.00	14.04
6	1.5	18.5	1.00	0.43
7	2.5	7.5	1.34	16.08
8	2.5	14.5	1.00	12.03
9	2.5	20.5	1.00	0.27
10	3.5	10.5	1.00	20.26
11	3.5	15.5	1.00	357
12	5.5	12.5	1.00	5.79
13	5.5	18.5	1.00	0.47
14	7.5	13.5	1.08	1.49
15	7.5	17.5	1.00	012
16	9.5	14.5	1.40	0.36
17	11.5	16.5	1.17	0.07
18	14.5	17.5	1.59	0.01
Total				100

This fatigue damage calculation procedure was repeated for all the 12 wave directions, the total long-term fatigue damage at each fatigue location was then computed using the directional probabilities that were presented in Table 5.7.

6.4.2 Discussion of the SLWR wave-induced fatigue performance

The time it takes for a point on the riser pipe to develop a crack through the wall thickness is the fatigue life at that point.

A summary of the SLWR fatigue performance for the D and C2 curves is presented in Table 6.6. The Table shows a summary of the performance at the critical riser sections. The minimum fatigue life is at the TDP. This minimum life is however well above the minimum fatigue life required as described in the acceptance criteria in section 5.7, when considering either C2 or D curve.

It should be noted that, a number of factors including FPSO offsets, different FPSO drafts, and marine growth at the TDP will contribute to the riser's TDP movement, thereby spreading the observed fatigue damage at the TDP over a wider length. The fatigue damage at the TDP as shown in Figure 6.9 is therefore conservative, as these factors are not taken into consideration.

It can also be seen from Figure 6.9 that the hog bend section, and the TDP area are the most critical to wave-induced fatigue damage, however, the performance is satisfactory in this study.

Fatigue performance at the SLWR top section has been considered for the arc length just below the section where the flex joint is supposed to occupy, as flex joint modeling is not considered in this study. The performance at the sag bend area is well above 10,000 years, this section of the SLWR is therefore of no significant concern with respect to wave-induced fatigue failure.

It is noted that the overall fatigue damage, resulting from the summation of long-term damages from each wave direction, and considering both the sea-state and directional probabilities give lower fatigue damages, compared to long-term fatigue damage per direction. This showed that fatigue damage based on single wave direction is a conservative approach. However, these results remain above the minimum required wave-induced fatigue life stipulated in the acceptance criteria.

Table 6.6 Fatigue Life in Years at Critical Locations

SLWR Location	D – Curve	C2 – Curve
Below flex joint	1255	1944
Sag bend	12206	17886
Hog bend	1234	1905
TDP	852	1297

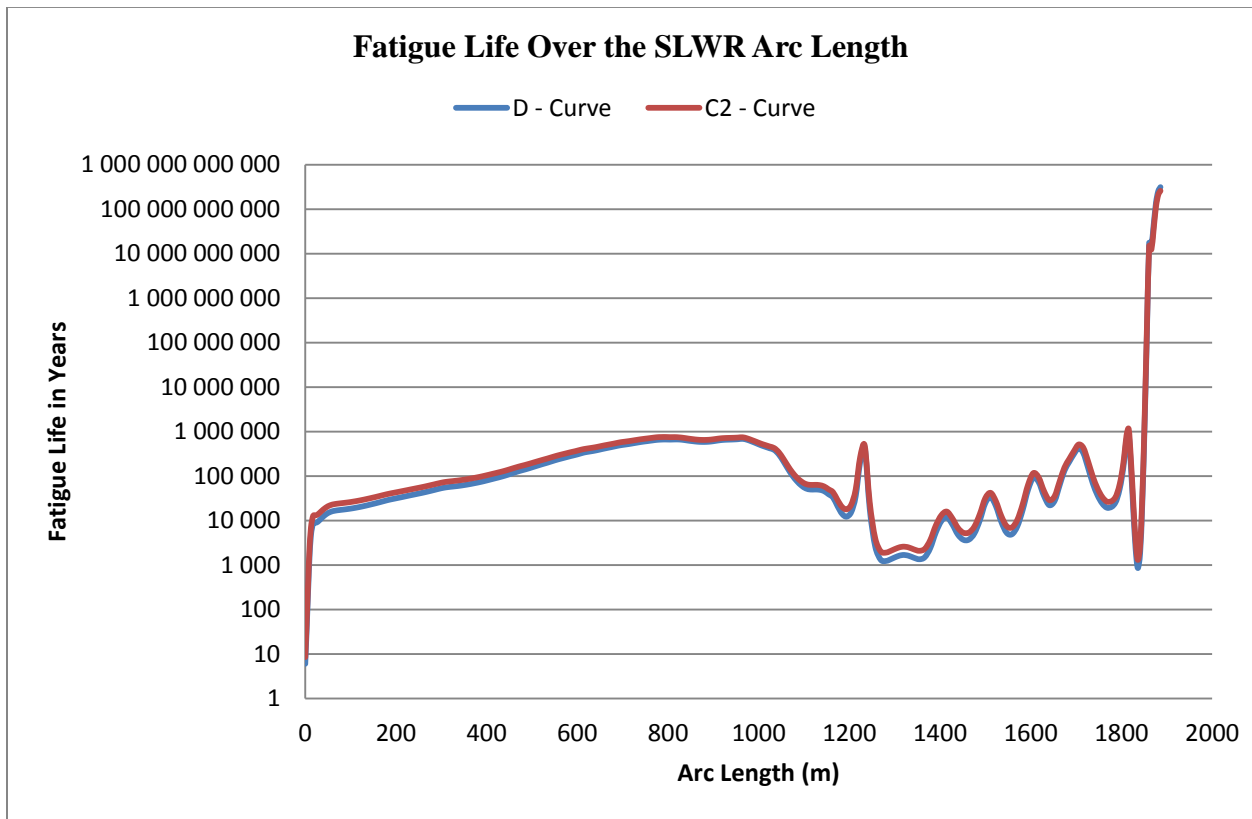


Figure 6.9 Calculated SLWR fatigue life considering mean position and one draft

Summary of the long-term fatigue damage results for the 12 wave directions is presented in Appendix C. Graphical representations of the wave-induced fatigue life along the entire riser arc length is also presented in the Appendix for each of the 12 wave directions. For each of the cases presented in the Appendix, a total exposure time of one year has been considered.

6.4.3 Vortex-Induced Vibration (VIV) Fatigue

Investigation of fatigue damage due to VIV is of importance in this study, this is due to the nature of current velocities in the WoS. In this study, consideration is given to unidirectional current profiles, acting in the SLWR main plane or perpendicular to the plane.

To perform the VIV analysis, the SLWR configuration is re-modeled in RIFLEX, the resulting static configuration is compared with the static configuration obtained in ORCAFLEX, and it was ensured that both configurations are the same, by subjecting the configuration to physical check, and by comparison of the static effective tensions.

VIV fatigue damage is then performed using VIVANA; the following is a brief description of the approach used in the VIV analysis, combining both RIFLEX and VIVANA:

- **Static analysis**

This is the first step in VIV fatigue calculation using VIVANA, the static shape of the SLWR must be determined. As mentioned above, this was done using RIFLEX, by replicating the SLWR configuration that was modeled in RIFLEX, and the mean offset position is considered.

- **Eigenvalue analysis**

The eigen-frequencies and mode shapes of the SLWR need to be determined, before fatigue damage calculations. The number of eigenvalues and eigenvectors calculated represents the total number of frequencies. At this initial stage the specified added mass for the riser is applied, this is referred to as the still water eigen-frequencies and mode shapes.

In this thesis work, up to 140 eigenvalues and eigenvectors are used to study the SLWR VIV response, this correspond to VIV response up to about 70 frequencies, to enable

consideration of all active VIV frequencies. This number of eigenvalues and eigenvectors is particularly required for the high current profiles in this study.

- **Identify dominating excitation frequencies**

From the calculated eigen-frequencies, there exists a subset of eigen-frequencies defining the complete set of active eigen-frequencies. At this stage, added mass is different from the previous value used for eigenvalue analysis, and require a number of iterations to determine the associated response frequency for each candidate frequency.

The added mass used at this stage in this thesis work ranges from -0.6 to +2.2. The maximum frequency among the active frequencies is identified by the software according to built-in criterion.

- **Response at the dominating frequency**

Using the frequency response method, the dynamic response at the identified dominating frequency above is calculated at this stage. The choice of frequency response method is suited to this process as the loads can be said to act at specific known discrete frequencies.

- **Post processing**

Once the dynamic responses are established, fatigue damage calculations can be performed.

The S-N curve method as previously defined is used in this study. D-curve and C2-curve are also considered, with SCF of 1.2.

For the VIV analysis, a total of fourteen current profiles were used. The current profiles are of varied severity with surface velocities in the range of 0.1 to 0.8 m/s. The analysis was performed for the in-plane and out-of plane unidirectional currents. The total number of load cases was therefore 28.

The current profiles probabilities of occurrence are presented in Table 6.7; these probabilities are used in determining the weighted fatigue damage contribution from each current profile.

The weighted fatigue damaged is obtained using the same formula as in wave-induced fatigue damage, where P_i represents the probability of occurrence of each current profile, and N_S is the number of current profiles considered. D_i is the fatigue damage per year for current i .

$$D_L = \sum_{i=1}^{N_S} D_i P_i$$

Taking into account the in-plane and out-of-plane currents, the total fatigue damage is obtained by using directional probabilities. A probability of 50% is assumed for the occurrence of each current direction, that is, when the riser is subjected to current profiles acting in the in-plane and out-of-plane directions to the riser.

6.4.4 Discussion of the SLWR fatigue damage due to VIV

The weighted VIV fatigue damage over the entire riser arc length, from the combination of the in-plane current profiles and the out-of-plane current profiles is presented in Figure 6.10. The riser sections that are most critical to fatigue damage due to VIV as seen from the Figure are the longest free span at the upper catenary, and the span between the buoyant section and the TDP.

The minimum fatigue lives due to VIV, when considering the C2 and D – curves are presented in Table 6.8. These minimum fatigue lives are below the allowable minimum VIV fatigue life as defined in the acceptance criteria.

The following are the general observations based on the VIV response:

- Current profiles projected in the in-plane direction to the SLWR resulted in less fatigue damage, compared to current profiles projected out-of-plane to the SLWR.
- A VIV suppression device is required to minimize the impact of VIV on the riser, since the minimum VIV fatigue life is below the specified acceptance level.

Table 6.7 Current Profile Probability of Occurrence

Current Profile No	Probability of Occurrence
1	0.1
2	0.1
3	0.1
4	0.1
5	0.1
6	0.1
7	0.1
8	0.1
9	0.1
10	0.02
11	0.02
12	0.02
13	0.02
14	0.02
Total	1

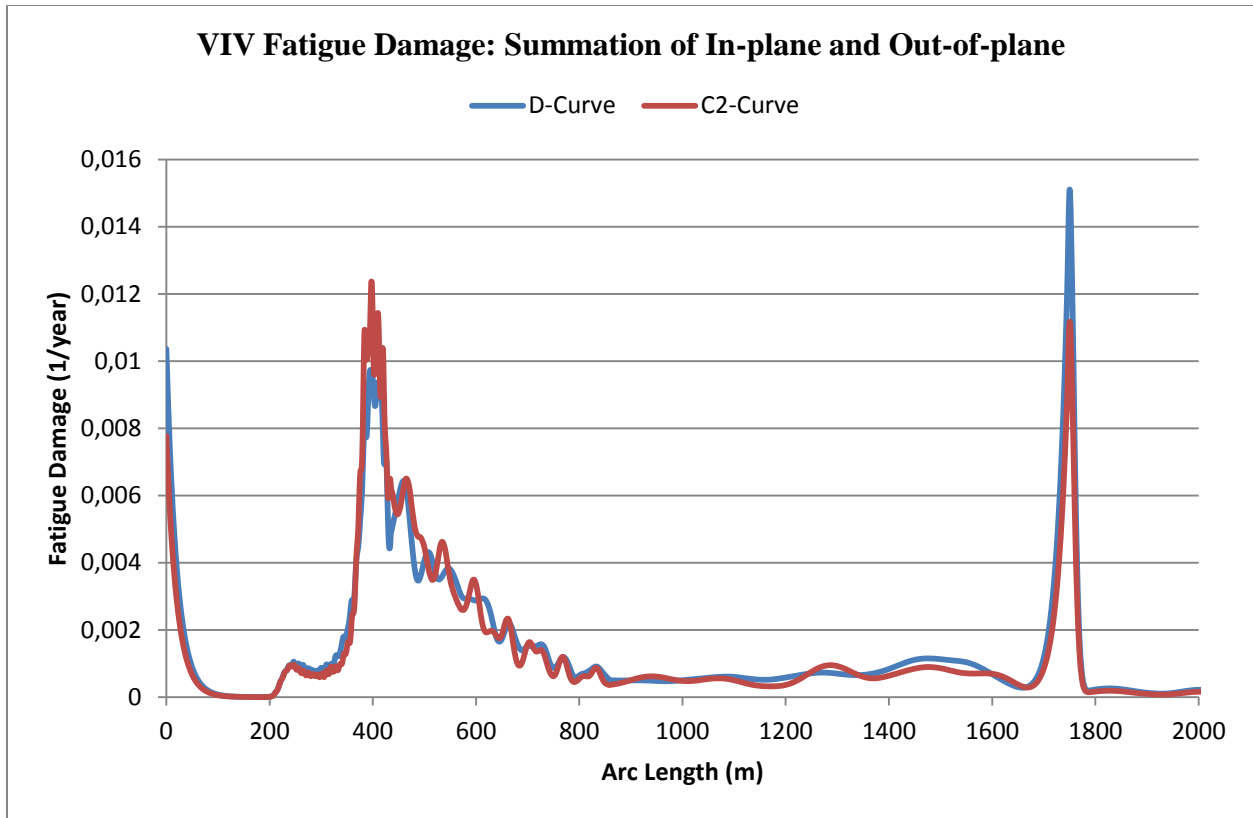


Figure 6.10 VIV fatigue damage resulting from combination of in-plane and out-of-plane currents

Table 6.8 Minimum VIV Fatigue Life in Years

SLWR Location	Fatigue Life in Years
D – curve	66
C2 – curve	81

The following are the locations along the arc length of the SLWR with fatigue lives below 500 years:

- Top riser section: between arc length 0 – 25 meters
- Upper catenary mid-section: between arc lengths 352 – 671 meters
- Lower catenary: between arc lengths 1710 - 1765

However, the total length of VIV suppression devices can only be determined by performing further works, this part of the study is not considered in this thesis work.

Fairings and helical strakes are commonly used VIV suppression devices; they can be used in combination or individually to reduce VIV impacts on the SLWR, they act to disrupt flow pattern in the vicinity of the riser.

Fairings are more efficient in the vertical or near-vertical riser configuration, and can therefore be used at the riser top section of the SLWR. Their design allows them to rotate such that they align with currents, thereby suppressing vortex shedding.

Helical strakes are widely used for VIV suppression. They are simple, effective, and efficient. In addition, helical strakes installation presents little changes. Due to their bluff body, they can provide early disruption of incoming flow pattern. However, this option increases riser's drag coefficient, and care should be taken to avoid excessive use, as this may have both design and cost implications.

Graphical representation of the raw VIV fatigue damage resulting from each current profile for both in-plane and out-of-plane VIV response calculations are presented in Appendix C.

CHAPTER 7 SLWR SENSITIVITY STUDIES

7.1 Introduction

In this chapter, sensitivity analysis is carried out to understand the SLWR behavior when changes are made to critical sections of the riser configuration, when different hang-off angles are used, and how net buoyancy used affects the riser integrity in extreme sea-states.

The different cases considered are as described in section 5.6. The parameter variation is selected to cover sufficient range, to ensure that a good understanding and clear judgment can be derived on how the SLWR configuration and behavior in extreme sea-states are influenced by these parameters. This knowledge can be used for further optimization as necessary.

The extreme sea-state combination of 100-year wave and 10-year current is considered in the sensitivity studies, since this combination give the worse response as seen in section 6.3.3.

A summary of the results representing the worst response is presented in the various sub-sections, while detailed results are presented in Appendix D.

7.2 Net Buoyancy Sensitivity Study

During the preliminary static configuration of the SLWR, it was observed that the net buoyancy or the amount of buoyancy elements used has direct influence on the static configuration and on the SLWR response in extreme sea-states. A parametric study is therefore carried out to understand how variation in net buoyancy affects the SLWR from turret moored FPSO.

The net buoyancies per meter considered in this sensitivity study are presented in Table 7.1; the difference in value considered is 100 N/m.

The following configuration parameters were considered for each of the four cases:

- Hang-off angle of 8 degrees in all cases
- Upper section length is 1239 m in all cases
- Buoyant section length is 420 m in all the cases
- Lower section length is 441 m in all cases

Table 7.1 Net Buoyancy Sensitivity Parameter

Net Buoyancy (N/m)				
500	600	700	800	900

The resulting static configurations for the five cases are as shown in Figure 7.1, for mean FPSO offset position. Subsequently, dynamic analysis was performed to determine how the SLWR integrity is influenced by a variation of the net buoyancy. The analysis was performed for the mean, near, and far offset positions for ULS and ALS design.

7.2.1 Net buoyancy sensitivity – static results

From the static configurations in Figure 7.1, it can be seen that an increase in net buoyancy force, while keeping constant the original riser section lengths, will result in slightly different riser configurations compared to the base case.

The following are the main differences in these configurations:

- Increase in sag bend height from the seabed for higher net buoyancy, and a sag bend height approaching seabed for lower net buoyancy.
- Increase in height between sag and hog bend for higher net buoyancy, and a decrease for lower net buoyancy.
- Horizontal distance to TDP is slightly shorter for decrease in net buoyancy, and slightly longer for higher net buoyancy.

From the configurations, it can be seen that the risk of a clash between the sag bend and the seabed when the riser is flooded with water, is increasing as the net buoyancy is reducing. To avoid such a situation, an adequate net buoyancy force should be used, following similar sensitivity studies, and detailed extreme response analysis.

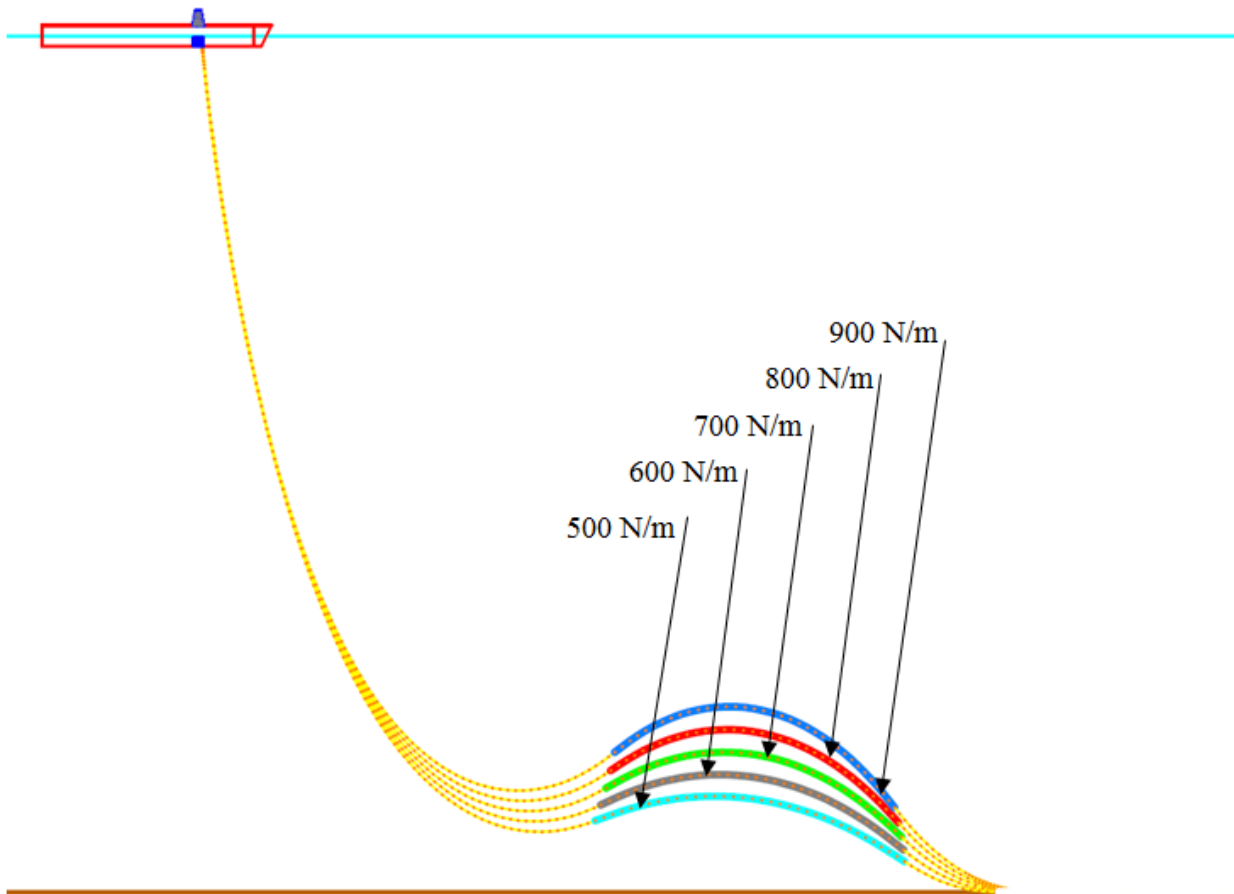


Figure 7.1 Static configuration: different net buoyancies – mean FPSO position

A summary of the static analysis results for the four cases and the base case is presented in Table 7.2; the following are the main observation from these results:

- Increase in net buoyancy generally results in decrease in top tension and vice-versa.
- The maximum static stress increases slightly with increase in net buoyancy, the maximum value is at the sag bend in all the five cases.
- The maximum static utilization increases slightly when increasing the net buoyancy.

Table 7.2 Net Buoyancy Sensitivity – Summary Static Results

	Net Buoyancy (N/m)				
	500	600	700	800	900
Max. Effective Top Tension (kN)	1258	1241	1224	1207	1190
Max. Bending Moment (kN.m)	267	271	275	280	283
Max. von Mises Stress (MPa)	247	250	251	253	254
Max. DNV Utilization (LRFD)	0.50	0.51	0.52	0.53	0.53

7.2.2 Dynamic response (ULS) – net buoyancy sensitivity

A summary of the dynamic behavior at the SLWR critical sections, that is, sag bend, hog bend, and the TDP is presented in Table 7.3 for ULS design.

The observed differences in the SLWR dynamic response, for the different net buoyancies can be summarized are as follow:

- In all cases, maximum effective tension and compression are observed when the FPSO and SLWR system is in the far offset position.
- The maximum effective top tension decreases as the net buoyancy force increases.
- The observed residual compression reduces when increasing net buoyancy; this showed that compression can be eliminated by increasing the net buoyancy of the SLWR; however, this translates to higher project costs, and is therefore not a recommended option, except if the integrity of the riser is considered unsafe. The maximum compression is at the SLWR sag bend, in all the cases considered.
- The maximum stress occurs in the near offset position. The maximum von Mises stress is observed at the sag bend in all cases except when the net buoyancy is 500 N/m. For this case, the maximum von Mises is at the TDP. A graphical representation of the changes in maximum von Mises stress is shown in Figure 7.2.

Table 7.3 Net Buoyancy Sensitivity – Summary Dynamic Response (ULS)

	Net Buoyancy (N/m)				
	500	600	700	800	900
Sag Bend					
Max. Effective Tension (kN)	967	782	658	575	521
Max. Compression (kN)	182	126	86	62	48
Max. Bending Moment (kN.m)	449	435	425	414	403
Max von Mises (MPa)	349	342	335	328	322
Max. DNV Utilization (LRFD)	0.81	0.78	0.77	0.75	0.73
Hog Bend					
Max. Effective Tension (kN)	942	736	594	497	431
Max. Compression (kN)	151	87	36	-	-
Max. Bending Moment (kN.m)	387	343	315	336	368
Max von Mises (MPa)	305	279	272	277	297
Max. DNV Utilization (LRFD)	0.85	0.74	0.67	0.64	0.68
TDP					
Max. Effective Tension (kN)	941	727	576	474	399
Max. Compression (kN)	59	-	-	-	-
Max. Bending Moment (kN.m)	467	423	400	384	377
Max von Mises (MPa)	357	329	314	305	300
Max. DNV Utilization (LRFD)	0.86	0.78	0.73	0.71	0.69

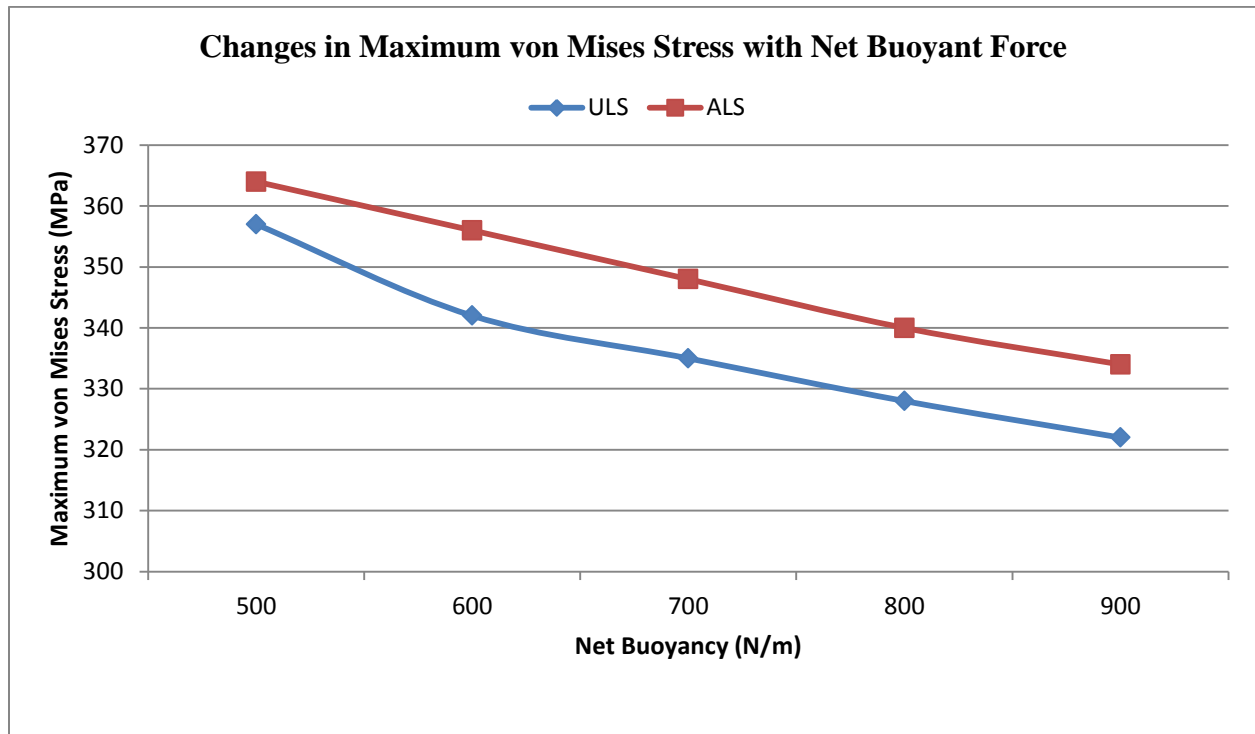


Figure 7.2 Maximum von Mises stresses for different net buoyancies

- The maximum von Mises stress reduces as the net buoyancy increases. The decrease is more significant at the TDP area; this shows that the decoupling efficiency of the lazy wave configuration increases as the net buoyancy increases.
- The maximum utilization is below unity in all the cases considered, this showed that, each of the configuration is a safe design for the extreme sea-state considered.

7.2.3 Net buoyancy sensitivity – comparison of sag, hog, and TDP

A comparison of the SLWR behavior at the critical sections, for the four cases showed similar behavior compared to the base case. For instance, the maximum stress and utilization at the sag bend and TDP occurred in the near offset position.

However, at the hog bend, the following trends were observed:

- Maximum stress and utilization occurred in the near offset position for net buoyancy

greater than or equal to 800 N/m.

- For net buoyancy less than or equal to 700 N/m, the maximum stress and utilization in this section is found in the far offset position.
- As stresses at the sag bend and TDP is reduced when increasing net buoyancy, the stress at the hog bend increase, particular in the near offset position. A plot of the maximum von Mises stresses along the SLWR arc length for the near offset position is presented in Figure 7.3.

From the dynamic analyses results, it can be summarized that the SLWR decoupling efficiency increases when the net buoyancy force is increased. However, since cost is one of the main drivers in selecting riser concept, and since buoyancy modules add costs to SLWR concept, it is sufficient to have a configuration that satisfies the design criteria with a margin.

7.3 Sensitivity Study on Height of Sag Bend above Seabed

The height of the sag bend above the seabed is primarily dependent on the SLWR upper section length, and the net buoyancy force. From section 7.2 it was seen that for the same SLWR upper section length, the height of the sag bend above the seabed changes when varying only the net buoyancy force.

The objective in this section is to study the SLWR extreme response behavior, considering a number similar configuration, however, with different sag bend heights above the seabed. The following are the main configuration parameters for the study:

- Hang-off angle of 8 degrees in all cases
- Net buoyancy force of 700 N/m in all cases
- Varied upper section length, to achieve the desired sag bend height
- Buoyant section length is 420 m in all the cases
- Lower section length is 441 m in all cases

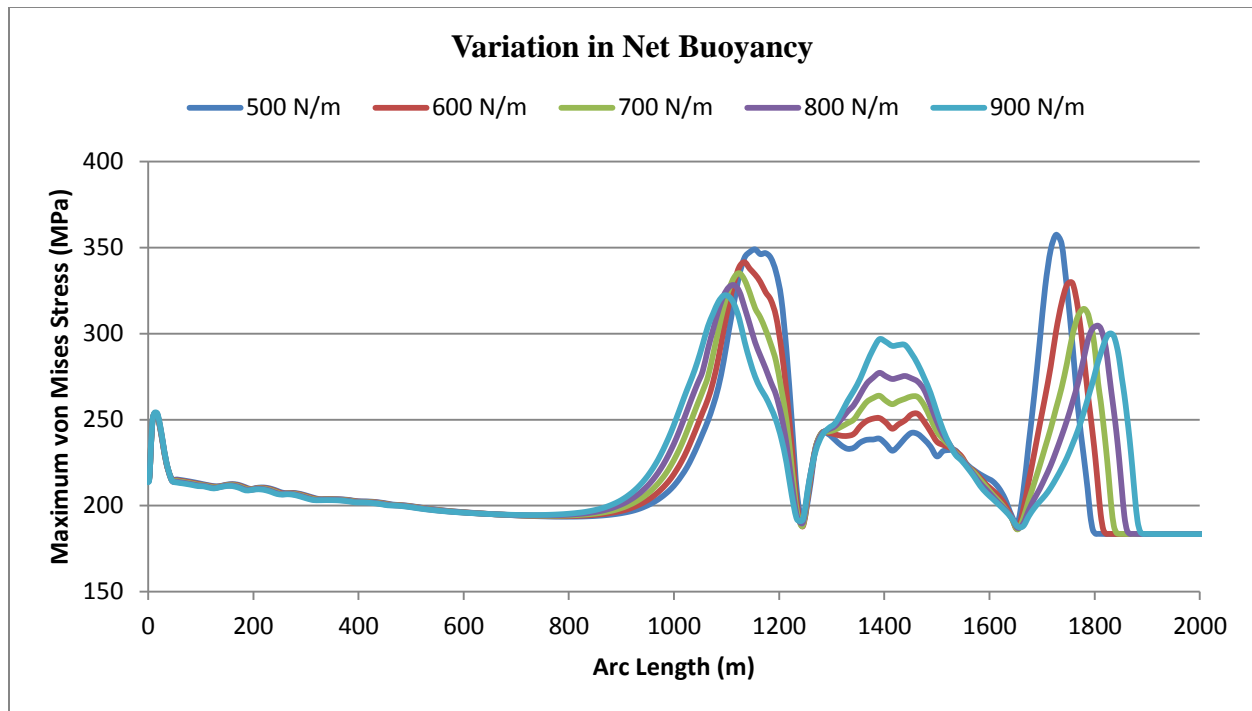


Figure 7.3 von Mises stresses for different net buoyancies – near offset position

One of the justifications for this sensitivity study is that the SLWR design is sometimes limited by top tension at the connection point, corresponding to the FPSO payload. Increasing the sag bend height, while keeping other parameters constant, translates to using less riser pipe at the upper section, and also affects the total riser payload.

Three cases are selected for the study; considering differences of 100 meters from case to case, they are presented in Table 7.4, also shown in the Table is the SLWR upper section lengths that resulted in the sag bend heights.

7.3.1 Height of sag bend sensitivity– static results

The static analysis was carried out using the same approach as in the base case, that is, environmental actions were not considered. The static configurations are as shown in Figure 7.4.

The following are observed from the configurations:

- The SLWR wave zone and TDP are closer to the hang-off location as the sag bend height increases.

Table 7.4 Height of Sag Bend above Seabed – Sensitivity Parameter

SLWR Upper Section Length (m)	Height Above Seabed (m)
1239	100
1100	200
950	300
820	400

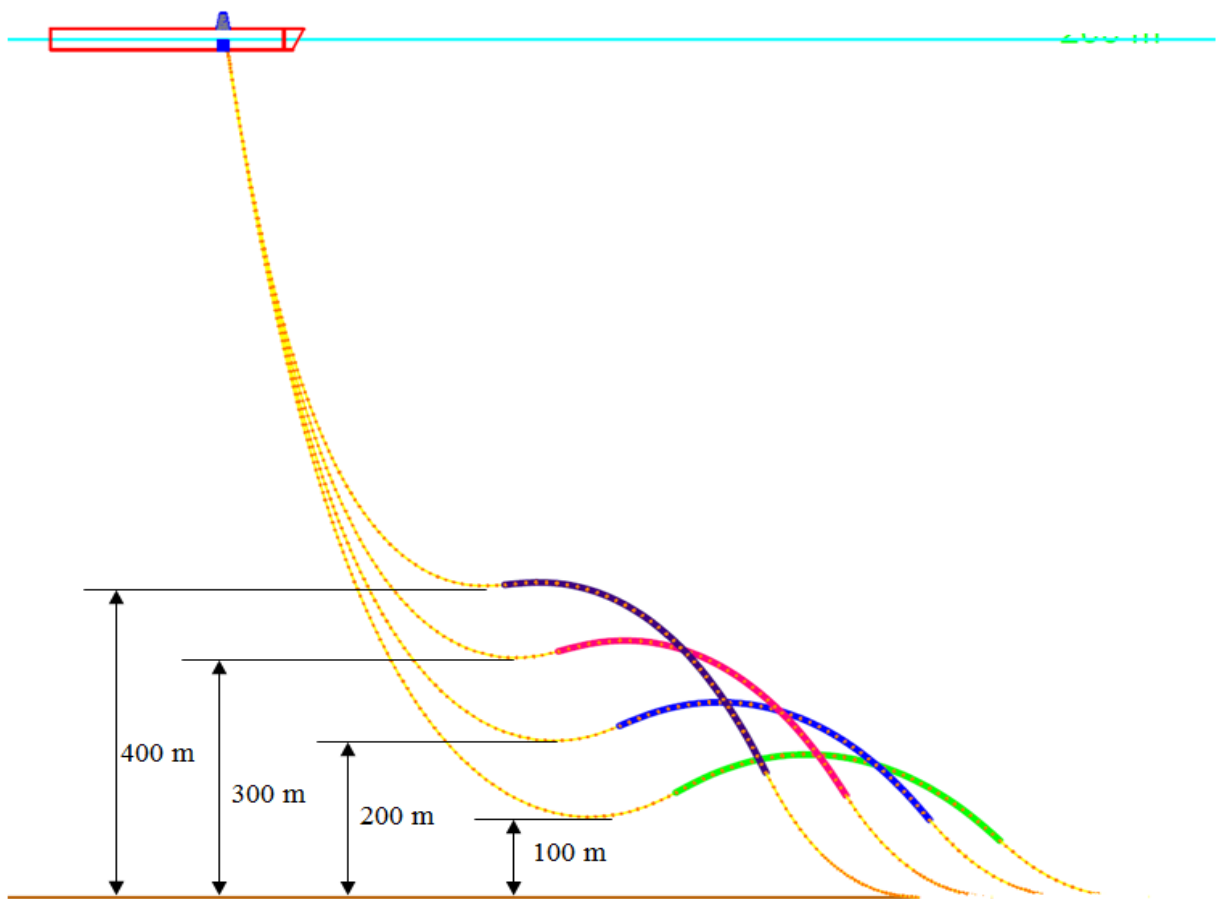


Figure 7.4 Static configuration: different sag bend heights – mean FPSO position

- The sag and hog bends are closer; both vertically and horizontally, when increasing the sag bend height, keeping net buoyancy and other parameters constant.

The static analysis results are summarized in Table 7.5, from the results, the following are observed:

- The effective tension at the top of the SLWR reduces with increase in sag bend height. This shows that as the sag bend height increases, the riser payload reduces.
- The SLWR static stress and utilization increase with increase in sag bend height from the seabed.

The advantage here is that, where the SLWR design is limited by the top tension at the connection point to the turret moored FPSO, increasing the sag bend height above the seabed may provide a viable solution.

However, excessive static stresses are to be avoided, especially in harsh environments, where environmental actions on the SLWR may be significant. Since all the configurations satisfy the LRFD design criteria, their integrity is therefore checked by performing dynamic analysis.

7.3.2 Dynamic response (ULS) – height of sag bend sensitivity

The dynamic analysis is performed for the intact and accidental mooring conditions. A summary of the dynamic response is presented in Table 7.6 for ULS design. The results represent the worst response when considering the near and far offset positions.

The following are the general observations from the dynamic analysis results:

- The maximum effective top tension occur in the far offset position, and decreases as the sag bend height increases when going from 100 to 300 meters.
- An increase in top tension is observed when the sag bend height is set to 400 meters. The increase is more significant in the accidental condition, and for far offset position. The variation in maximum effective top tension is presented in Figure 7.5.

Table 7.5 Height of Sag Bend above Seabed – Summary Static Results

	Height of Sag Bend Above Seabed (m)			
	100	200	300	400
Max. Effective Tension (kN)	1224	1103	971	856
Max. Bending Moment (kN.m)	275	302	332	348
Max von Mises (MPa)	251	263	276	284
Max. DNV Utilization (LRFD)	0.52	0.57	0.62	0.64

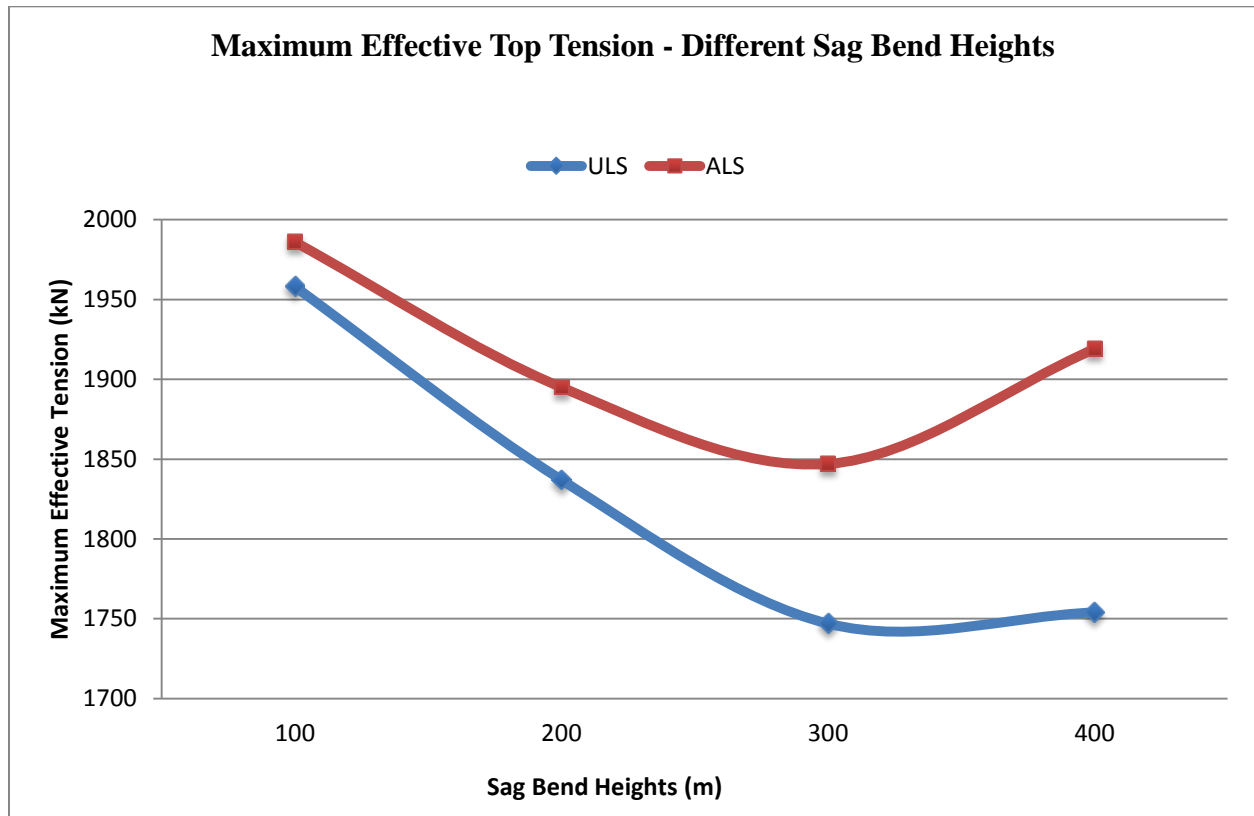


Figure 7.5 Maximum effective top tensions for different sag bend heights

Table 7.6 Height of Sag Bend above Seabed – Summary Dynamic Response (ULS)

	Height of Sag Bend Above Seabed			
	(m)			
	100	200	300	400
Sag Bend				
Max. Effective Tension (kN)	658	692	776	939
Max. Compression (kN)	86	115	163	218
Max. Bending Moment (kN.m)	425	479	561	650
Max von Mises (MPa)	335	370	422	480
Max. DNV Utilization (LRFD)	0.77	0.85	0.98	1.12
Hog Bend				
Max. Effective Tension (kN)	594	614	701	859
Max. Compression (kN)	36	92	150	209
Max. Bending Moment (kN.m)	315	392	476	564
Max von Mises (MPa)	272	308	362	422
Max. DNV Utilization (LRFD)	0.67	0.79	0.93	1.1
TDP				
Max. Effective Tension (kN)	576	570	617	729
Max. Compression (kN)	-	-	-	-
Max. Bending Moment (kN.m)	400	428	481	539
Max von Mises (MPa)	314	332	366	404
Max. DNV Utilization (LRFD)	0.73	0.77	0.85	0.94

- Residual compression in the sag and hog bends is more significant for higher sag bend heights, as seen from Table 7.6, and the maximum compression is at the SLWR sag bend, in all the cases considered.
- The maximum von Mises stress increases as the height of sag bend is increasing; also the contribution from environmental loads is more significant as the sag bend height increases. Changes in the maximum von Mises stress with increasing sag bend heights is as shown in Figure 7.6.
- The maximum stress is above the allowable stress when the sag bend height is set to 200 meters and above. For the 200 meters case, this is observed only at the sag bend, while for 300 meters and above, the maximum stress is above the allowable at all the critical sections.
- The maximum utilization for all the cases considered except one, is below unity. When the sag bend height is set to 400 meters, the DNV utilization is above unity, this is therefore an unsafe design.

It can be summarized from these observations that the SLWR payload decreases as the sag bend height increases, but to a limit. However, the maximum stress and utilization increase as the sag bend height increases. Therefore the decoupling efficiency reduces as the sag bend height increases.

7.4 Buoyant Section Length Sensitivity Study

The following have been established from the sensitivity analyses in sections 7.2 and 7.3:

- For the same configuration, increasing the net buoyancy provides better decoupling at the TDP, and improves extreme response at the critical sections of the SLWR.
- For the same configuration, but with different upper section length, therefore different height of sag bend; the closer the sag bend height to the seabed, the better the decoupling efficiency, and therefore improved extreme response.

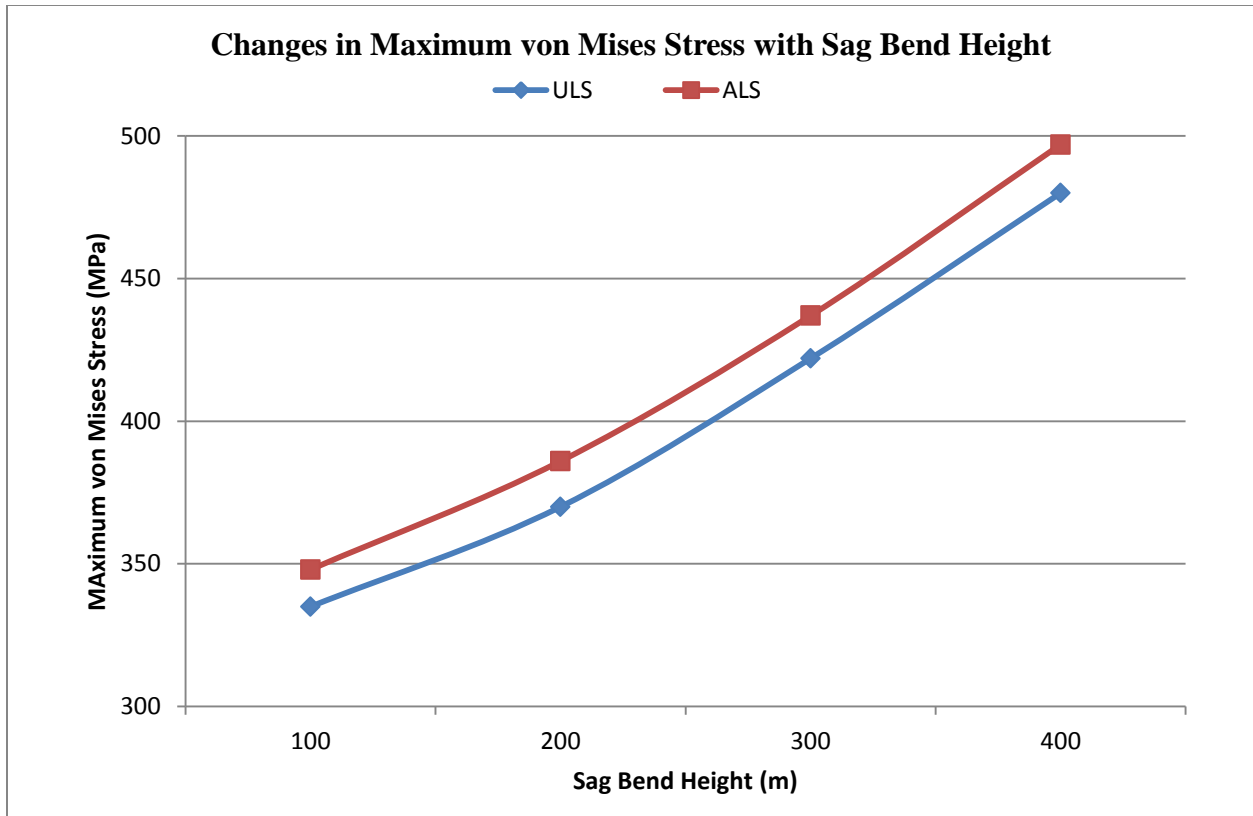


Figure 7.6 Maximum von Mises stress for different sag bend heights

In this section, further sensitivity study is performed by combining the knowledge from the previous two case studies, taking the following into consideration:

- Hang-off angle of 8 degrees
- Net buoyancy force of 700 N/m
- Fixed sag bend height of 100 m in all cases
- Varied the buoyant section length
- Varied upper section length
- Varied lower section length

The various buoyant section lengths that are considered represent an equivalent number of buoyancy modules, which are equally spaced at 12 meters interval. Changes in the buoyant section length also require changes to the SLWR upper and lower section lengths, to achieve the same sag bend height above the seabed.

The buoyant section lengths considered in this study are presented in Table 7.7, alongside with upper and lower section lengths for each configuration. The resulting static configuration for the four cases and the base case is as shown in Figure 7.7, for mean FPSO offset position.

The overall objective of this sensitivity study is to understand the SLWR response in extreme sea-states, for a riser with the same payload, but different buoyant section lengths.

7.4.1 Buoyant section length sensitivity - static results

The static analysis was performed taking into consideration only the functional loads. The following are observed from the static configuration:

- Longer buoyant section lengths give configurations with higher hog bend.
- The TDP is farther away from the connection point, since the length of the riser is longer, and the same hang-off angle is used.

A summary of the static analysis results is presented in Table 7.8. The results give an indication of how the sag bend height influences the static stresses, notwithstanding the difference in buoyant section lengths, and the total riser length.

The observed static analysis response can be summarized as follows:

- The effective top tension is the same for each configuration; this is expected as the sag bend height determines the riser payload.
- The maximum von Mises stress is at the sag bend for each configuration, and the value is approximately the same for all the cases considered.
- The maximum utilization is also equal for all the cases considered.

Table 7.7 Buoyant Section Length Sensitivity Parameter

Sag Bend Height = 100 m		
Upper Section Length (m)	Lower Section Length (m)	Buoyant Section Length (m)
1214	406	360
1232	424	396
1239	441	420
1246	458	444
1259	481	480

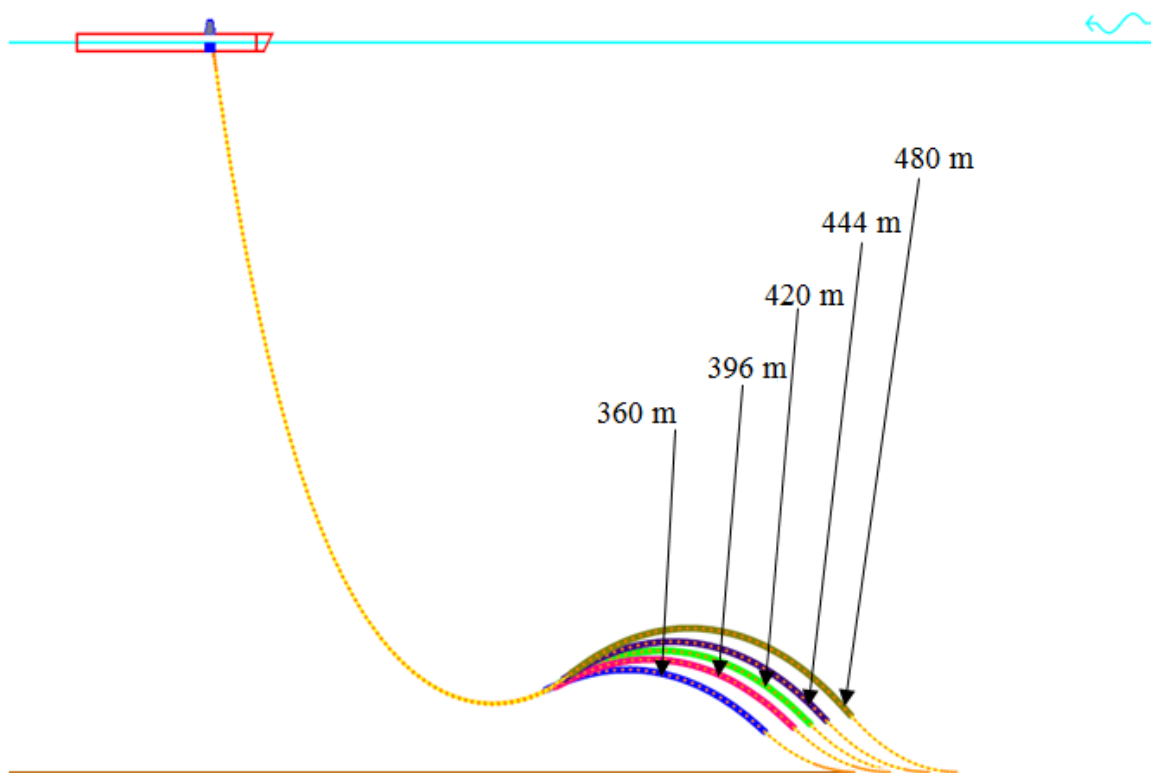
**Figure 7.7** Static configuration: different buoyant section length – mean FPSO position

Table 7.8 Buoyant Section Length Sensitivity – Summary Static Results

	Buoyant Section Length (m)				
	360	396	420	444	480
Max. Effective Tension (kN)	1222	1226	1224	1222	1222
Max. Bending Moment (kN.m)	275	275	275	276	276
Max von Mises (MPa)	251	251	251	251	251
Max. DNV Utilization (LRFD)	0.52	0.52	0.52	0.52	0.52

These observations further establish that for the same sag bend height, the SLWR payload remain the same, and that the riser top tension is a function of the depth of the sag bend.

The results also show that for the same sag bend height, maximum static stresses remain the same, even when increasing the buoyant section length. The behavior at the hog bend and TDP are also similar in all five cases.

7.4.2 Dynamic response (ULS) – buoyant section length sensitivity

Dynamic analyses was performed for both ULS and ALS design, to check the integrity of each of the configurations, and how their behaviors are affected by varying the buoyant section lengths.

Since each of the four configurations give static responses similar to the base case, it will be interesting to see how they behave when subjected to environmental actions from waves and current. A summary of the dynamic responses in extreme sea-state is presented in Table 7.9 for ULS design. The worst response from the far or near position is presented.

The following are the general observations from the extreme response behavior:

- The maximum effective top tension remains approximately the same for all the cases, when in the mean offset position, even in the extreme sea-state.

Table 7.9 Buoyant Section Length Sensitivity – Summary Dynamic Response (ULS)

	Buoyant Section Length (m)				
	360	396	420	444	480
Sag Bend					
Max. Effective Tension (kN)	808	716	658	627	582
Max. Compression (kN)	123	97	86	78	70
Max. Bending Moment (kN.m)	450	433	425	415	401
Max von Mises (MPa)	351	340	335	329	320
Max. DNV Utilization (LRFD)	0.80	0.78	0.77	0.75	0.73
Hog Bend					
Max. Effective Tension (kN)	766	650	594	545	486
Max. Compression (kN)	104	68	36	34	13
Max. Bending Moment (kN.m)	405	355	315	313	292
Max von Mises (MPa)	315	284	272	264	257
Max. DNV Utilization (LRFD)	0.81	0.72	0.67	0.65	0.57
TDP					
Max. Effective Tension (kN)	759	632	576	508	436
Max. Compression (kN)	-	-	-	-	-
Max. Bending Moment (kN.m)	426	412	400	390	379
Max von Mises (MPa)	331	322	314	308	301
Max. DNV Utilization (LRFD)	0.77	0.75	0.73	0.72	0.70

- The maximum effective top tension decreases as the buoyant section length increases, when in the far offset position. This shows that there is more contribution to the effective top tension from the environmental actions when the buoyant section length is shorter. The effective top is as shown in Figure 7.8, for both ULS and ALS design.
- Residual compression is observed at the sag and hog bends in all the cases considered. However, the compression becomes smaller when increasing the buoyant section length. This behavior is similar to what is observed in section 7.2, net buoyancy sensitivity, and this later approach appears more efficient.
- The maximum von Mises stress generally reduces as the buoyant section length is increasing. An overview of the changes in the maximum von Mises stress with increasing buoyant section lengths is as shown in Figure 7.9. The maximum stress is below the allowable stress for all the cases considered.
- The maximum utilization for all the cases considered is below unity, therefore each of the four configurations is considered as safe design, considering extreme response from the sea state under consideration.

In summary, an increase or decrease in buoyant section length of the SLWR, for a configuration with constant sag bend height, has no significant influence on the static behavior. Residual compression under dynamic loadings can be eliminated by increasing the buoyant section length.

Also, under environmental loadings, the decoupling efficiency of the SLWR increases as the buoyant section length increases.

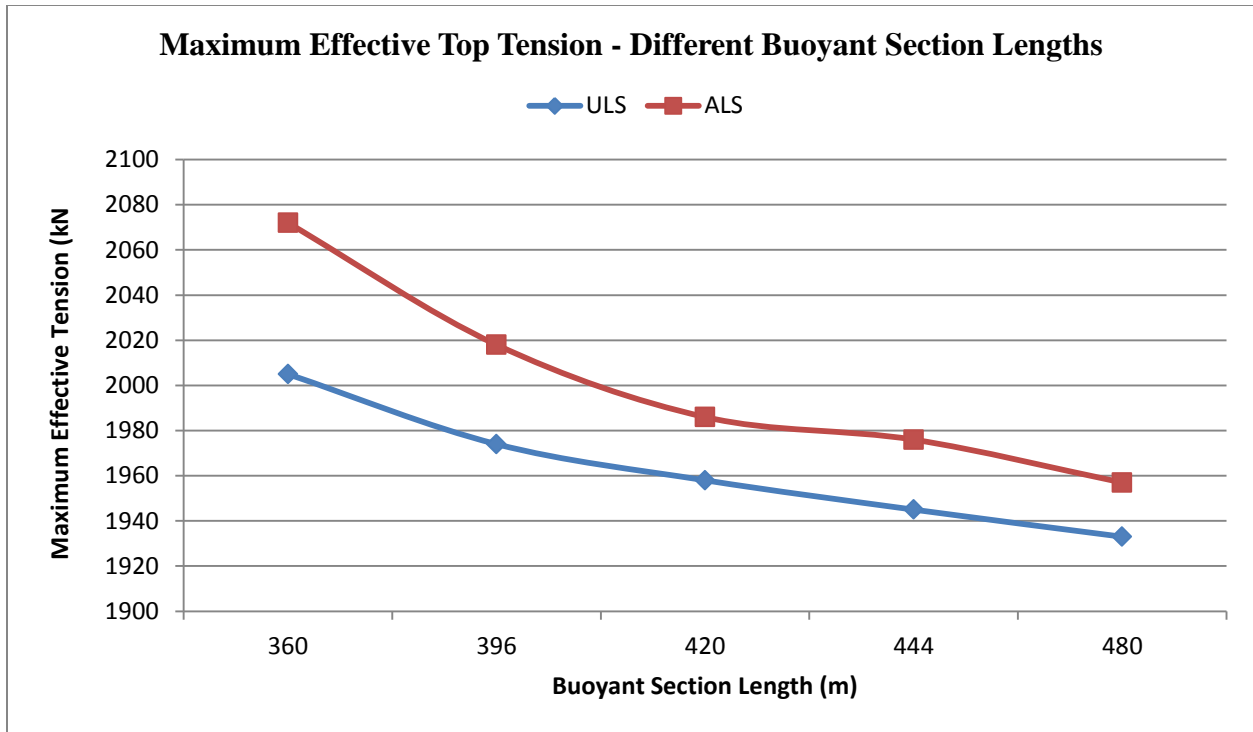


Figure 7.8 Maximum effective top tension for different buoyant section lengths

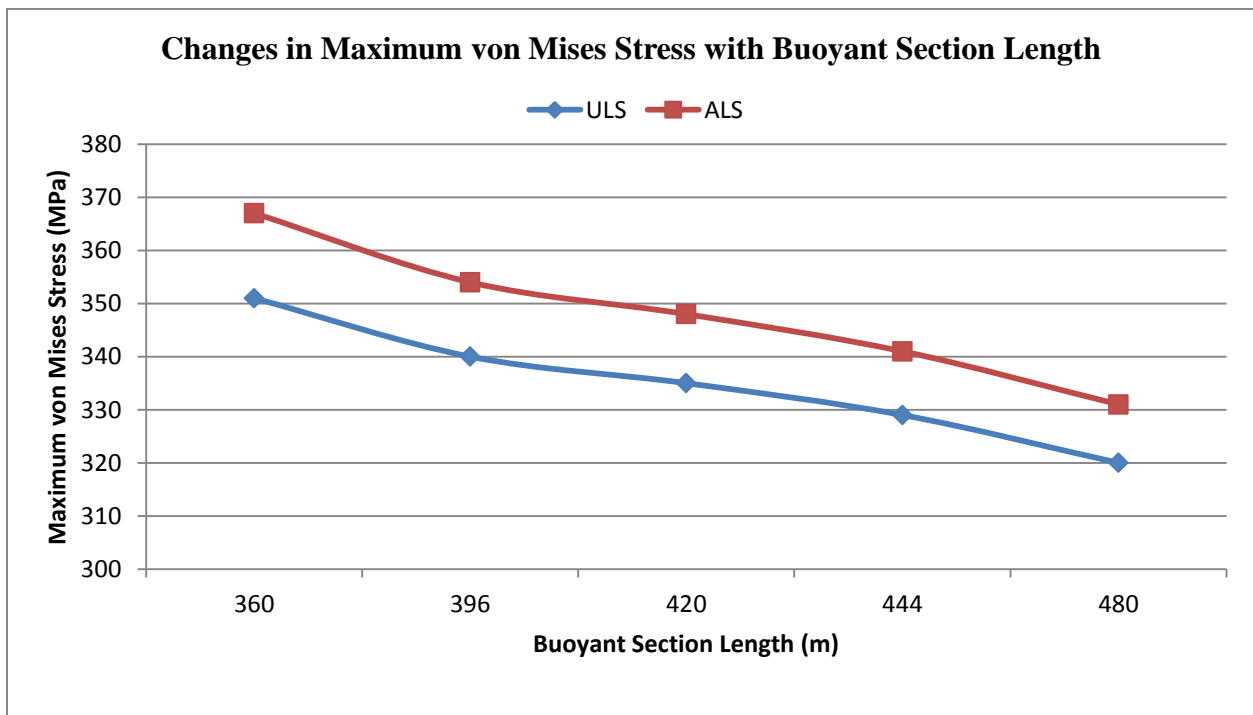


Figure 7.9 Maximum von Mises stresses for different buoyant section lengths





7.5 Sensitivity on Hang-off Angle

It was established in section 7.3 that a configuration with sag bend height closer to the seabed, will in general provide better decoupling efficiency, and therefore give better extreme response behavior under the harsh environmental conditions being considered.

It was also established in section 7.4 that a wider spread of the buoyant section length, provides better decoupling efficiency at the TDP, and therefore an improved extreme response.

This knowledge is combined in this section to study the SLWR extreme response for different hang-off angles. To study this behavior, four hang-off angles are considered, and compared to the base case hang-off angle.

The hang-off angle sensitivity study is performed by observing the following:

- Fixed sag bend height of 100 m
- Fixed net buoyancy per unit length of 700 N/m
- Fixed buoyant section length of 420 m in all the cases
- Varied upper section length
- Varied lower section length
- Hang-off angle is varied, in addition to the base case angle, the following angles are considered:
 -  6 degrees
 -  7 degrees
 -  9 degrees
 -  10 degrees

The resulting static configurations for all the cases are presented in Figure 7.10, for mean offset position.

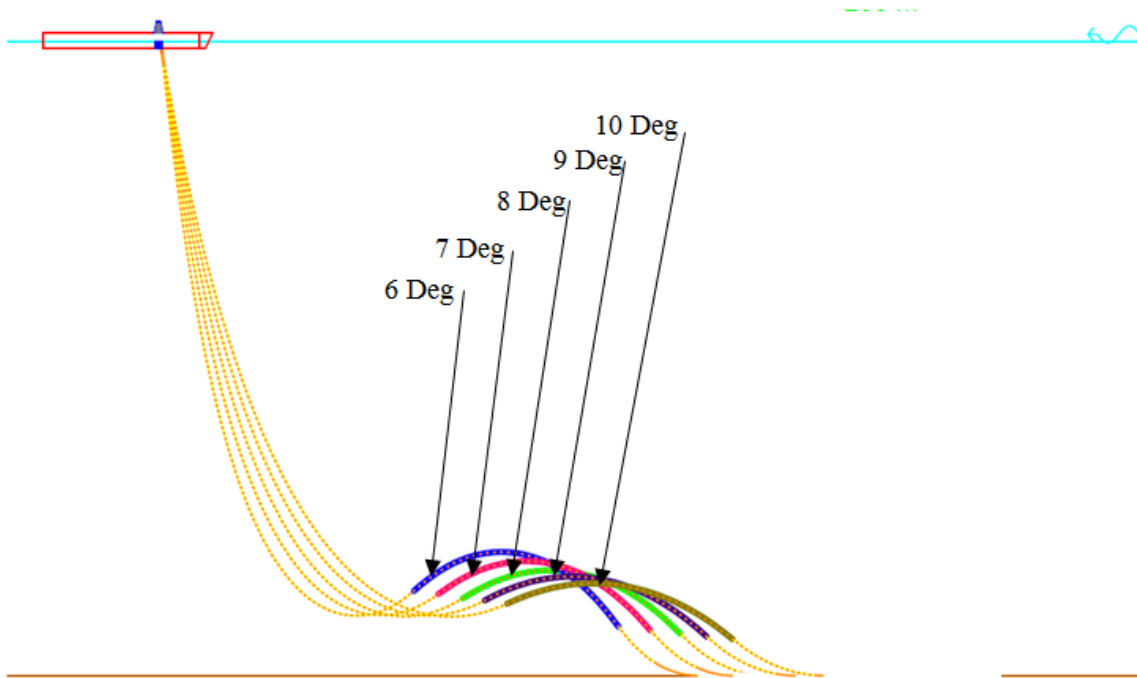


Figure 7.10 Static configuration: different hang-off angles – mean FPSO position

7.5.1 Hang-off angle sensitivity - static results

Considering only functional loads, the following are observed from static analysis:

- As the top angle increases, the wave zone become longer
- The height between the sag bend and the hog bend become smaller
- The TDP is further away from the connection point on the FPSO

A summary of the static analysis results is presented in Table 7.10, for mean FPSO offset position, when considering only functional loads. The following are observed from the results:

- Top tension increases as the hang-off angle increases
- The static stresses become smaller as the hang-off angle become bigger
- The LFRD utilization also become smaller as the hang-off angle become bigger

Table 7.10 Hang-off Angle Sensitivity – Static Analysis Results

	Hang-off Angles (Degrees)				
	6	7	8	9	10
Max. Effective Tension (kN)	1176	1197	1224	1247	1275
Max. Bending Moment (kN.m)	372	318	275	242	214
Max von Mises (MPa)	298	268	251	239	230
Max. DNV Utilization (LRFD)	0.68	0.60	0.52	0.48	0.44

From the static analysis, it can be said that where excessive static stresses are of serious concern, an increase in hang-off angle, could be a viable solution, provided this is provided for on the FPSO.

7.5.2 Dynamic response (ULS) – hang-off angle sensitivity

The dynamic response analysis is performed for both ULS and ALS design. From the results, it can be summarized that the SLWR dynamic response is better for a configuration with the same sag bend height and larger hang-off angle. A summary of the results is presented in Table 7.11, for ULS design.

The worst responses at each of the critical sections are presented in the Table, from the results, we can summary the strength response of the SLWR when increasing hang-off angle as follows:

- The maximum effective top tension increases as the hang-off angle is increasing, the changes in maximum effective top tension as hang-off angle is increasing is presented in Figure 7.11, for the far offset position.
- Residual compression is observed at the sag and hog bends in all the cases considered. The observed compression increases as the hang-off angle is increasing.
- The maximum von Mises stress generally reduces as the hang-off angle is increasing. Figure 7.12 gives an overview of how the maximum von Mises stress changes with increasing hang-off angle.

Table 7.11 Hang-off Angle Sensitivity – Summary Dynamic Response (ULS)

	Hang-off Angle (Degrees)				
	6	7	8	9	10
Sag Bend					
Max. Effective Tension (kN)	435	541	658	816	983
Max. Compression (kN)	64	72	86	95	111
Max. Bending Moment (kN.m)	534	475	425	386	351
Max von Mises (MPa)	405	367	335	311	289
Max. DNV Utilization (LRFD)	0.93	0.84	0.77	0.71	0.66
Hog Bend					
Max. Effective Tension (kN)	345	458	594	751	932
Max. Compression (kN)	9	27	36	65	85
Max. Bending Moment (kN.m)	396	347	315	345	360
Max von Mises (MPa)	312	281	267	278	287
Max. DNV Utilization (LRFD)	0.73	0.65	0.67	0.71	0.73
TDP					
Max. Effective Tension (kN)	309	423	576	729	914
Max. Compression (kN)	-	-	-	-	-
Max. Bending Moment (kN.m)	462	428	400	377	358
Max von Mises (MPa)	354	332	314	300	288
Max. DNV Utilization (LRFD)	0.82	0.77	0.73	0.70	0.68

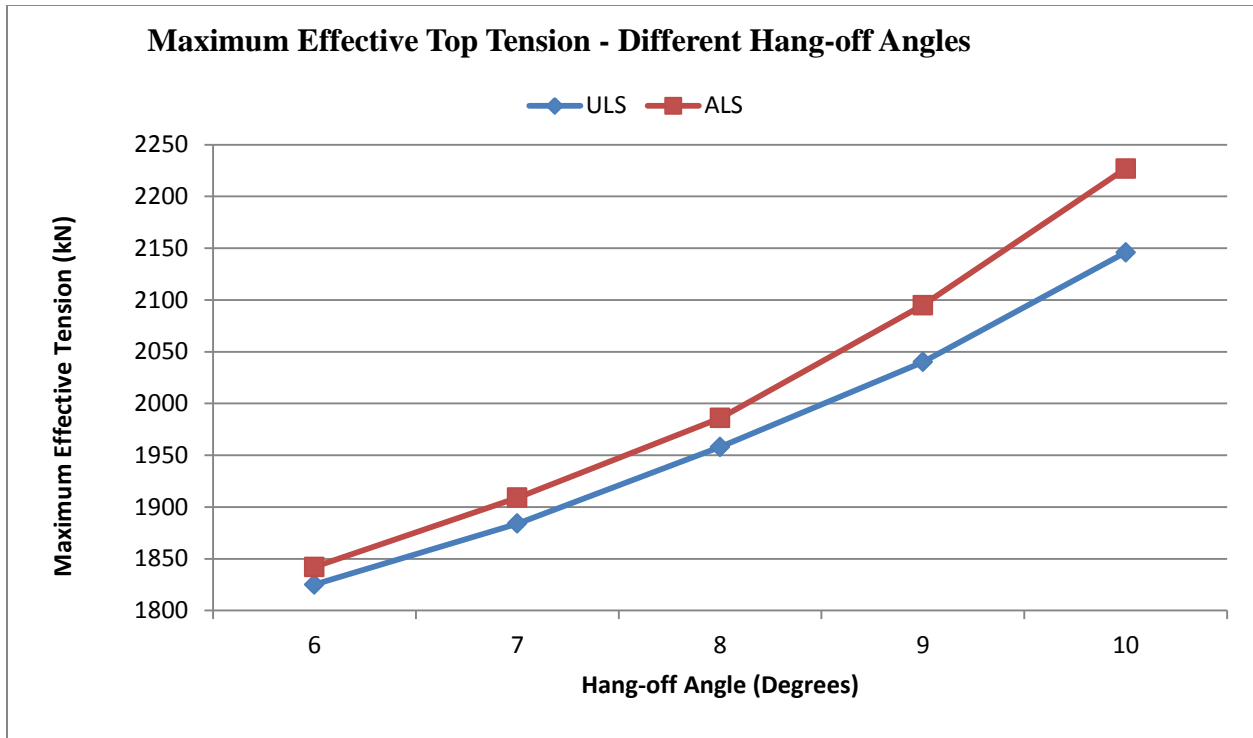


Figure 7.11 Maximum effective top tension for different hang-off angles

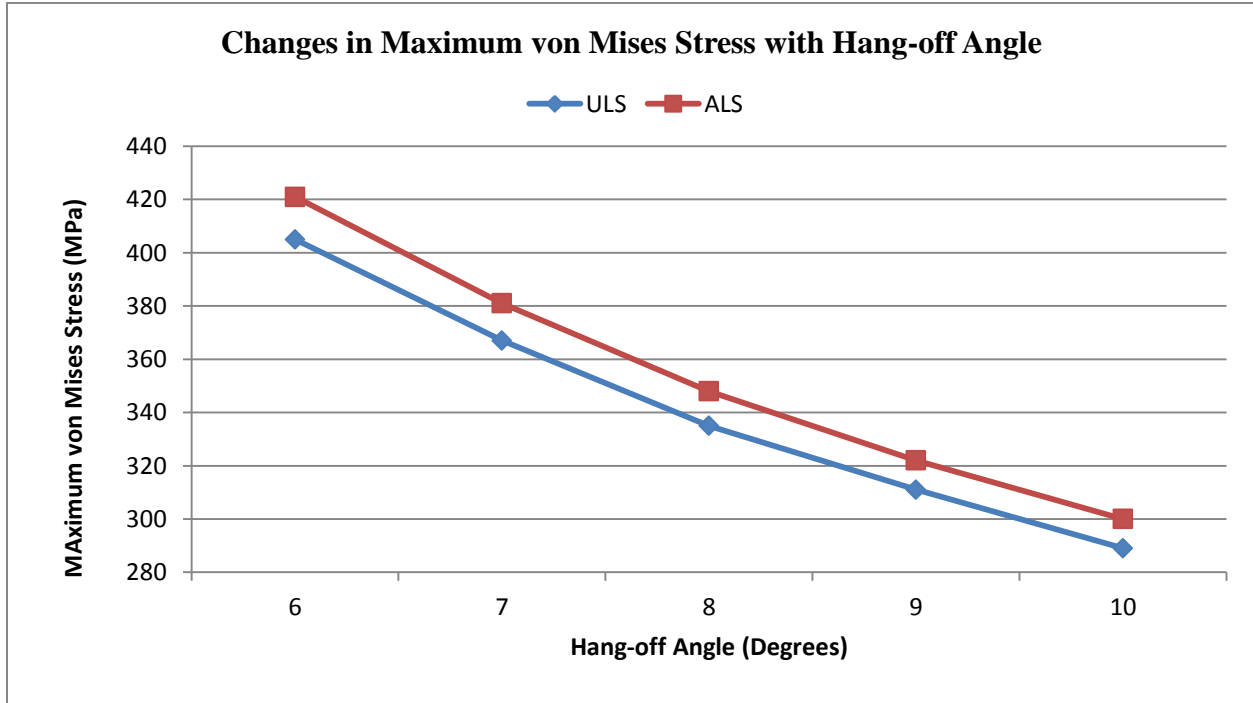


Figure 7.12 Maximum von Mises stress for different hang-off angles

- The maximum stress is above the allowable when the hang-off angle is set to 6 and 7 degrees. In all the cases, the maximum stress is at the sang-bend.
- It is observed that the maximum stresses at the sag and hog bends, and the TDP are approximately equal when the hang-off angle is set to 10 degrees.
- The maximum utilization is below unity in all the cases considered, and can therefore be considered as safe design. The maximum utilization is achieved when the hang-off angle is 6 degrees, and decreases as the angle increases.

In summary, this sensitivity study showed that a configuration with large hang-off angle will provide higher top tension, improved decoupling, and therefore better extreme response.

7.6 Internal Content Sensitivity

This sensitivity study is carried out to establish the dynamic behavior of the SLWR considering the case when the riser is empty. This is necessary if the riser is to be considered empty at any point in time during the design life.

For this study, only the base case configuration is considered, and analyses are performed for the mean, near, and far offset positions, also both ULS and ALS design are considered.

Consideration is given to the following:

- SLWR configuration – same as base case
- Content density – 0 kg/m^3
- Design pressure – 0 MPa

Considering the diameter of the SLWR and the light weight when empty, the SLWR become more buoyant, the resulting static configuration is as shown in Figure 7.13 for the mean offset position.

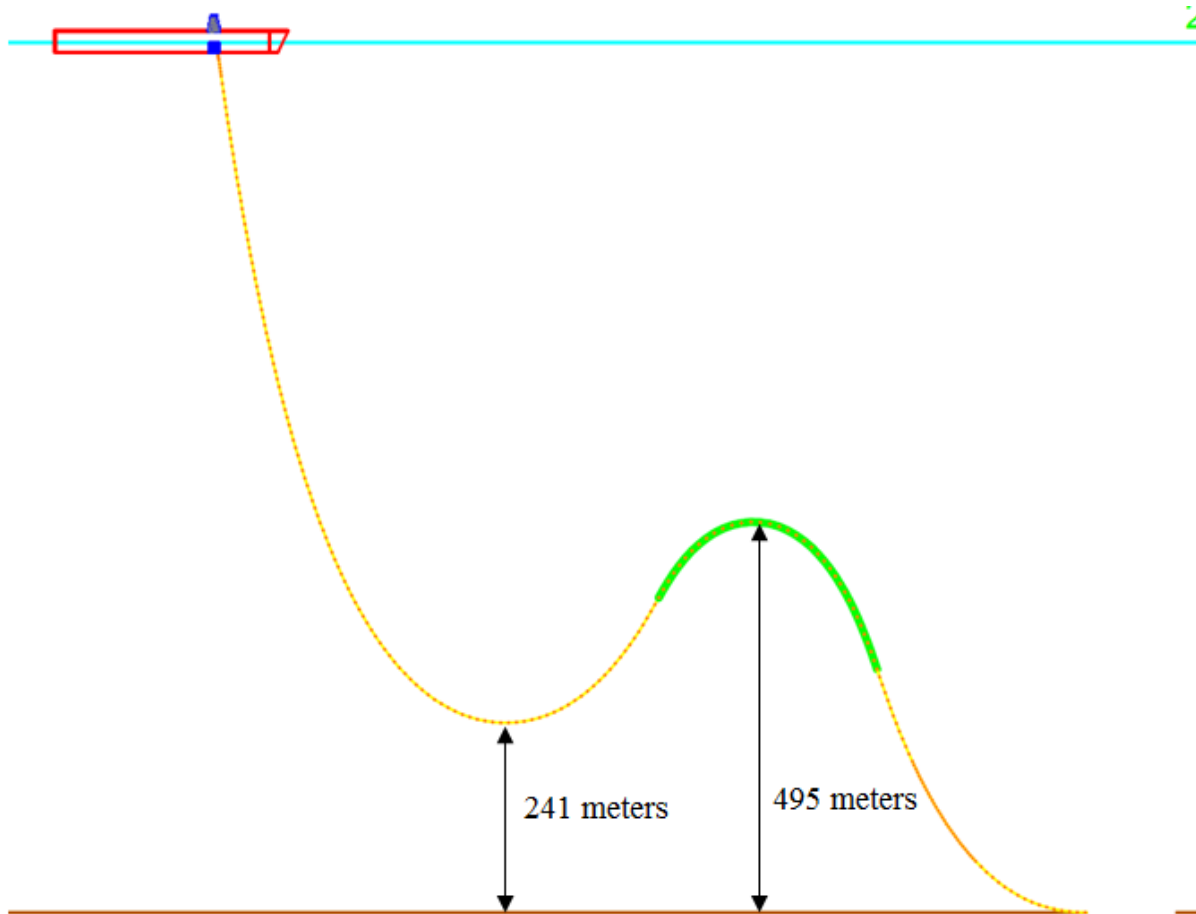


Figure 7.13 SLWR configuration – empty riser condition in mean offset position

7.6.1 Empty SLWR - static analysis

From the static configuration, the main changes in the SLWR configuration as seen from physical assessment are as follows:

- Increase in sag bend height from 100 to 241 meters above the seabed.
- Increase in the height between the sag and hog bends, from 80 to 254 meters.
- The above resulted in a configuration with higher wave zone compared to the base case, as expected.
- Also, the horizontal distance to the TDP from the connection point increased from 1116

to 1168 meters, almost at the end of the riser pipe arc length.

A summary of the static analysis results is presented in Table 7.12 for the critical riser locations. The following are the general observation from the static results:

- The effective top tension is about 55 percent of the effective tension for the case when filled with production fluid.
- The effective tensions at the sag and hog bends, and the TDP are equal as expected. This is similar to the case when filled with production fluid.
- The maximum static stress is observed at the SLWR hog bend for the empty riser condition; this stress is below the allowable stress limit. This behavior is different compared to the case when filled with production fluid, where maximum static stress is observed at the sag bend.
- The maximum static DNV utilization, based on functional loads factor of safety, is below unity.

From the summary results, it can be concluded that the SLWR will not fail under static conditions when the riser pipe is empty. However, there is need to study the behavior in dynamic environment.

7.6.2 Dynamic response (ULS) – content sensitivity

A summary of the dynamic analysis results is presented in Table 7.13. The following are the general observation from the dynamic behavior:

- Similar to the content filled condition, residual compression is observed at the sag bend area, however, the compression is minimal.
- The maximum stress is found at the hog bend in the near offset position. This stress is above the allowable limit. The maximum DNV utilization is above unity.

The dynamic analysis results showed that the SLWR configuration cannot withstand the extreme sea-state conditions, and since the utilization is above unity, the riser may fail.

The condition whereby the SLWR become empty should be avoided during the field's life. Alternatively, the configuration may be modified to accommodate this condition; such modifications have not been considered in this study.

Table 7.12 Static Results – Empty SLWR

FPSO Mean Position			
Hang-off Angle (°)	8		
Effective Top Tension (kN)	672		
Critical Locations			
	Sag Bend	Hog Bend	TDP
Effective Tension (kN)	112	112	112
Bending Moment (kN.m)	259	409	227
von Mises Stresses (MPa)	192	296	172
DNV Utilization (LRFD)	0.24	0.51	0.22

Table 7.13 Content Sensitivity – Summary Dynamic Response (ULS)

100-year wave + 10-year current Empty Content	FPSO Position				
	Intact			Accidental	
	Near	Far	Mean	Near	Far
Max. Top Angle	27.1	16.6	18.4	26.9	16.2
Min. Top Angle	8.4	0.1	0.0	8.1	0.1
Max. Effective Top Tension (kN)	1153	1162	1152	1148	1167
Sag Bend					
Max. Effective Tension (kN)	181	276	229	175	287
Max. Compression (kN)	86	101	99	85	101
Max. Bending Moment (kN.m)	395	254	314	409	243
Max. von Mises Stresses (MPa)	284	188	228	294	181
Max. DNV Utilization (LRFD)	0.50	0.23	0.33	0.45	0.19
Hog Bend					
Max. Effective Tension (kN)	88	177	136	83	187
Max. Compression (kN)	-	-	-	-	-
Max. Bending Moment (kN.m)	637	410	480	658	398
Max. von Mises Stresses (MPa)	454	299	344	469	291
Max. DNV Utilization (LRFD)	1.22	0.53	0.70	1.05	0.41
TDP					
Max. Effective Tension (kN)	65	149	114	61	157
Max. Compression (kN)	-	-	-	-	-
Max. Bending Moment (kN.m)	367	238	273	378	233
Max. von Mises Stresses (MPa)	266	179	202	274	176
Max. DNV Utilization (LRFD)	0.47	0.25	0.30	0.42	0.20

7.7 Sensitivity Studies Summary

The following is a summary of the knowledge gained on how to optimize the SLWR configuration:

Increasing the net buoyancy force can eliminate residual compression that is observed in the sag bend area of the SLWR, and provide better decoupling efficiency. However, such a solution will increase project cost. For this study, a net buoyancy of 700 N/m is found to be adequate.

The closer the sag bend height to the seabed, the better is the decoupling efficiency, as is seen in the extreme response in this study. A sag bend height of 100 meters above the seabed is found adequate for the SLWR configuration in this study.

A longer buoyant section length will provide improved decoupling efficiency compared to a shorter one. This will also lower the stresses and utilization at the critical sections of the SLWR. A buoyant section length of 420 meters is found adequate for the configuration in this study.

Increasing the hang-off angles also provide improved decoupling efficiency, and therefore lower stresses at the critical sections of the riser. A hang-off angle of 8 degrees used for the base case study is found adequate in this thesis work.

It was found that this SLWR configuration is not suitable for the condition where the riser pipe is empty. As the stress at the hog bend will become excessive, and may lead to the riser failure.

It should be noted that analysis for fatigue performance is performed for only the base case configuration, if it is desired to consider any of the other configurations in future studies or work, fatigue performance study is recommended.

CHAPTER 8 FABRICATION AND INSTALLATION OF SLWR

8.1 Introduction

The discussion in this chapter is based on previous works and industrial experience on the fabrication and installation of steel catenary risers (SCRs) of different configurations, including steel lazy wave risers (SLWRs). The objective is to give a general overview of the technical feasibility of fabrication and installation of SLWRs in deepwater, harsh environments. Due to time constraints, the scope of work does not include the actual installation analyses.

As described in section 3.7, the ease of fabrication and installation are among the many factors that are driving the selection of deepwater riser concepts. One of the challenges facing SCRs installation is the limit in the availability of installation vessels that can accommodate the riser top tension, which increases with water depth.

8.2 SLWR Fabrication

Fabrication of the SLWRs can be performed onshore and/or offshore. Onshore fabrication of girth welds has an added advantage because the welds can be inspected in a controlled space in order to ascertain that the required level of weld integrity is attained. The fabrication material as described in chapter 5 is carbon steel, the grade is X65, and line pipe will be used.

Some of the steps used in riser fabrication are described below:

- Welding of joint together to form quad joints or longer lengths based on the capacity of the fabrication yard
- Setting of the resultant multiple joints to align with other previous fabricated riser sections, and welding together
- Setting of spacers in plastic skin and in place while injection ends are put in position
- Pulling of riser pipe forward, and then repetition of the steps

8.2.1 Welding of SLWRs

The girth weld may limit the SLWR fatigue performance as seen from the fatigue performance calculations in section 6.4. Previous works including work by Karunakaran et al. (2013) have

also established the importance of the girth weld on SCRs fatigue performance. A number of automatic welding techniques that can be used include:

- Pulsed Gas Metal Arc Welding (PGMAW)
- Pulsed Gas Tungsten Arc Welding (PGTAW)
- Flux Core Arc Welding (FCAW)
- Gas Metal Arc Welding (GMAW)
- Gas Tungsten Arc Welding (GTAW)

The experience from BC-10 project by Subsea 7, where PGTAW technique was used to achieve high quality girth welds can be transferred in carrying out the SLWR welding. A pictorial representation showing typical mechanized PGTAW and grinding of weld cap to improve the riser fatigue performance is shown in Figure 8.1.

8.3 SLWR Installation

Installation of SCRs in deepwater requires vessels with good offshore stability, capacity to accommodate large riser top tension, and ability to effectively and efficiently accommodate a large quantity of steel riser pipe.

Some of the vessels that meet these requirements and have been used for SCRs installation include Seven Oceans, Seven Seas, and Seven Borealis, owned by Subsea 7. The Seven Borealis is designed to withstand installation conditions in harsh environments, such as offshore West of Shetland, a pictorial view of the vessel is shown in Figure 8.2.

The methods used in pipeline installation can also be employed in the installation of SLWRs, this methods include:

- S-Lay
- J-Lay, and
- Reeled-Lay

The S-Lay method has a long history in rigid pipe installation; however, with increasing water depths, methods such as J-Lay and Reeled-Lay emerged, and these methods are proven for deepwater riser installations.

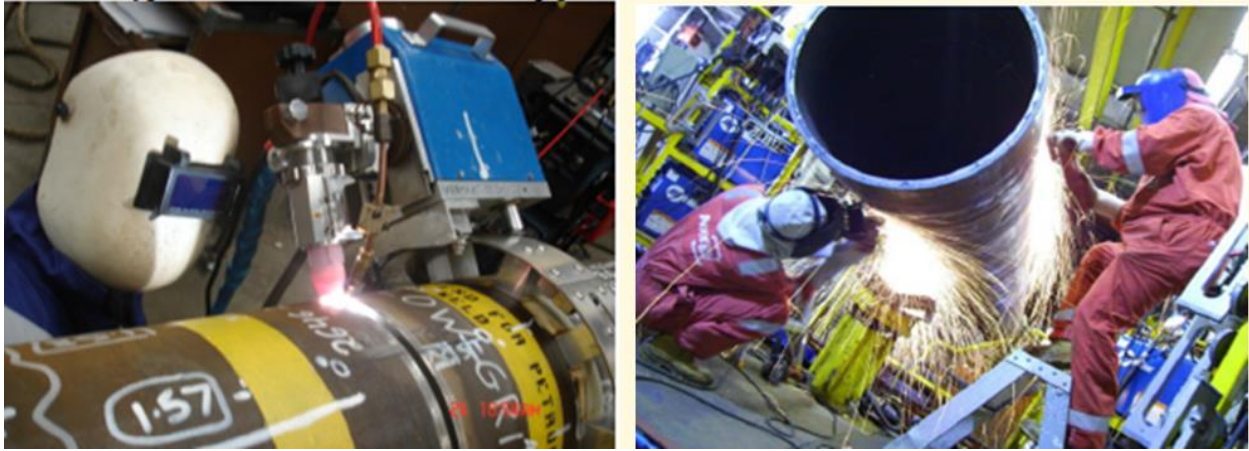


Figure 8.1 Mechanized PGTAW and grinding of weld cap to improve fatigue performance



Figure 8.2 Seven Borealis (Subsea 7, Norway)

The Reeled-Lay method was employed in the installation of the first SLWR in ultra-deepwater offshore Brazil.

Normally, installation of SCRs is carried out by direct transfer to FPSO from installation vessels. An alternative approach is pre-lay, abandonment and recovery technique which has advantages over the direct transfer technique, including decoupling of the subsea installation from FPSO, reduction in waiting on weather, and lower risk in severe environmental conditions. This installation technique however requires adequate preparations and planning to be successful.

Preparation and planning of the pre-lay, abandonment, and recovery technique requires a consideration of the following (Thomas et al., 2010):

- A pre-lay SLWR configuration
- Pre-abandonment
- Recovery
- Transfer after recovery

Pre-lay configuration: it is required to develop a pre-lay configuration that allows for efficient laying flexibility while maintaining the SLWR configuration as designed in the riser final in-place position. This will require several iterations, with consideration for various pre-lay configurations and the subsequent recovery pattern.

Pre-abandonment: when laid on seafloor, the SLWRs buoyant section forms a “hump”, a crucial aspect of pre-abandonment is maintaining the hump stability, and this is based on selection of suitable riser lay tension, which will optimize the hump height, and balance the riser-soil friction force. Also of importance at this stage is prevention of overstraining of the flex joint, this can be achieved by providing the flex joint with adequate bottom tension.

Recovery: at this stage, emphasis is on optimized vessel route that will provide adequate clearance from other subsea structures during the SLWR recovery. Also of importance is hump stability, as well as riser and flex joint integrity.

Transfer after recovery: at the stage, emphasis is on proper placement of the installation vessel in relation to the FPSO; to avoid excessive top tension at the connection point to the FPSO, to

maintain integrity of the riser and flex joint, and to avoid a second TDP being formed.

In addition to the steps described above, it is important to make contingency plans that can be used to mitigate risks associated with the installation procedure. It is also important to put into consideration the possibility of a direct transfer to FPSO, should the FPSO arrive early.

8.3.1 SLWR Hook-Up

Another challenge associated with deepwater riser installation is connecting the riser to the deepwater floater. For SLWR deployment in conjunction with an FPSO, it is possible to pre-install the riser before the FPSO is delivered; this can be achieved by decoupling the hook-up operations from the riser installation.

This option has an added advantage, in that the risk of keeping the installation vessel on hold, while the FPSO is being moored is avoided, however, the option comes with its particular challenges as already discussed.

To contain the SLWR close to the touchdown point (TDP), the riser may be anchored to seabed using suction piles; this can be done both in the temporary position and in the in-place position.

The riser top end also needs to be protected when laying the riser down temporarily, including immobilization of the flex joint to avoid damage of the elastomer due to deepwater hydrostatic pressure and thermal shrinkage. A typical riser flex joint is as shown in Figure 8.3.

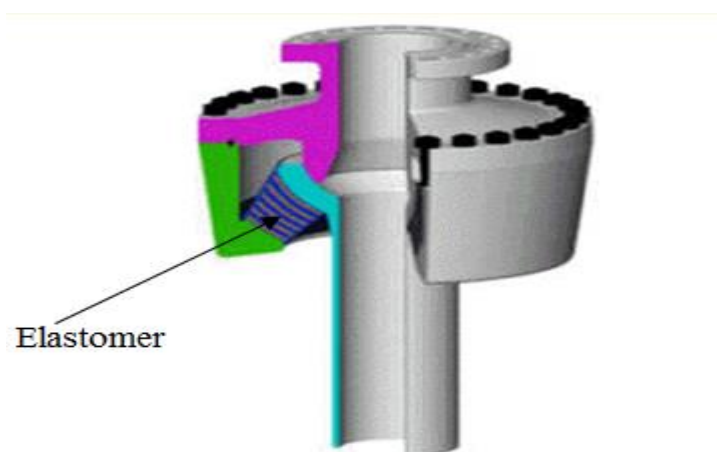


Figure 8.3 Typical SCR flex joint (Oilstates, 2014)

CHAPTER 9 CONCLUSION AND RECOMMENDATIONS

9.1 Conclusion

A riser concept that is suitable for deployment in deepwater, harsh environment is presented in this thesis work. The concept is a low lazy wave configuration made from high strength, low carbon steel of grade X65. The harsh environment considered is the extreme condition offshore of the West of Shetland.

The concept has been considered in conjunction with a high motion vessel, and detailed analyses has been performed to check the integrity of this concept in extreme sea-states, also detailed analyses has been performed to check the fatigue performance of the system; with consideration for both wave induced fatigue damage and fatigue damage due to vortex induced vibration.

The high motion vessel used in this study is a Floating, Production, Storage and Offloading (FPSO) system, with internal turret mooring system. The FPSO is a standard North Sea deepwater floater, with the internal turret system located at 55 meters forward of the amidships. The FPSO has the capability to weathervane up to 360° , and the turret system is permanent. The permanent option has been considered as the danger of typhoon and drifting iceberg are considered very low.

The steel lazy wave riser (SLWR) has been modeled in ORCAFLEX, and several analyses were carried out to establish the suitable configuration for the location under consideration. After establishing a suitable configuration with satisfactory static stresses and effective tension that are below the allowable limit, the SLWR was subjected to full-filling extreme strength analyses.

Riser Integrity

The strength response in the extreme sea-states showed that the concept can withstand the extreme conditions offshore West of Shetland. The maximum stress is found in the SLWR sag bend area, and the contribution of environmental actions from the extreme sea state, to the stresses at the touchdown point (TDP), and the critical sections is considered fairly low.

With this configuration, a maximum DNV utilization of 77 percent was achieved in the extreme conditions, also the maximum von Mises stress of 335 MPa is below the allowable limit, and therefore the configuration is considered safe.

In the extreme sea-state, some residual compression is however observed at the sag bend area, the maximum value for ultimate limit state (ULS) design is 86 kN. The observed compression is minimal and there is no danger of riser buckle.

Through sensitivity studies, it was observed that if undesirable, compression can be eliminated by the increasing the net buoyancy or increasing the buoyant section length.

For this configuration, the empty riser condition showed the stress at the hog bend is excessive, and may lead to riser failure. This should be avoided or modifications should be made to the configuration to minimize the stress at the hog bend.

Fatigue Performance

The wave-induced fatigue performance analysis of the SLWR was performed using a total of 216 load cases. A total of twelve wave directions were considered, and for each wave direction, a total of 18 load cases were considered.

The analyses results showed satisfactory wave-induced fatigue performance, a minimum fatigue life of 852 years was observed at the SLWR TDP, considering the D-curve. The minimum life is well above the acceptance limit of 250 years.

The top section of the riser, from 0 to about 8 meters showed very low fatigue performance; this section will in practice be covered with flex joint. However, flex joint modeling is not considered in this thesis work, therefore the fatigue life at top is not taken into account.

Calculation of fatigue damage due to vortex induced vibration (VIV) gave a minimum fatigue life below the acceptance limit of 500 years. The problem of VIV is not new to the offshore industry, and there are proven measures to mitigate the occurrence of fatigue damage due to VIV.

The minimum fatigue life due to VIV is observed at the TDP area, and in the middle section of

the SLWR upper catenary, where the longest span exists. The minimum fatigue life between these two areas is about 80 years; this is far below the acceptance limit.

For this configuration, strakes has been proposed as a solution to mitigate the observed fatigue damage due to VIV, the required amount of strakes is estimated to cover about 20% of the riser arc length, at the identified locations.

Sensitivity Study

Various sensitivity analyses were performed to have better understanding of the SLWR configuration, and the behavior in extreme sea states. From the sensitivity studies, it can be seen that to optimize the lazy wave configuration, the hang-off angle, the net buoyancy force, the buoyant section length, and the height of the sag bend above the seabed are of great importance.

Summary

The low lazy wave configuration presented in this study is found suitable for deepwater harsh environment. The low configuration minimizes buoyancy modules requirements, and therefore a reduction in overall project cost. The configuration also reduces the risk of interferences as a result of a reduction in riser foot-print.

Strength analysis results showed that the SLWR will perform well in extreme conditions, in the typical harsh environmental conditions found offshore West of Shetland.

Wave induced fatigue performance was satisfactory, and the minimum fatigue life at the TDP is well above the minimum acceptable limit, however, strakes is required to suppress VIV fatigue at certain section of the riser.

The addition of buoyancy elements at certain sections of the riser decouples the FPSO high motions from the TDP area, therefore the improved extreme response and fatigue performance at the TDP. This riser concept is also a cost effective option compared to other solutions that can be used to improve riser fatigue performance.

9.2 Recommendation

This thesis work has provided background knowledge on the integrity of a steel lazy wave riser

configuration for deployment in a typical deepwater harsh environment.

The study was quite extensive with various sensitivity studies to see how changes in the SLWR configuration and the amount buoyancy modules will affect the SLWR integrity. However, it can be said that further work still need to be carried out, especially with regards to suppression of VIV fatigue damage, and ease of installation.

In view of the above, the following are recommendations for further works that need to be considered prior to deployment of this concept in the location that was considered.

- A constant hydrodynamic coefficient was considered in the present study, sensitivity studies may be carried out for conditions where the drag coefficient varies with Reynolds number, and the roughness of the riser pipe.
- Introduction of strakes at the identified sections of the SLWR, and further VIV response analyses to see how effective the introduced strakes suppress the VIV fatigue damage.
- Fatigue analyses may also be performed for some of the other configurations in the sensitivity studies, for example, a configuration with greater hang-off angle than what is considered in this study.
- Detailed installation analyses. This requires information regarding a suitable weather window, when the sea-state is suitable for the installation works. The ease of installation of the lazy wave riser and buoyancy modules should be established. Experience from past projects such as the Parque das Conchas (BC-10) SLWR installation can be built on in the work.
- Analysis may be performed to investigate the behavior of the SLWR when flooded with sea water, as this was not considered in this thesis work due to lack of associated environmental data for such an analysis.

REFERENCES

- 2B1ST. 2012. *Turret* [Online]. 2b1st Consulting. Available: <http://www.2b1stconsulting.com/turret/> [Accessed 07 February 2014].
- ANDRADE, E. Q., AGUIAR, L. L., SENRA, S. F., SIQUEIRA, E. F. N., TORRES, A. L. F. L. & MOURELLE, M. M. 2010. Optimization Procedure of Steel Lazy Wave Riser Configuration for Spread Moored FPSOs in Deepwater Offshore Brazil. *Offshore Technology Conference*. Houston, Texas.
- API 1998. Design of Risers for Floating Production Systems (FPSs) and Tension-Leg Platforms (TLPs). *Recommended Practice, API-RP-2RD*. American Petroleum Institute.
- API 2005. Design and Analysis of Station Keeping Systems for Floating Structures. *Recommended Practice, API-RP-2SK*. American Petroleum Institute.
- API 2006. Design and Operation of Subsea Production Systems - General Requirements and Recommendations. *Recommended Practice, API-RP-17A, 4th Edition*. American Petroleum Institute.
- BAI, Y. & BAI, Q. 2005. *Subsea Pipelines and Risers*, London, Elsevier Ltd.
- BALMORAL. 2014. *Distributed Buoyancy Modules* [Online]. Balmoral Offshore Engineering. Available: <http://www.balmoral-offshore-engineering/2-surf-distributed-buoyancy.php> [Accessed 06 June 2014].
- CARTER, B. A. & RONALDS, B. F. 1998. Deepwater Riser Technology. *Society of Petroleum Engineers*.
- DNV 2007. Environmental Conditions and Environmental Loads. *Recommended Practice, DNV-RP-C205*. Det Norske Veritas.
- DNV 2009. Offshore Riser Systems. *Offshore Service Specification DNV-OSS-302*. Norway: Det Norske Veritas.
- DNV 2010a. Dynamic Risers. *Offshore Standard, DNV-OS-F201*. Det Norske Veritas AS.
- DNV 2010b. Global Performance Analysis of Deepwater Floating Structures. *Recommended Practice, DNV-RP-F205*. Det Norske Veritas.
- DNV 2012. Fatigue Design of Offshore Steel Structures. *Recommended Practice, DNV-RP-C203*. Det Norske Veritas AS.
- DUGGAL, A. S., HEYL, C. N. & RYU, S. 2009. Station-keeping of FPSOs In Extreme Environments. *International Society of Offshore and Polar Engineers*, D-09-004 ISOPE Conference Paper.
- ENGLAND, L. T., DUGGAL, A. S. & QUEEN, L. A. 2001. A comparison Between Turret and Spread Moored F(P)SOs for Deepwater Field Developments. *Deep Offshore Technology*.
- GUDMESTAD, O. T. 2013. Marine Operations: Vessel Motions. *OFF600 - Lecture Notes*. Stavanger, Norway: University of Stavanger.
- GUO, B., SONG, S. & GHALAMBOR, A. 2005. *Offshore Pipelines*, Oxford, Elsevier.
- HAMILTON, J. & PERRETT, G. R. 1986. Deepwater Tension Leg Platform Designs. *Proceedings of International Symposium on Developments in Deep Waters*. The Royal Institution of Naval Architects, London.
- HANSEN, V. L. 2011. *Dry Tree Semi - New Deepwater Floater?* [Online]. Available: http://www.dnv.com/industry/oil_gas/publications/updates/oil_and_gas_update/2011/01_2011/drytreeseininewdeepwaterfloater.asp [Accessed 14 January 2014].
- HOWELLS, H. & HATTON, S. A. 1997. Challenges for Ultra-Deep Water Riser Systems. . *Floating Production Systems*. IIR, London.
- HUANG, S. & HATTON, S. 1996. Rigid Bottom Weighted Large Diameter Risers - Concept, Analysis and

- Design -. *Technology for Deep Hostile Seas*. Aberdeen, United Kingdom.
- KARUNAKARAN, D., LEGRAS, J.-L. & JONES, R. 2013. Fatigue Enhancement of SCRs: Design Applying Weight Distribution and Optimized Fabrication. *Offshore Technology Conference*. Houston, TX, USA.
- KARUNAKARAN, D. & MELING, T. S. Robust SCR Design against Fatigue in Deepwater Harsh Environment. Deep Offshore Technology, 2006 Houston, Texas.
- KARUNAKARAN, D. & OLUFSEN, A. An Efficient Metal Riser Configuration for Ship and Semi Based Production Systems. International Offshore and Polar Engineering Conference 1996 Los Angeles.
- KATLA, E., MORK, K. & HANSEN, V. L. 2001. Dynamic Risers: Introduction and Background to the New DNV Offshore Standard (OS-F201) *Offshore Technology Conference*. Houston, Texas.
- KAVANAGH, W. K., LOU, J. & HAYS, P. 2003. Design of Steel Risers in Ultra Deep Water – The Influence of Recent Code Requirements on Wall Thickness Design for 10,000ft Water Depth. *Offshore Technology Conference*. Houston, Texas.
- MAHONEY, T. R. & BOUVARD, M. J. 1986. Flexible Production Riser System for Floating Production Applications in the North Sea. *Offshore Technology Conference - OTC 5163*. Houston, Texas.
- MELING, T. S. 2013. Deepwater Floating Production Systems in Harsh Environment - A Look at a Field Development Offshore Norway and Need for Technology Qualification. *Offshore Technology Conference*. Rio de Janeiro, Brazil.
- NORSOK 2004. Well Integrity in Drilling and Well Operations. *NORSOK Standard D-010*. Norway.
- NORSOK 2007. Actions and Action Effects. *NORSOK Standard N-003*. Norway: Standards Norway.
- ODLAND, J. 2012a. Offshore Field Development: Floating Production Systems. *OFF500 - Lecture Notes*. Stavanger, Norway: University of Stavanger.
- ODLAND, J. 2012b. Offshore Field Development: Platform concepts and design issues. *OFF500 - Lecture Notes*. Stavanger, Norway: University of Stavanger.
- ODLAND, J. 2012c. Offshore Field Development: Tension Leg Platforms and Deep-Draft Floaters. *OFF500 - Lecture Notes*. Stavanger, Norway: University of Stavanger.
- OGP 2010. Regulators' use of Standards *Report No. 426* International Association of Oil & Gas Producers.
- OILSTATES. 2014. *SCR FlexJoints Products* [Online]. Available: <http://www.oilstates.com/fw/main/SCR-FlexJoint%C2%AE-Products-369.html> [Accessed 02 June 2014].
- OLUFSEN, A., LOLAND, G., GORF, P. & WEBB, S. 2003. Evaluation Ranks Deepwater, Harsh Environments Floater, Riser Concepts. *Oil and Gas Journal*, 101, 39-46.
- PAIK, J. K. & THAYAMBALLI, A. K. 2007. *Ship-Shaped Offshore Installations: Design, Building, and Operation*, Cambridge University Press.
- PETROMIN 2012. An Innovative Flexible Riser Solution for Large Diameter, Ultra-deepwater Asian Fields. *Technology*. Petromin Pipeliner.
- PHIFER, E. H., KOPP, F., SWANSON, R. C., ALLEN, D. W. & LANGNER, C. G. 1994. Design and Installation of Auger Steel Catenary Risers. *Offshore Technology Conference - OTC 7620*. Houston, Texas.
- SAINT-MARCOUX, J. & LEGRAS, J. 2014. Impact on Risers and Flowlines Design of the FPSO Mooring in Deepwater and Ultra Deepwater. *Offshore Technology Conference*. Houston, Texas.
- SARPKAYA, T. 1976. Vortex Shedding and Resistance in Harmonic Flow about Smooth and Rough Cylinders. *Proceedings of the 1st International Conference on the Behaviour of Offshore Structures (BOSS '76)*. The Norwegian Institute of Technology.
- SARPKAYA, T. 1977. In-line and Transverse Forces on Cylinders in Oscillatory Flow at High Reynolds Numbers. *Journal of Ship Research* 21,2000-216.
- SENRA, S. F., ANDRADE, E. Q., MOURELLE, M. M. & TORRES, A. L. F. L. Challenges Faced in the Design of

- SLWR Configuration for the Pre-Salt Area. Ocean, Offshore and Arctic Engineering, OMAE2011, 2011 Rotterdam, The Netherlands.
- SONG, R. & STANTON, P. 2007. Deepwater Tieback SCR: Unique Design Challenges and Solutions. *Offshore Technology Conference*. Houston, Texas.
- SONG, R. & UPPU, K. 2012. Assessment of Riser System Selection. *Deepwater Technology Asia*. Jakarta.
- STANTON, P., KAVANAGH, W. K., GARRETT, D. & MORK, K. 2010. New Code for the Design of Dynamic Risers for Floating Production Installations. *Offshore Technology Conference*. Houston, Texas.
- THOMAS, B., BENIRSCHKE, A. & SARKAR, T. 2010. Parque das Conchas (BC-10) Steel Lazy Wave Riser Installation, Pre-abandonment, Recovery and Transfer Challenges. *Offshore Technology Conference - OTC 20605*. Houston, Texas.

APPENDIXES

Appendix A – Wall Thickness Sizing

A.1 Wall Thickness Sizing for SLWR – Code Check Overview

Kilometer Post

Start End

Material Input

SMYS [MPa]

SMTS [MPa]

f_y temp [MPa]

f_u temp [MPa]

Young's modulus [GPa]

Poisson's ratio [-]

Anisotropy factor [-]

Hardening factor [-]

Fabrication factor [-]

Suppl. req. U fulfilled

Load Input

	Pressure [barg]	@ level [m]	Content mass density [kg/m ³]
Design	<input type="text" value="344"/>	<input type="text" value="-12"/>	<input type="text" value="800"/>
System test	<input type="text" value="396"/>	<input type="text" value="-12"/>	<input type="text" value="1025"/>

Incidental to design pressure ratio [-]

Water depth [m] and mass density [kg/m³]

	Functional	Environmental
Moment [kNm]	<input type="text" value="0"/>	<input type="text" value="0"/>
Axial force [kN]	<input type="text" value="0"/>	<input type="text" value="0"/>
Strain [%]	<input type="text" value="2,2"/>	<input type="text" value="2,2"/>

Load condition factor [-]

Design Input

Failure mode	Condition	Safety class	Corr.	Der.
Burst	Operation	<input type="text" value="High"/>	<input checked="" type="checkbox"/>	<input type="checkbox"/>
Burst	System test	System test	<input checked="" type="checkbox"/>	<input type="checkbox"/>
Collapse	<input type="text" value="Empty"/>	<input type="text" value="High"/>	<input checked="" type="checkbox"/>	<input type="checkbox"/>
Propagating buckling	<input type="text" value="Empty"/>	<input type="text" value="High"/>	<input checked="" type="checkbox"/>	<input type="checkbox"/>
Load comb., LCC, lc = a				
Load comb., LCC, lc = b				
Load comb., DCC, lc = a	<input type="text" value="Operation"/>	<input type="text" value="High"/>	<input checked="" type="checkbox"/>	<input type="checkbox"/>
Load comb., DCC, lc = b				

Results

Calc.	t _{req.} [mm]	Utilisation [-]	Utilisation [-]
<input checked="" type="checkbox"/>	<input type="text" value="19,82"/>	<input type="text" value="0,762"/>	<div style="width: 76.2%; height: 10px; background-color: #90EE90;"></div>
<input checked="" type="checkbox"/>	<input type="text" value="17,97"/>	<input type="text" value="0,682"/>	<div style="width: 68.2%; height: 10px; background-color: #90EE90;"></div>
<input checked="" type="checkbox"/>	<input type="text" value="16,12"/>	<input type="text" value="0,422"/>	<div style="width: 42.2%; height: 10px; background-color: #90EE90;"></div>
<input checked="" type="checkbox"/>	<input type="text" value="23,43"/>	<input type="text" value="0,821"/>	<div style="width: 82.1%; height: 10px; background-color: #90EE90;"></div>
<input checked="" type="checkbox"/>	<input type="text" value="-"/>	<input type="text" value="-1,000"/>	
<input checked="" type="checkbox"/>	<input type="text" value="-"/>	<input type="text" value="-1,000"/>	
<input checked="" type="checkbox"/>	<input type="text" value="15,22"/>	<input type="text" value="0,794"/>	<div style="width: 79.4%; height: 10px; background-color: #90EE90;"></div>
<input checked="" type="checkbox"/>	<input type="text" value="24,87"/>	<input type="text" value="0,991"/>	<div style="width: 99.1%; height: 10px; background-color: #90EE90;"></div>

A.2 Wall Thickness Sizing for SLWR – Pressure Containment Report

DNV-OS-F101 - SUBMARINE PIPELINE SYSTEMS - 2007

Pipeline Engineering Tool (PET)

Pressure Containment (bursting) report

Project: SLWR - Wall Thickness Check by Orimolade.pet

Section: SLWR

KP Start: 0,000

KP End: 1,000

Date: 25.04.2014



RELEVANT INPUT PARAMETER S:	Operation	System test
Nominal inner steel diameter [mm]:	254,00	
Nominal steel wall thickness [mm]:	25,40	
Fabrication tolerance [%]:	12,50	
Corrosion allowance [mm]:	3,00	
Specified minimum yield stress [MPa]:	448,2	
Specified minimum tensile strength [MPa]:	530,9	
Derating in yield stress due to temperature [MPa]:	0,0	
Derating in tensile strength due to temperature [MPa]:	0,0	
Depth [m]:	1100,0	
Density of external fluid [kg/m ³]:	1025,0	
Material strength factor [-]:	1,00	1,00
Internal pressure at reference level [bar]:	344,0	396,0
Reference level for internal pressure [m]:	-12,0	-12,0
Density of internal fluid [kg/m ³]:	800,0	1025,0
Incidental to design pressure ratio [-]:	1,10	1,00
Safety Class :	HIGH	SYSTEM TEST
Corroded wall thickness :	YES	YES
Derated material properties :	NO	NO
INTERMEDIATE RESULTS:	Operation	System test
Characteristic yield stress [MPa]:	448,2	448,2
Characteristic ultimate strength [MPa]:	530,9	530,9
Steel wall thickness used in code check [mm]:	19,23	19,23
Pressure containment resistance, yielding limit state [bar]:	696,8	696,8
Pressure containment resistance, ultimate [bar]:	717,7	717,7
Pressure containment resistance, minimum [bar]:	696,8	696,8
Local design pressure [bar]:	429,4	505,4
Local incidental pressure [bar]:	463,8	505,4
External pressure [bar]:	110,6	110,6
Pressure difference [bar]:	353,2	394,8
Material resistance factor [-]:	1,15	1,15
Safety class resistance factor [-]:	1,308	1,046
FINAL RESULTS:	Operation	System test
Code check, utility with given wall thickness [-]:	0,76	0,68
Required nominal wall thickness [mm]:	19,82	17,97

Appendix B – Brief Description of the Software Programs Used

B.1 ORCAFLEX Software Program

B.1.1 Introduction

This is the main analysis software that was used in this thesis work. The software program is primarily designed for static and dynamic analysis of a number of offshore structures, which include rigid and flexible risers, mooring system, and installation. It is a product of Orcina Ltd, and this description is based on the software user manual.

Its time domain features allows for non-linear time domain analysis, and this can be carried out for specific part of a system or for the entire system. It can be used in performing both extreme response analyses in different sea-states, and for fatigue analysis of offshore marine risers among others.

The current version, 9.7, can be used to perform a number of code checks when designing or analyzing offshore systems, including:

- DNV-OS-F201
- DNV-OS-F101
- PD-80010, and
- API-RP-1111

B.1.2 An overview of ORCAFLEX software program

The software is user-friendly, and provides good pictorial representation of each part of a system as the user is building the system. Experience user can take advantage of this feature and make the best of the modeling time.

The software program is started on a computer in which it is installed in a similar manner to other basic software. This can be done from the desktop, from the start menu, or through other available shortcuts.

A 3-D view representing the marine environment is presented to the user when the program

starts; the view shows the sea surface, the seabed, and a dark empty space representing the surrounding environment. A pictorial representation of this main window is as shown in Figure B.1, where the blue line represents the sea surface, and the brown line represents the seabed.

The menu bar has various commands including commands for opening, saving, printing and exporting. It has data and object editing facilities. It provides access to facilities that are used for modeling, starting, stopping, and replaying analyses. It can be used when accessing different views of the model. Provide commands used in obtaining analyses results, and can be used to access multiple windows and workspace.

The toolbar can be described as a shortcut to the menu bar, it provides a shortcut to access most of the commands that are found in the menu bar. In other words, it provides for a quick access to most of the commands used in modeling, analyses and obtaining results. A list of the key tools that are found in OrcaFlex and their functions is presented in Table D.1.

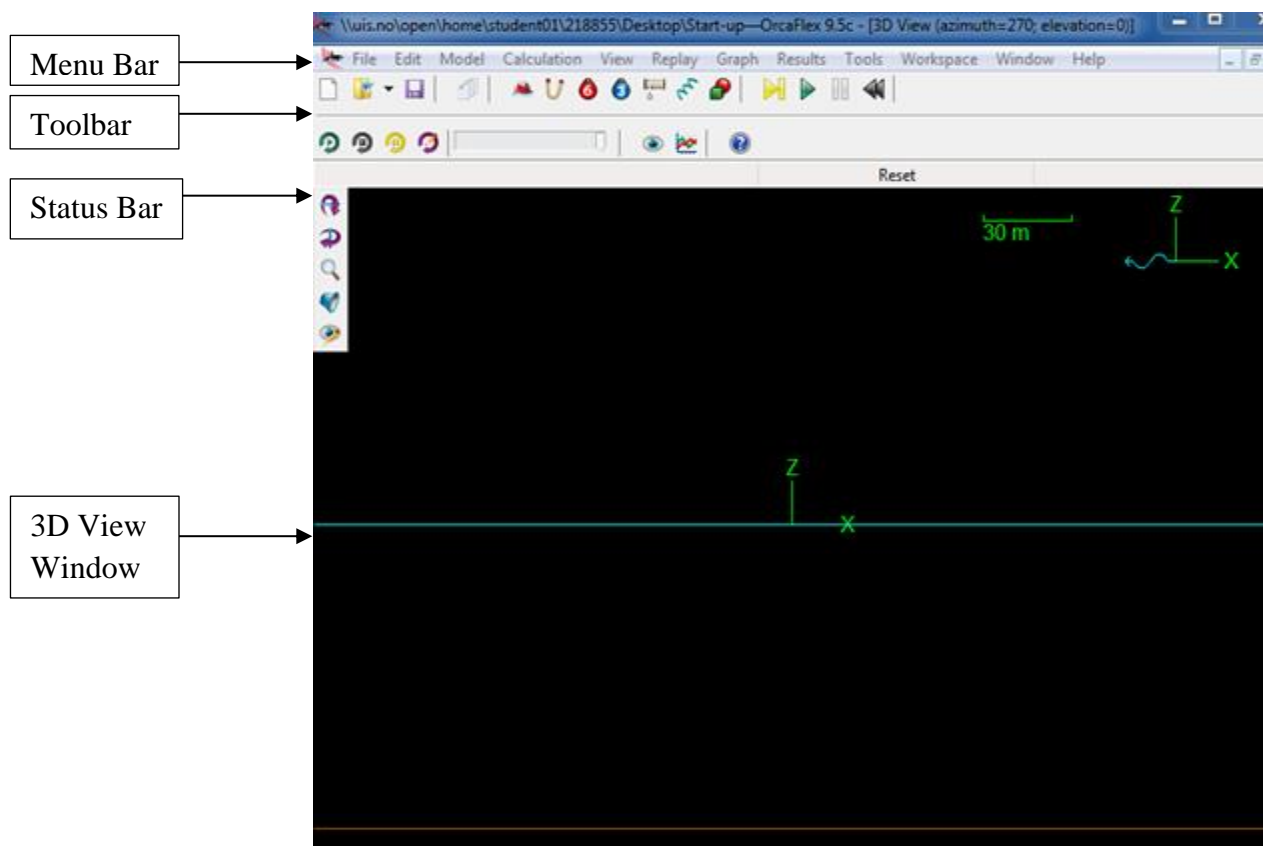






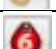




















Figure B.1 OrcaFlex main window

Table B.1 OrcaFlex Tools

Tool	Task	Description
	New	Deletes all objects from the model and resets data to default values
	Open	Open a saved OrcaFlex file – either a data file (.dat or .yml) or a simulation file (.sim)
	Save	Save an OrcaFlex file – either a data or simulation file
	Model Browser	Toggles the visibility of the Model Browser
	New Vessel	Creates new vessel – the vessel (object) is placed at the position of next mouse CLICK within a 3D view.
	New Line	Creates new line
	New 6D Buoy	Creates new 6D buoy
	New 3D Buoy	Creates new 3D buoy
	New Winch	Creates new winch
	New Link	Creates new link
	New Shape	Creates new shape
	Single Statics	Start the single statics calculation.
	Run Dynamic Simulation	Start a dynamic simulation.
	Pause Dynamic Simulation	Pause the simulation
	Reset	Reset the model, discarding any existing results.
	Start/Stop Replay	Starts or stops the replay of a simulation
	Step Replay	Step the replay forwards or backwards one frame at a time. Click the button to step forwards; press down SHIFT and CLICK to step backwards
	Edit Replay Parameters	Adjust the Replay Parameters, such as the period of simulation to replay, the time interval between frames, the replay speed etc
	Add 3D View	Add another 3D View Window. Having multiple views on screen allows you to watch different parts of the system simultaneously, or to see different views at the same time (for example a plan and an elevation).
	Select Results	Display the results form, which allows you to choose from the currently available selection of graphs and results tables. Graphs such as Time Histories, XY Graphs and Range Graphs may be created before a simulation has been run, thus allowing you to watch the variables during a simulation.
	OrcaFlex Help	Opens the OrcaFlex on-line help system.
	Rotate Up / Down / Left / Right	Change the view direction, for the active 3D View, by the view rotation increment
	Zoom In / Zoom Out	Click the zoom button to zoom in (decrease view size) or SHIFT+CLICK it to zoom out (increase view size).
	Change Graphics Mode	Toggles the graphics mode between wireframe and shaded.
	Edit View Parameters	Adjust the View Parameters for the active 3D View

The status bar provides information about how current action is progressing, and is divide into message box, state indicator, and information box.

The 3D view window shows the current model in a pictorial form. The main window can also be divided into sub-windows, showing graphs, spreadsheets, and texts.

B.1.3 Modeling and analysis in ORCAFLEX

The sequence of analyses in ORCAFLEX is as shown in Figure B.2, if the static analysis does not converge it is impossible to perform a dynamic analysis, and will require the user to modify the configuration, or time steps.

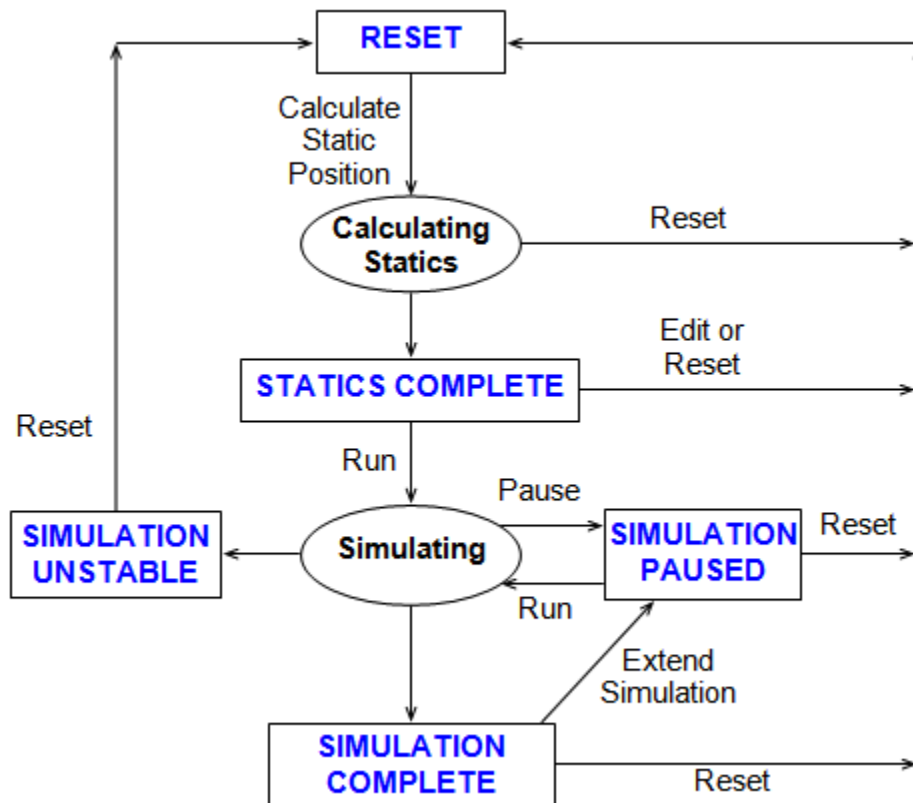


Figure B.2 Model states

The coordinate system in ORCAFLEX is as shown in Figure B.3, this comprise of a general global coordinate system, denoted GXYZ and local coordinates systems for each of the modeled objects.

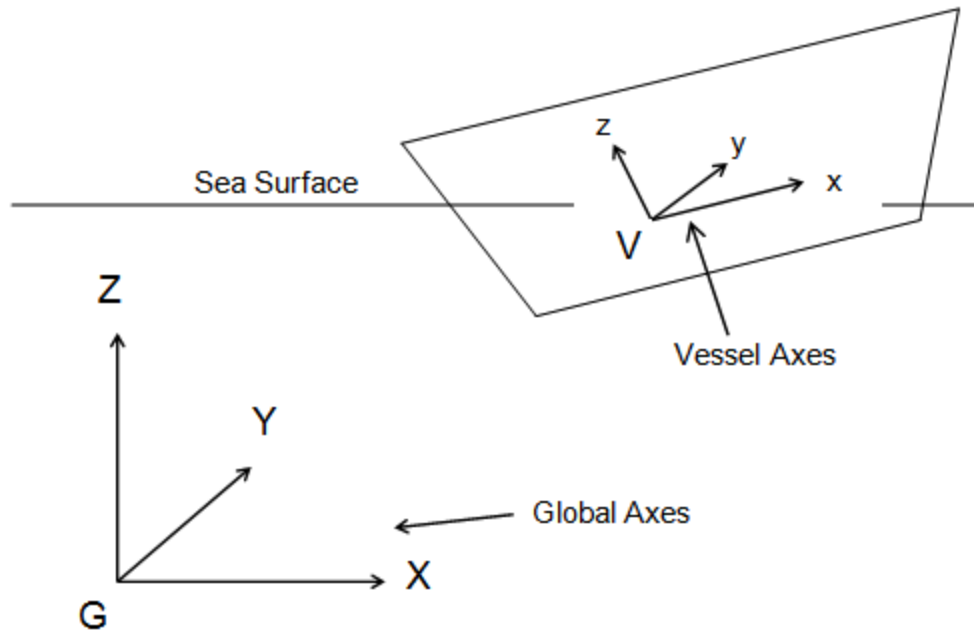


Figure B.3 ORCAFLEX coordinate systems

The various headings and directions in ORCAFLEX is as shown in Figure B.4, they are specified by providing the azimuth angle for a direction, measured counter-clockwise.

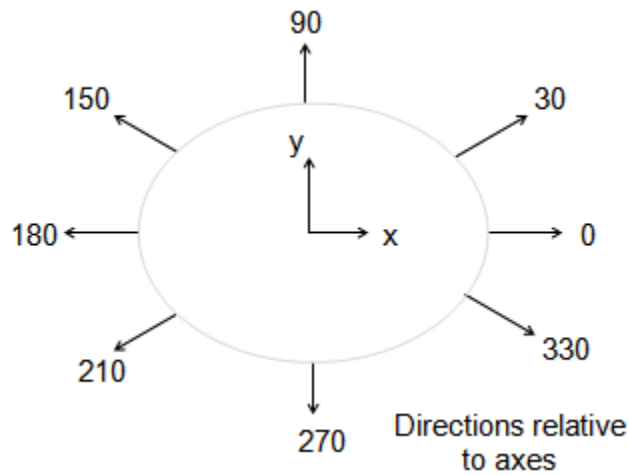


Figure B.4 ORCAFLEX headings and directions

A description of how the simulation time is specified and how this can be divided into different stages is shown in Figure B.5; this information is particularly useful if a one wants to capture

part of simulation rather than the entire simulation period.

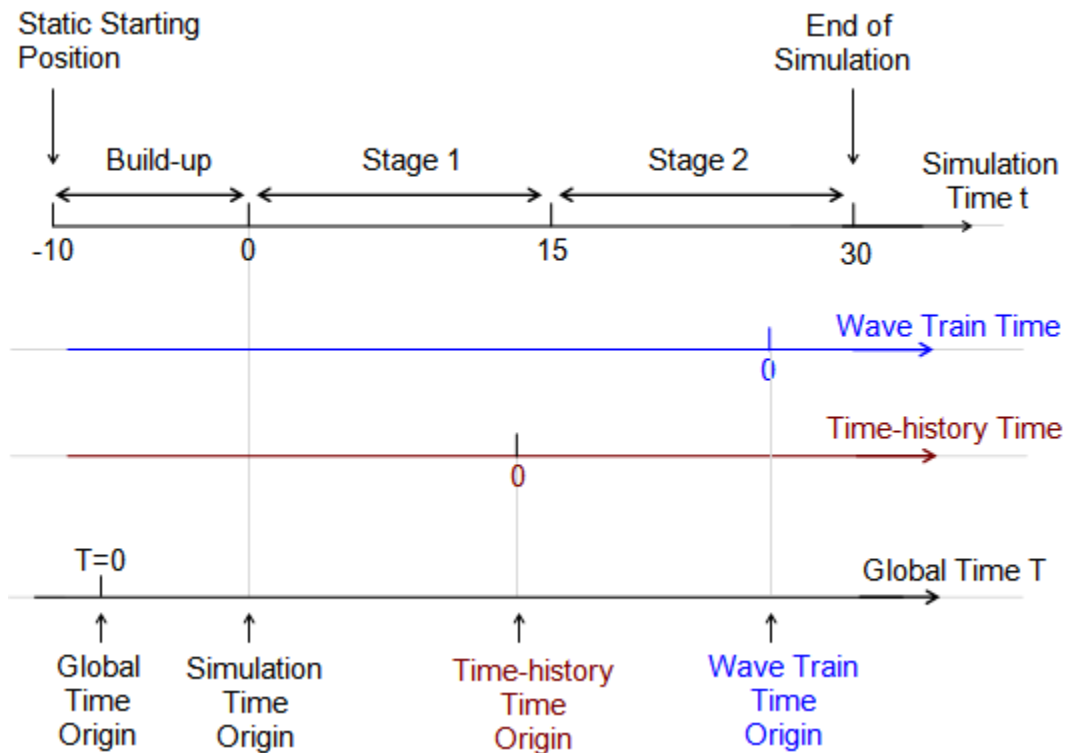


Figure B.5 Setting up simulation time and stages

B.1.4 LRFD calculation

To determine the LRFD result, the environmental and functional loads are separated, to achieve this; the combined load from the model is treated as linear superposition of functional load and environmental load.

That is:

$$M_{x,E}(t) = M_x(t) - M_{x,F}$$

$$M_{y,E}(t) = M_y(t) - M_{y,F}$$

$$Te_E(t) = Te(t) - Te_F$$

Thus, in the static state, there is no environmental load contribution when determining the LRFD.

The load effects used in the DNV-OS-F201 LRFD calculations can be represented by the

following equations:

$$T e_d = \gamma_F T e_F + \gamma_E T e_E$$

$$M_{x,d} = \gamma_F M_{x,F} + \gamma_E M_{x,E}$$

$$M_{y,d} = \gamma_F M_{y,F} + \gamma_E M_{y,E}$$

$$|M_d| = \sqrt{M_{x,d}^2 + M_{y,d}^2}$$

These design loads, moment and tension, are evaluated individually for about four times in ORCAFLEX, using different permutations of the partial load factors stated in Table 6.1 of the main report, and using the combinations with the greatest magnitude. The final result is in accordance with the code check criteria as defined in section 4 of the main report.

B.2 RIFLEX Software Program

This software program is designed for analysis of flexible riser systems, but it can as well be used for analysis of other slender structures, including steel marine risers. It is a product of MARINTEK, and this description is based on the general user manual.

The software program comprises of four modules as shown in Figure B.6, and for a full dynamic analysis, all four modules must be run.

In this thesis work, only the INPMOD and STAMOD were used, and are described below:

INPMOD MODULE: the user defines all the input parameters for the design analysis in this module, including riser configuration, support vessel, and environmental conditions. The module reads the input and prepares a database for use in subsequent analyses. Examples of the INPMOD used in this thesis are presented in this Appendix.

STAMOD MODULE: the static configuration of the model is determined by this module. The module can perform several kinds of static analyses. The results serve as input to subsequent dynamic analyses, or may be used directly for parametric studies. Examples of the STAMOD used in this thesis work are also presented in this Appendix.

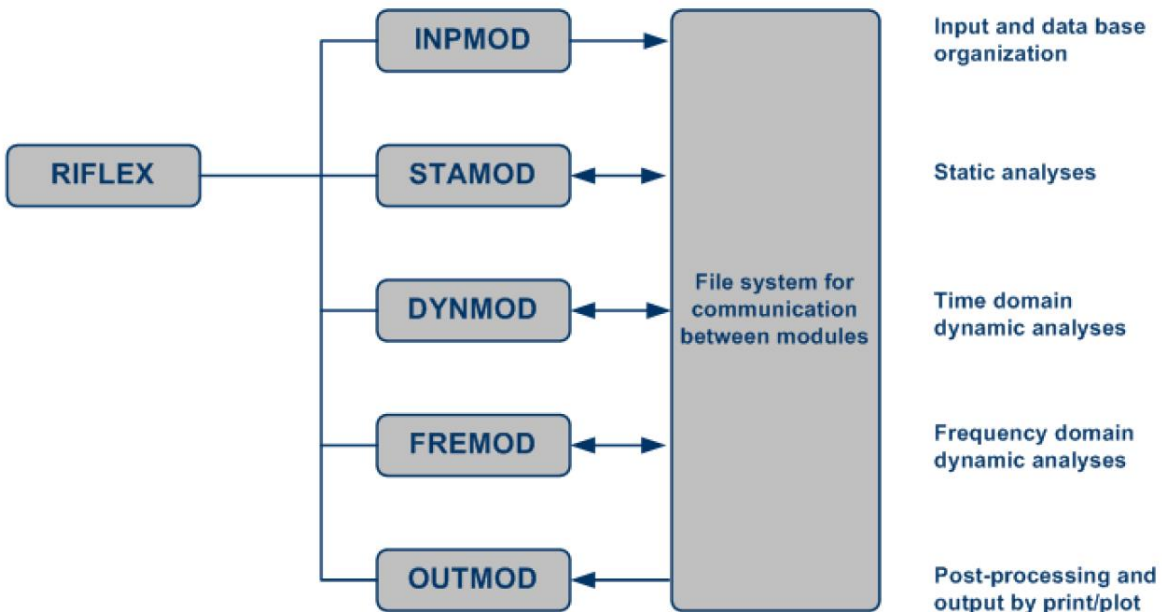


Figure B.6 RIFLEX program structure

B.3 VIVANA Software Program

This software program is semi-empirical and is designed for vortex induced vibration (VIV) prediction. It is a product of MARINTEK, and is applicable to slender structures under the action of ocean current. The software is linked to RIFLEX, that is, the INPMOD and STAMOD analyses are performed in RIFLEX. The description in this section is based on VIVANA user manual.

The general structure of the relation between RIFLEX and VIVANA is shown in Figure B.7. For complete VIV response calculations, the following are considered:

- Initial RIFLEX analysis from INPMOD and STAMOD modules
- Computation of eigen-frequencies and normal modes by the VIVEIG module
- Calculation of initial important parameters in INIVIV
- Dynamic response analyses in VIVRES module
- Fatigue damage calculations from VIVRES results in VIVFAT module

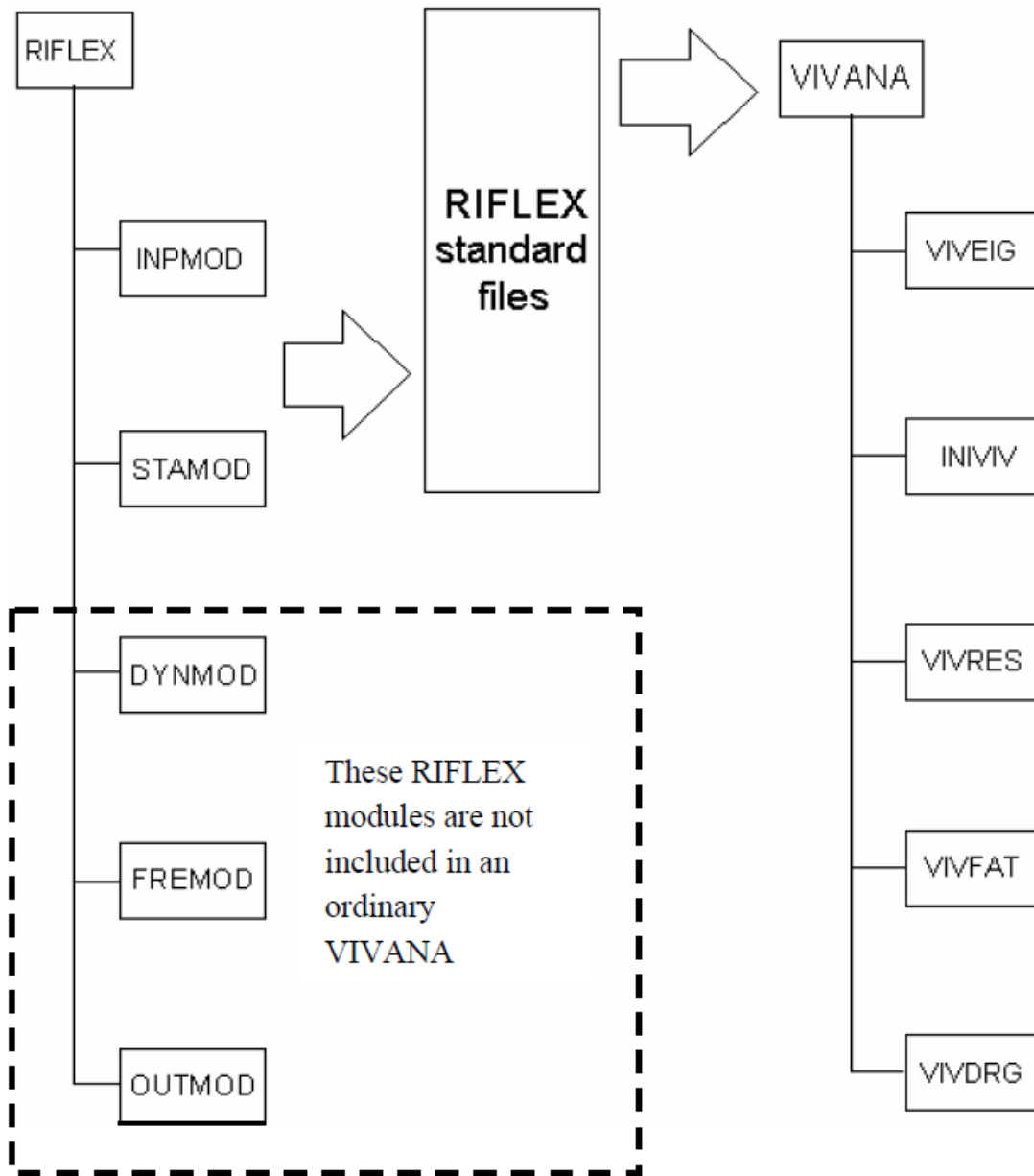


Figure B.7 VIVANA and RIFLEX overall structure

B.4 RIFLEX FILES

This sub-section provides information on some of the RIFLEX files used in the VIV fatigue analysis simulations.

B.4.1 INPMOD

Two set of INPMOD files were created for each current direction considered, the first defines the configuration and current profiles 1 to 10, and the second defines the configuration and current profiles 11 to 14.

INPMOD SET 1, In-plane Current

```

*** I N P M O D INPUT FILE ***
'-----
'
INPMOD IDENTIFICATION TEXT 3.6
'
SLWR from Turret Moored FPSO
10" API X65 Steel Grade Riser Pipe, 1100 m WD
Adekunle Peter Orimolade - April 2014
'
UNIT NAME SPECification
' UTime  ULength  UMass   UForce   GRAV   GCONS
  s      m      kg      N      9.81  1.0
' seconds meter kilograms Newtons          m/s^2
'-----
'----- RISER SYSTEM SPECIFICATION -----
'-----
'   Super nodes
'   Lines
'   Segments
'
'   Elements
'-----
NEW SINGLE RISER
'-----
'iatyp idris
AR LONG
ARBITRARY SYSTEM AR
'nsnod  nlin  nsnfix  nves  no-of rigid-snodes
  4     3     2     1     0
'ibtang  zbot  ibot3D
  1    -1100  0
' Seafloor support conditions
' stfbot  stfjaxi  stflat  frijaxi  frilat
  1.0E6  1.0E5    1.0E0   0.3     0.5
' ilinty  isnod1  isnod2
  1     1     2
  2     2     3

```

```

3 3 4
,
' Boundary Conditions - upper end
' isnod ipos ix iy iz irx iry irz
1 1 1 1 1 1 1 1 GLOBAL
' x0 y0 z0 x1 y1 z1 rot dir
0 0 -500 60 0 -12 82
,
' Boundary Conditions - lower end
' isnod ipos ix iy iz irx iry irz
4 0 1 1 1 1 1 1 GLOBAL
' x0 y0 z0 x1 y1 z1 rot dir
2100 0 -500 1380.41 0.0 -1100
,
,
' Free nodes
' isnod X Y Z
2 1239 0 -500
3 1659 0 -500
,
' xg, yg, zg: Coordinates for vessel contact
' ives idhfr xg yg zg headng
1 ASGA 0.0 0.0 0.0 0.0
,
-----
'----- LINE DATA -----
'-----
NEW LINE DATA
'-----
' ilinty nseg icnlty ifluty
1 6 0 98
' icmpty icnlty iexwty nelseg slgth
1 0 0 4 2
1 0 0 16 8
1 0 0 40 20
1 0 0 54 270
1 0 0 110 550
1 0 0 78 389
'-----
NEW LINE DATA
'-----
' ilinty nseg icnlty ifluty
2 2 0 98
' icmpty icnlty iexwty nelseg slgth
1 0 3 255 255
1 0 3 165 165

```

NEW LINE DATA

```

'-----
'ilinty nseg icnlty ifluty
 3   3   0   98
'icmpty icnlty iexwty nelseg slgth
 1   0   0   125   125
 1   0   0   150   150
 1   0   0   33   166

```

```

'-----
'Total                2100

```

```

'10" Pipe with coating and Cd=1
'-----

```

NEW COMPONENT CRS1

```

'icmpty temp
 1  10
'ams  ae      ai  rgyr  ast  wst  dst  thst
235  0.16188  0.05067  0.0990  0.02191  0.001414  0.3040  0.0250
'iea iej igt ipress imf
 1  1  1  0
'ea
 4.536E9
'ej
 4.449E7
'gt
 3.422E7
'Hydrodynamic force coefficients
'cqx  cqy  cax  cay  clx  cly  icode  d
 0.0  1.0  0.  1.0  0.  0.  2  0.454
'tb  ycurmx
 1  1

```

```

'Distributed Buoyancy Module
'-----

```

NEW COMPONENT EXT1

```

'icmpty
 3
'AMS  AE      RGYR  FRAC
815.83  2.065  0.6166  0.1403
'Hydrodynamic force coefficients
'CDX  CDY  AMX  AMY  CDLX  CDLY
 1.0  1.0  0.5  1.0  0  0

```



```

'
'-----INTERNAL FLUID OIL-----
NEW COMPONENT FLUID
' icmpty
  98
'
' rhoi vveli pressi dpres idir
  800.0 0.0 34.5e3 0.0 2
'
'-----INTERNAL FLUID SEA WATER-----
NEW COMPONENT FLUID
' icmpty
  99
'
' rhoi vveli pressi dpres idir
  1025.0 0.0 0.0 0.0 2
'
'----- ENVIRONMENTAL DESCRIPTION -----
'-----
ENVIronment IDENtification
' Descriptive text one line (A60)
  Current conditions
'idenv
  ENV
'
WATErdepth AND WAVetype
'wdepth noirw norw ncusta
  1100 0 0 10
'
ENVIronment CONStants
'airden watden wakivi
  1.3 1025 1.35E-6
'
'----- Profile 1
NEW CURRENT STATE
' Omni dir 1year extream
' icusta ncuelv
  1 6
' curelv curdir curvel
  -10.0 180 0.067
  -50.0 180 0.058
  -200.0 180 0.044
  -500.0 180 0.039
  -1000.0 180 0.034

```

```

-1500.0 180 0.022
,
'----- Profile 2
NEW CURRENT STATE
' Omni dir 1year extream
' icusta ncuelv
  2   6
' curelv  curdir curvel
  -10.0 180 0.105
  -50.0 180 0.092
  -200.0 180 0.081
  -500.0 180 0.069
  -1000.0 180 0.060
  -1500.0 180 0.042
,
'----- Profile 3
NEW CURRENT STATE
' Omni dir 1year extream
' icusta ncuelv
  3   6
' curelv  curdir curvel
  -10.0 180 0.139
  -50.0 180 0.122
  -200.0 180 0.112
  -500.0 180 0.093
  -1000.0 180 0.081
  -1500.0 180 0.057
,
'----- Profile 4
NEW CURRENT STATE
' Omni dir 1year extream
' icusta ncuelv
  4   6
' curelv  curdir curvel
  -10.0 180 0.174
  -50.0 180 0.152
  -200.0 180 0.141
  -500.0 180 0.115
  -1000.0 180 0.099
  -1500.0 180 0.071
,
'----- Profile 5
NEW CURRENT STATE
' Omni dir 1year extream
' icusta ncuelv
  5   6
' curelv  curdir curvel

```

```

-10.0 180 0.210
-50.0 180 0.182
-200.0 180 0.171
-500.0 180 0.137
-1000.0 180 0.116
-1500.0 180 0.085
,
'----- Profile 6
NEW CURRENT STATE
' Omni dir 1year extream
' icusta ncuelv
  6 6
' curelv curdir curvel
  -10.0 180 0.251
  -50.0 180 0.215
  -200.0 180 0.202
  -500.0 180 0.160
  -1000.0 180 0.135
  -1500.0 180 0.100
,
'----- Profile 7
NEW CURRENT STATE
' Omni dir 1year extream
' icusta ncuelv
  7 6
' curelv curdir curvel
  -10.0 180 0.297
  -50.0 180 0.253
  -200.0 180 0.238
  -500.0 180 0.185
  -1000.0 180 0.155
  -1500.0 180 0.116
,
'----- Profile 8
NEW CURRENT STATE
' Omni dir 1year extream
' icusta ncuelv
  8 6
' curelv curdir curvel
  -10.0 180 0.355
  -50.0 180 0.300
  -200.0 180 0.281
  -500.0 180 0.215
  -1000.0 180 0.178
  -1500.0 180 0.135
,

```

```
'----- Profile 9
NEW CURRENT STATE
' Omni dir 1year extream
' icusta ncuelv
  9   6
' curelv  curdir curvel
  -10.0  180  0.435
  -50.0  180  0.363
  -200.0 180  0.339
  -500.0 180  0.254
  -1000.0 180 0.208
  -1500.0 180 0.160
,
'----- Profile 10
NEW CURRENT STATE
' Omni dir 1year extream
' icusta ncuelv
  10  6
' curelv  curdir curvel
  -10.0  180  0.510
  -50.0  180  0.422
  -200.0 180  0.391
  -500.0 180  0.290
  -1000.0 180 0.235
  -1500.0 180 0.182
,
'-----
'----- SUPPORT VESSEL DATA -----
'-----
TRANSfer FUNcTION FILE
'chftra
Aasgard-A.rif
,
END
INPMOD SET 2, In-plane Current

'*** I N P M O D INPUT FILE ***
'-----
,
INPMod IDENtification TEXT 3.6
,
SLWR from Turret Moored FPSO
10" API X65 Steel Grade Riser Pipe, 1100 m WD
Adekunle Peter Orimolade - April 2014
,
```

UNIT NAME SPECification

```
' UTime  ULength UMass  UForce  GRAV  GCONS
  s      m      kg      N      9.81  1.0
' seconds meter kilograms Newtons          m/s^2
```

----- RISER SYSTEM SPECIFICATION -----

```
' Super nodes
' Lines
' Segments
' Elements
```

----- NEW SINGLE RISER -----

```
' iatyp idris
AR LONG
ARBITRARY SYSTEM AR
' nsnod nlin nsnfix nves no-of rigid-snodes
  4    3    2    1    0
' ibtang zbot ibot3D
  1  -1100  0
' Seafloor support conditions
' stfbot stfjaxi stflat frijaxi frilat
  1.0E6  1.0E5  1.0E0  0.3  0.5
' ilinty isnod1 isnod2
  1    1    2
  2    2    3
  3    3    4
'
' Boundary Conditions - upper end
' isnod ipos ix iy iz irx iry irz
  1    1    1    1    1    1    1    1 GLOBAL
' x0 y0 z0 x1 y1 z1 rot dir
  0    0  -500    60    0  -12  82
'
' Boundary Conditions - lower end
' isnod ipos ix iy iz irx iry irz
  4    0    1    1    1    1    1    1 GLOBAL
' x0 y0 z0 x1 y1 z1 rot dir
  2100    0  -500  1380.41  0.0  -1100
'
' Free nodes
' isnod X Y Z
  2    1239  0  -500
  3    1659  0  -500
'
```

' xg, yg, zg: Coordinates for vessel contact

'ives idhfr xg yg zg headng
1 ASGA 0.0 0.0 0.0 0.0

'----- LINE DATA -----

NEW LINE DATA

' ilinty nseg icnlty ifluty

1 6 0 98

'icmpty icnlty iexwty nelseg slgth

1 0 0 4 2

1 0 0 16 8

1 0 0 40 20

1 0 0 54 270

1 0 0 110 550

1 0 0 78 389

NEW LINE DATA

' ilinty nseg icnlty ifluty

2 2 0 98

'icmpty icnlty iexwty nelseg slgth

1 0 3 255 255

1 0 3 165 165

NEW LINE DATA

' ilinty nseg icnlty ifluty

3 3 0 98

'icmpty icnlty iexwty nelseg slgth

1 0 0 125 125

1 0 0 150 150

1 0 0 33 166

'Total -----
2100

'10" Pipe with coating and Cd=1

NEW COMPONENT CRS1

' icmpty temp

1 10

'ams ae ai rgyr ast wst dst thst

235 0.16188 0.05067 0.0990 0.02191 0.001414 0.3040 0.0250

```

'iea iej igt ipress imf
  1 1 1 0
'ea
  4.536E9
'ej
  4.449E7
'gt
  3.422E7
'Hydrodynamic force coefficients
'cqx cqy cax cay clx cly icode d
  0.0 1.0 0. 1.0 0. 0. 2 0.454
'tb      ycurmx
  1      1
'
'Distributed Buoyancy Module
'-----
NEW COMPONENT EXT1
'icmpty
  3
'AMS    AE      RGYR    FRAC
  815.83 2.065  0.6166 0.1403
'
'Hydrodynamic force coefficients
'CDX CDY AMX AMY CDLX CDLY
  1.0 1.0 0.5 1.0 0 0
'
'-----INTERNAL FLUID OIL-----
NEW COMPONENT FLUID
'icmpty
  98
'
'rhoi vveli pressi dpres idir
  800.0 0.0 34.5e3 0.0 2
'
'-----INTERNAL FLUID SEA WATER-----
NEW COMPONENT FLUID
'icmpty
  99
'
'rhoi vveli pressi dpres idir
  1025.0 0.0 0.0 0.0 2
'
'----- ENVIRONMENTAL DESCRIPTION -----
'-----

```

```

,
ENVIronment IDENtification
'Descriptive text one line (A60)
  Current conditions
'idenv
ENV
,
WATERdepth AND WAVetype
'wdepth noirw norw ncusta
  1100  0  0  4
,
ENVIronment CONSTants
'airden watden wakivi
  1.3  1025  1.35E-6
,
-----
'----- Profile 11
NEW CURRENT STATE
'Omni dir 1year extream
'icusta ncuelv
  1  6
'curelv curdir curvel
  -10.0  180  0.545
  -50.0  180  0.449
  -200.0  180  0.415
  -500.0  180  0.306
  -1000.0  180  0.247
  -1500.0  180  0.192
,
'----- Profile 12
NEW CURRENT STATE
'Omni dir 1year extream
'icusta ncuelv
  2  6
'curelv curdir curvel
  -10.0  180  0.591
  -50.0  180  0.484
  -200.0  180  0.445
  -500.0  180  0.326
  -1000.0  180  0.262
  -1500.0  180  0.205
,
'----- Profile 13
NEW CURRENT STATE
'Omni dir 1year extream
'icusta ncuelv

```



```

3    6
' curelv  curdir  curvel
  -10.0  180  0.658
  -50.0  180  0.535
 -200.0  180  0.490
 -500.0  180  0.355
-1000.0  180  0.283
-1500.0  180  0.223
,
' ----- Profile 14
NEW CURRENT STATE
' Omni dir 1year extream
' icusta ncuelv
  4    6
' curelv  curdir  curvel
  -10.0  180  0.793
  -50.0  180  0.636
 -200.0  180  0.577
 -500.0  180  0.412
-1000.0  180  0.325
-1500.0  180  0.259
,
'-----
'----- SUPPORT VESSEL DATA -----
'-----
TRANSfer FUNCtion FILE
'chftra
Aasgard-A.rif
,
END

```

B.4.2 STAMOD

The data presented represent the base STAMOD input file, for each current profile the corresponding “icurin” number must be specified to account for current effect from that particular current profile.

```

'*** STAMOD INPUT FILE ***
,
STAMod CONTrol INFOrmation 3.6
,
'Three lines of identification text (A60)

```

```
,
SLWR from Turret Moored FPSO
10" API X65 Steel Grade Riser Pipe, 1100 m WD
Adekunle Peter Orimolade - April 2014
'---
'irunco idris ianal iprdat iprcat iprfem iprform iprpor
  1  LONG  1  5  1  1  0  0
'---
RUN IDENTification
'idres
SHAPE
'---
ENVIronment REFERENCE IDENTifier
'idenv
ENV
'---
STATIC CONDition INPUT
'nlcomp icurin curfac lcons
  0  1  1.0  1
'---
COMPUTational PROCEDURE
FEM
FEM ANALYSIS PARAMeters
'
LOAD GROUP DATA
'nstep maxit racu
  10  50  1.E-5
'lotype
  VOLU
'
LOAD GROUP DATA
'nstep maxit racu
  100  50  1.E-5
'lotype
  DISP
'
LOAD GROUP DATA
'nstep maxit racu
  10  50  1.E-5
'lotype
  FRIC
'
LOAD GROUP DATA
'nstep maxit racu
  10  50  1.E-5
'lotype
```

```

CURR
'-----
END
'-----
' --
'PARAMETRIC VARIATION DEFINITION
' nstvar iofpos icuvar ifovar maxipv racupv
' 10 1 0 0 1 0.00001
'STATIC OFFSET INCREMENT
' iref dxoff dyoff dzof irot drot
' -1 0.2 0.0 0.0 0 0.0
'
'STAMOD PRINT CONTROL
' istep isfor ispos
' 10 0 1
'
'END

```

B.4.3 VIVANA

The third input file is the VIVANA file, and a sample is presented here for the C2-curve.

```

VIVANA CONTROL INFORMATION
'
SLWR from Turret Moored FPSO VIV Analysis
10" API X65 Steel Grade Riser Pipe, 1100 m WD
Adekunle Peter Orimolade - April 2014
'
' idris idstat idenv temp
LONG SHAPE ENV 20
'-----
'
WORK ARRAY DIMENSION
' nwiwa
9000000
'-----
'
EIGENVALUE ANALYSIS PARAMETERS
' neig nvec
35 35
' eps1 eps2 eps3 ksr maxit kex shift maxniv
0.0 0.0 0.0 1 7 0 0.0 0

```

'
'
EIGENVALUE PRINT OPTIONS

```
' npeig npvec  
  35   35
```

'
'
SECTION PROPERTY SPECIFICATION

```
' nsegp  
  11  
' isegp iexczo iaddma iliftc idampg istrou  
  1  0    0    0    0    1  
  2  0    0    0    0    1  
  3  0    0    0    0    1  
  4  0    0    0    0    1  
  5  0    0    0    0    1  
  6  0    0    0    0    1  
  7  0    0    0    0    1  
  8  0    0    0    0    1  
  9  0    0    0    0    1  
 10  0    0    0    0    1  
 11  0    0    0    0    1
```

'
'
PROPERTY EXCITATION ZONE

```
' nexzon  
  2  
' iprono cprpid fhmin fhmax  
  2  Exc_norm 0.125  0.2  
  1  Excit_02 0.125  0.2
```

'
'
PROPERTY DAMPING FACTORS

```
' ndpfac  
  4  
' iprono cprpid fstill flowv fhighv
```

1	Dmp_norm	1.0	1.0	1.1
2	Damp_01	1.0	0.8	1.14
3	Damp_02	1.0	0.9	1.13
4	Damp_03	1.2	0.3	1.12

PROPERTY STROUHAL SPECIFICATION

```
' nstrsp
  2
' iprono cprpdi npudsc strou
  1 Strou_01 16 0.
' reynum strnum
  40. 0.1
  100. 0.18
  200. 0.19
  400. 0.195
  1000. 0.20
  4000. 0.205
  10000. 0.21
  40000. 0.215
  100000. 0.22
  200000. 0.4
  300000. 0.45
  500000. 0.45
  800000. 0.25
  1000000. 0.23
  4000000. 0.25
  10000000. 0.27
```

```
' iprono cprpid npudsc strou
  2 Strou_02 0 0.17
```

PROPERTY ADDED MASS

```
' nadcur
  2
' iprono cprpid nampt
  1 Admas_01 12
```

'fhat addmco

0.0 -0.6
 0.15 -0.6
 0.16 -0.3
 0.17 1.7
 0.18 2.0
 0.2 2.2
 0.21 2.0
 0.24 1.7
 0.27 1.5
 0.33 1.2
 0.40 1.0
 0.5 1.0

,

'iprono cprpid nampt

2 Admas_02 10

'fhat addmco

0.0 -0.4
 0.16 -0.2
 0.17 1.5
 0.18 2.0
 0.2 2.2
 0.21 2.0
 0.24 1.7
 0.27 1.5
 0.33 1.2
 0.5 1.2

,

,

PROPERTY LIFT COEFFICIENT

'nlccur

1

'iprono cprpid nlcpt

1 Test_211 26

'fhat acl0 aclmax clmax cla0

0.120 0.149 0.100 0.10 0.000
 0.125 0.266 0.200 0.10 0.000
 0.127 0.400 0.214 0.10 0.016
 0.130 0.451 0.235 0.10 0.040

```

0.135 0.505 0.270 0.10 0.080
0.140 0.530 0.350 0.14 0.110
0.150 0.588 0.450 0.20 0.180
0.160 0.658 0.500 0.35 0.240
0.165 0.746 0.500 0.50 0.300
0.168 0.890 0.460 0.78 0.350
0.172 0.900 0.430 0.80 0.400
0.175 0.837 0.400 0.70 0.200
0.180 0.761 0.400 0.40 0.100
0.185 0.706 0.400 0.30 0.000
0.190 0.666 0.400 0.20 0.000
0.200 0.615 0.380 0.10 0.000
0.210 0.592 0.350 0.10 0.000
0.220 0.575 0.313 0.10 0.000
0.230 0.539 0.275 0.10 0.000
0.240 0.504 0.238 0.10 0.000
0.250 0.420 0.200 0.10 0.000
0.270 0.312 0.160 0.10 0.000
0.280 0.247 0.140 0.10 0.000
0.290 0.186 0.120 0.10 0.000
0.300 0.160 0.100 0.10 0.000
0.310 0.136 0.090 0.10 0.000

```

RESPONSE ANALYSIS PARAMETERS

' reldam gives damping as fraction of critical damping

```

' reldam  conlim  max_iter  iprint  ilim  iuddf
  0.01    0.010    30      1      2

```

' idomfrq

' 2

' 1

VIVANA RESULT PRINT

```

' iprelf  iprstf  iprdrg  iprrsp  iprcng
  0      0      0      0      0

```

VIVRESPONSE FATIGUE DAMAGE

```
' nsect npcs ioppr
  0  4  0
' dscfa dscfy dscfz  asi  wsti
  1.2  1.2  1.2
'
' NOTE: rfact scales stresses from Pa (STAMOD) to MPa for
'   fatigue analysis using SN curves
' nosl limind fatlim rfact
  1  0  0.0  .000001
' rmi1 rci1
  3.0  11.901
'-----
'
END
```


Appendix C – Fatigue Results

This section of the appendix give wave-induced fatigue damage results for each of the 12 wave directions considered. It also gives plots of VIV fatigue damage covering all the 14 current profiles.

C.1 Fatigue Response Results – Wave Heading 0

Table C.1.1 Fatigue Response Summary C2-curve

Worst Damage	
Damage over total exposure	0.00121
Total exposure time (years)	1.0
Life (years)	825
Arc Length (m)	9.0
Theta (deg)	180.0

Table C.1.2 Fatigue Response Summary D-curve

Worst Damage	
Damage over total exposure	0.00188
Total exposure time (years)	1.0
Life (years)	531
Arc Length (m)	9.0
Theta (deg)	180.0

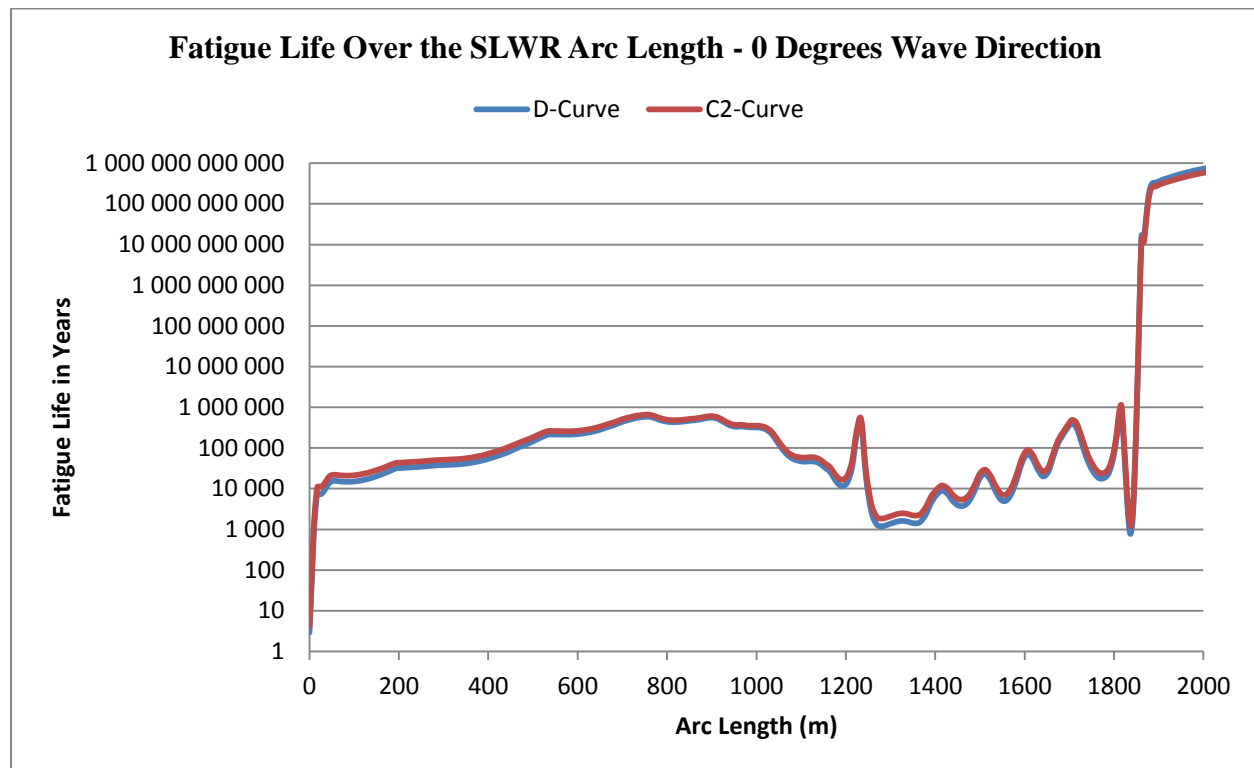


Figure C.1 Wave Induced Fatigue Life – 0 Degrees Wave Direction

C.2 Fatigue Response Results – Wave Heading 30

Table C.2.1 Fatigue Response Summary C2-curve

Worst Damage	
Damage over total exposure	0.00121
Total exposure time (years)	1.0
Life (years)	828
Arc Length (m)	9.0
Theta (deg)	157.5

Table C.2.2 Fatigue Response Summary D-curve

Worst Damage	
Damage over total exposure	0.00188
Total exposure time (years)	1.0
Life (years)	532
Arc Length (m)	9.0
Theta (deg)	157.5

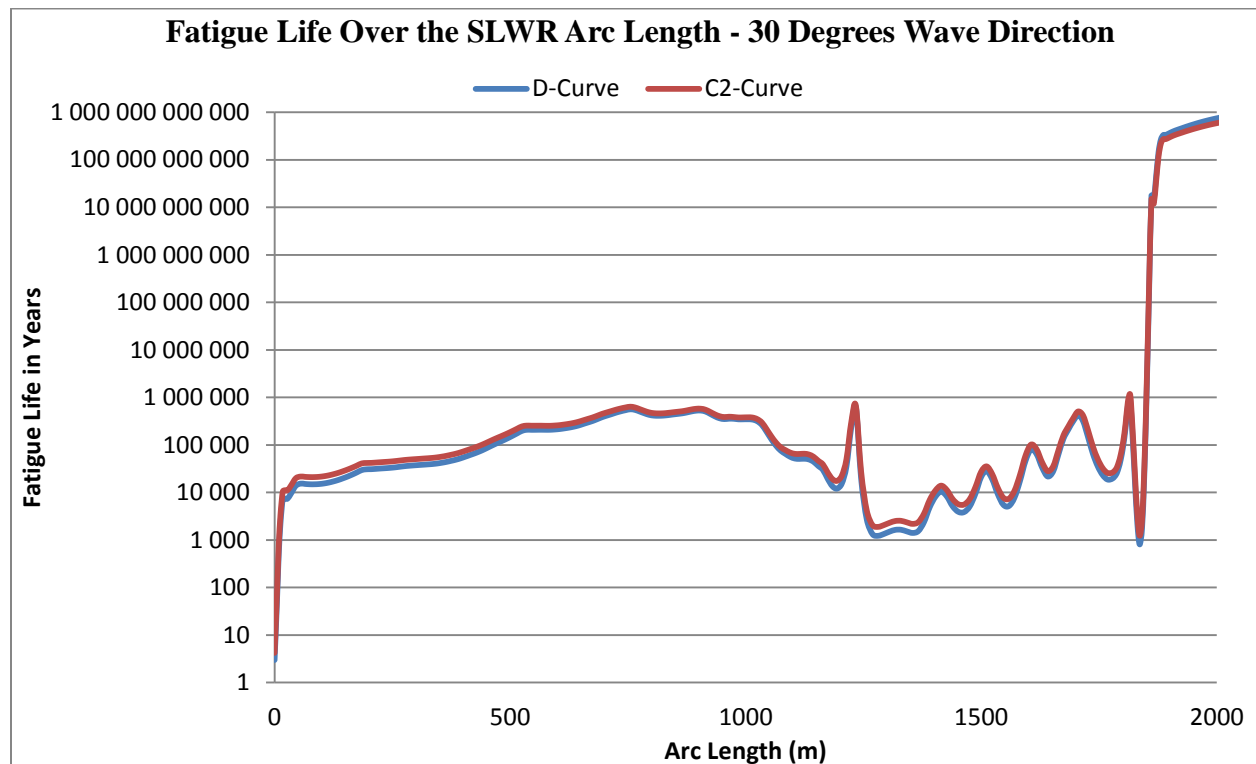


Figure C.2 Wave Induced Fatigue Life – 30 Degrees Wave Direction

C.3 Fatigue Response Results – Wave Heading 60

Table C.3.1 Fatigue Response Summary C2-curve

Worst Damage	
Damage over total exposure	0.00132
Total exposure time (years)	1.0
Life (years)	756
Arc Length (m)	9.0
Theta (deg)	112.5

Table C.3.2 Fatigue Response Summary D-curve

Worst Damage	
Damage over total exposure	0.00205
Total exposure time (years)	1.0
Life (years)	487
Arc Length (m)	9.0
Theta (deg)	112.5

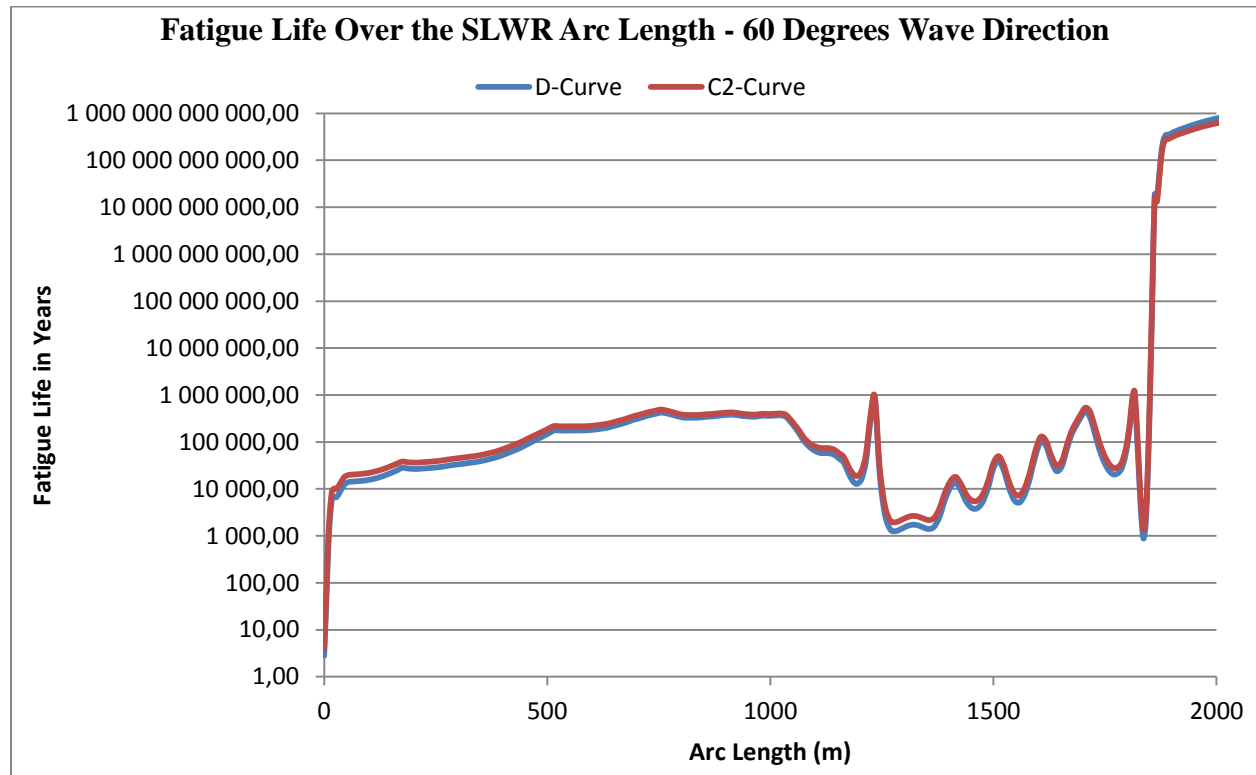


Figure C.3 Wave Induced Fatigue Life – 60 Degrees Wave Direction

C.4 Fatigue Response Results – Wave Heading 90

Table C.4.1 Fatigue Response Summary C2-curve

Worst Damage	
Damage over total exposure	0.00153
Total exposure time (years)	1.0
Life (years)	652
Arc Length (m)	9.0
Theta (deg)	90

Table C.4.2 Fatigue Response Summary D-curve

Worst Damage	
Damage over total exposure	0.00238
Total exposure time (years)	1.0
Life (years)	421
Arc Length (m)	9.0
Theta (deg)	90

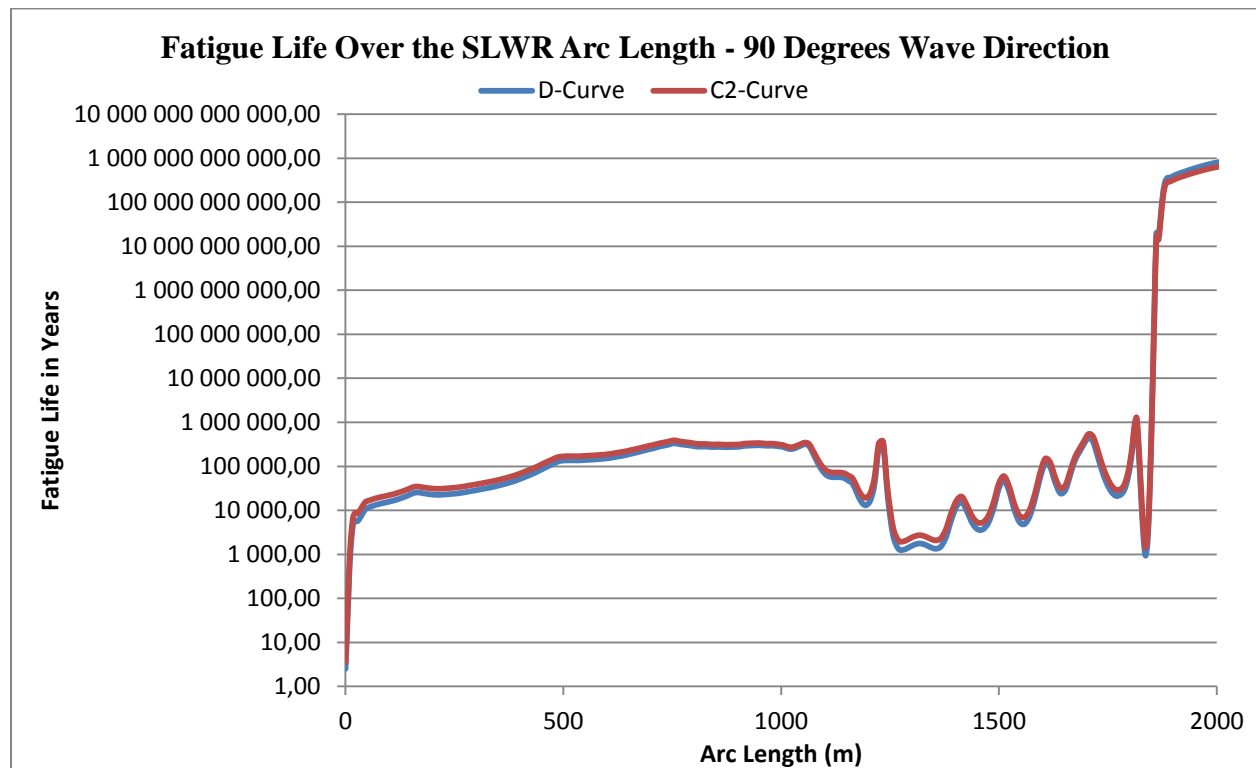


Figure C.4 Wave Induced Fatigue Life – 90 Degrees Wave Direction

C.5 Fatigue Response Results – Wave Heading 120

Table C.5.1 Fatigue Response Summary C2-curve

Worst Damage	
Damage over total exposure	0.00172
Total exposure time (years)	1.0
Life (years)	581
Arc Length (m)	9.0
Theta (deg)	67.5

Table C.5.2 Fatigue Response Summary D-curve

Worst Damage	
Damage over total exposure	0.00266
Total exposure time (years)	1.0
Life (years)	376
Arc Length (m)	9.0
Theta (deg)	67.5

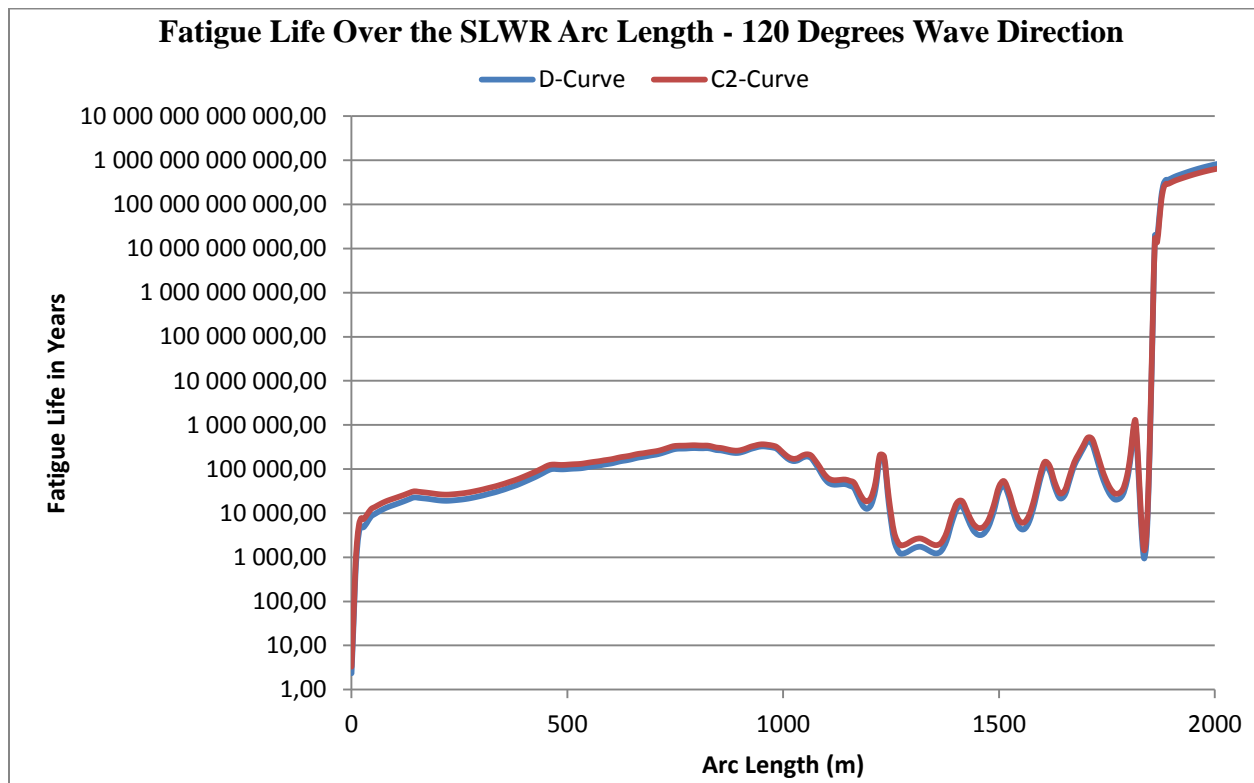


Figure C.5 Wave Induced Fatigue Life – 120 Degrees Wave Direction

C.6 Fatigue Response Results – Wave Heading 150

Table C.6.1 Fatigue Response Summary C2-curve

Worst Damage	
Damage over total exposure	0.00200
Total exposure time (years)	1.0
Life (years)	501
Arc Length (m)	9.0
Theta (deg)	22.5

Table C.6.2 Fatigue Response Summary D-curve

Worst Damage	
Damage over total exposure	0.00308
Total exposure time (years)	1.0
Life (years)	325
Arc Length (m)	9.0
Theta (deg)	22.5

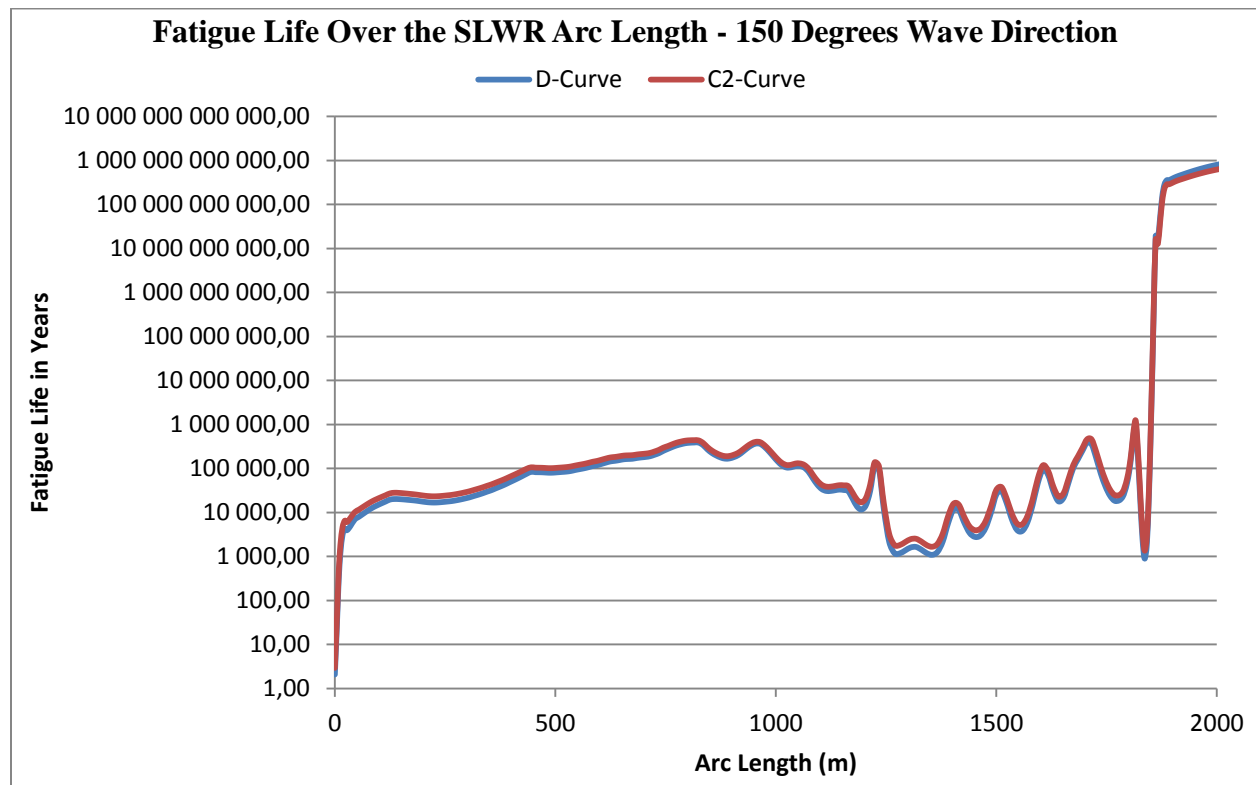


Figure C.6 Wave Induced Fatigue Life – 150 Degrees Wave Direction

C.7 Fatigue Response Results – Wave Heading 180

Table C.7.1 Fatigue Response Summary C2-curve

Worst Damage	
Damage over total exposure	0.00213
Total exposure time (years)	1.0
Life (years)	469
Arc Length (m)	9.0
Theta (deg)	0.0

Table C.7.2 Fatigue Response Summary D-curve

Worst Damage	
Damage over total exposure	0.00328
Total exposure time (years)	1.0
Life (years)	305
Arc Length (m)	9.0
Theta (deg)	0.0

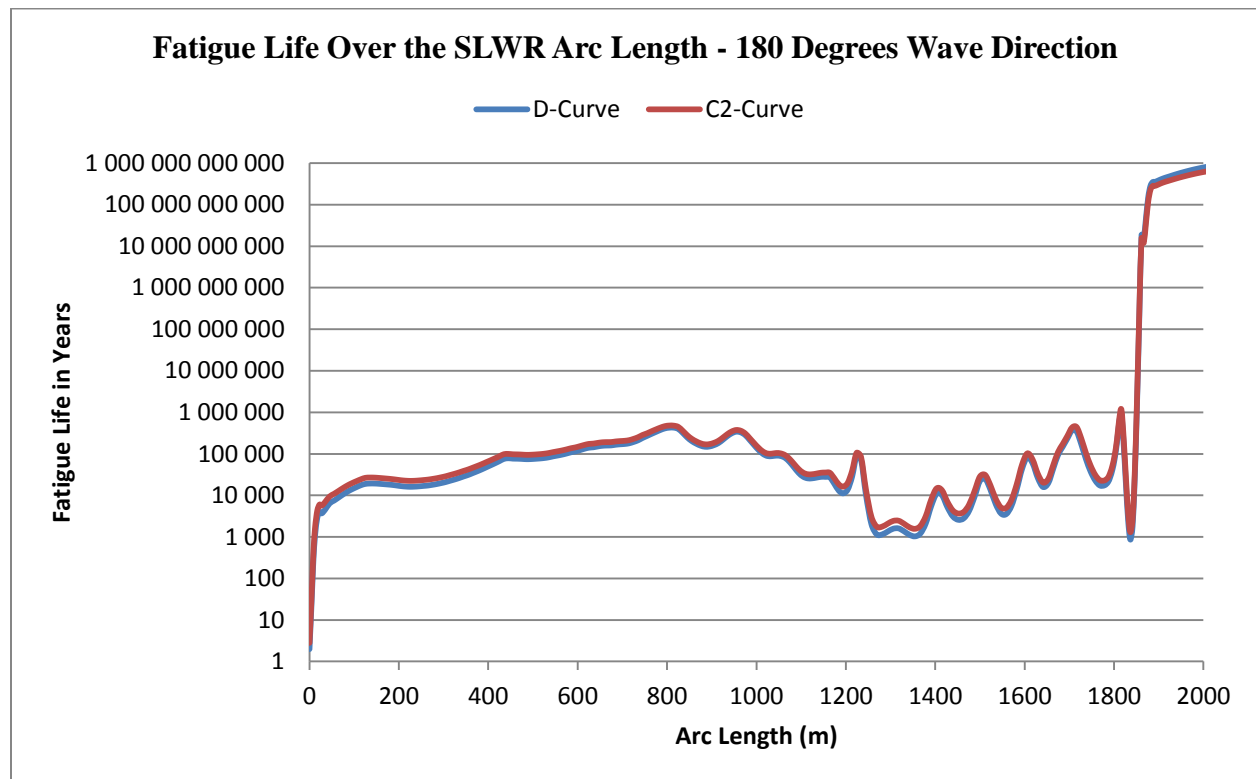


Figure C.7 Wave Induced Fatigue Life – 180 Degrees Wave Direction

C.8 Fatigue Response Results – Wave Heading 210

Table C.8.1 Fatigue Response Summary C2-curve

Worst Damage	
Damage over total exposure	0.00200
Total exposure time (years)	1.0
Life (years)	501
Arc Length (m)	9.0
Theta (deg)	337.5

Table C.8.2 Fatigue Response Summary D-curve

Worst Damage	
Damage over total exposure	0.00308
Total exposure time (years)	1.0
Life (years)	325
Arc Length (m)	9.0
Theta (deg)	337.5

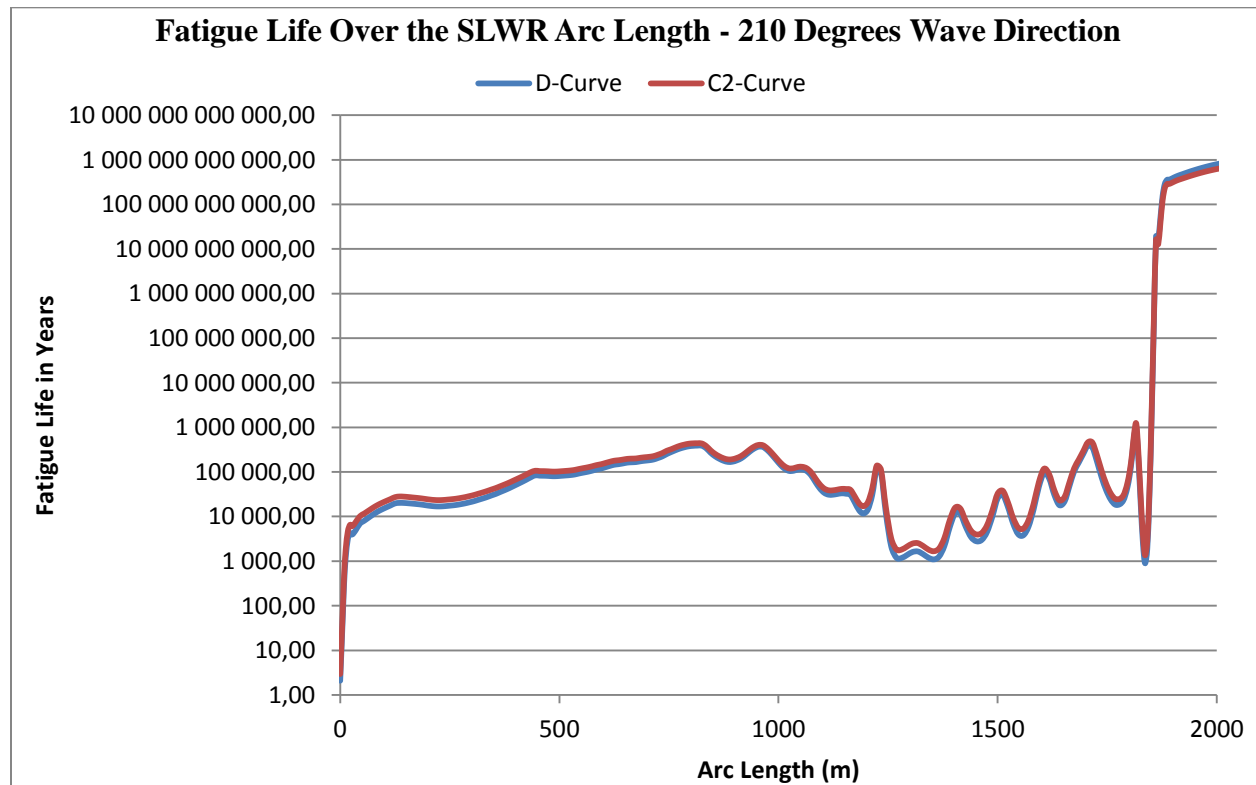


Figure C.8 Wave Induced Fatigue Life – 210 Degrees Wave Direction

C.9 Fatigue Response Results – Wave Heading 240

Table C.9.1 Fatigue Response Summary C2-curve

Worst Damage	
Damage over total exposure	0.00172
Total exposure time (years)	1.0
Life (years)	581
Arc Length (m)	9.0
Theta (deg)	292.5

Table C.9.2 Fatigue Response Summary D-curve

Worst Damage	
Damage over total exposure	0.00288
Total exposure time (years)	1.0
Life (years)	376
Arc Length (m)	9.0
Theta (deg)	292.5

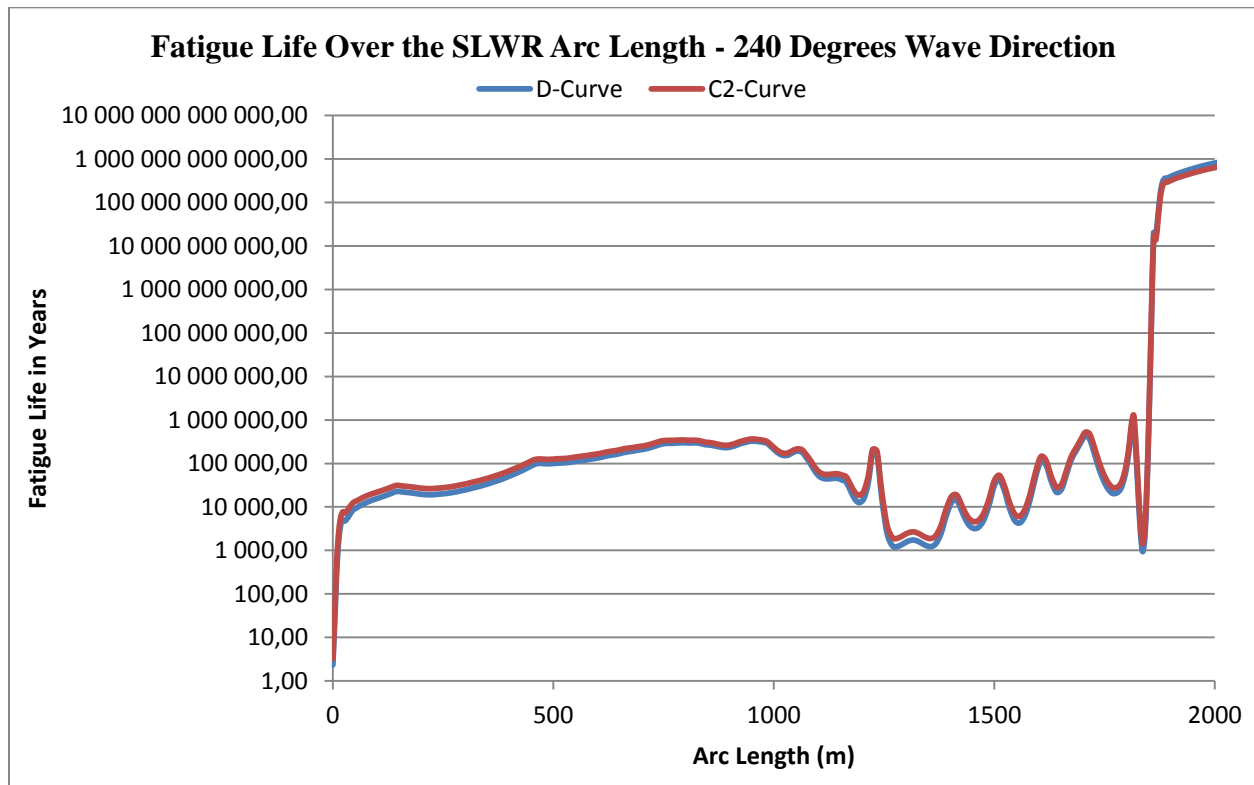


Figure C.9 Wave Induced Fatigue Life – 240 Degrees Wave Direction

C.10 Fatigue Response Results – Wave Heading 270

Table C.10.1 Fatigue Response Summary C2-curve

Worst Damage	
Damage over total exposure	0.00153
Total exposure time (years)	1.0
Life (years)	652
Arc Length (m)	9.0
Theta (deg)	270

Table C.10.2 Fatigue Response Summary D-curve

Worst Damage	
Damage over total exposure	0.00238
Total exposure time (years)	1.0
Life (years)	421
Arc Length (m)	9.0
Theta (deg)	270

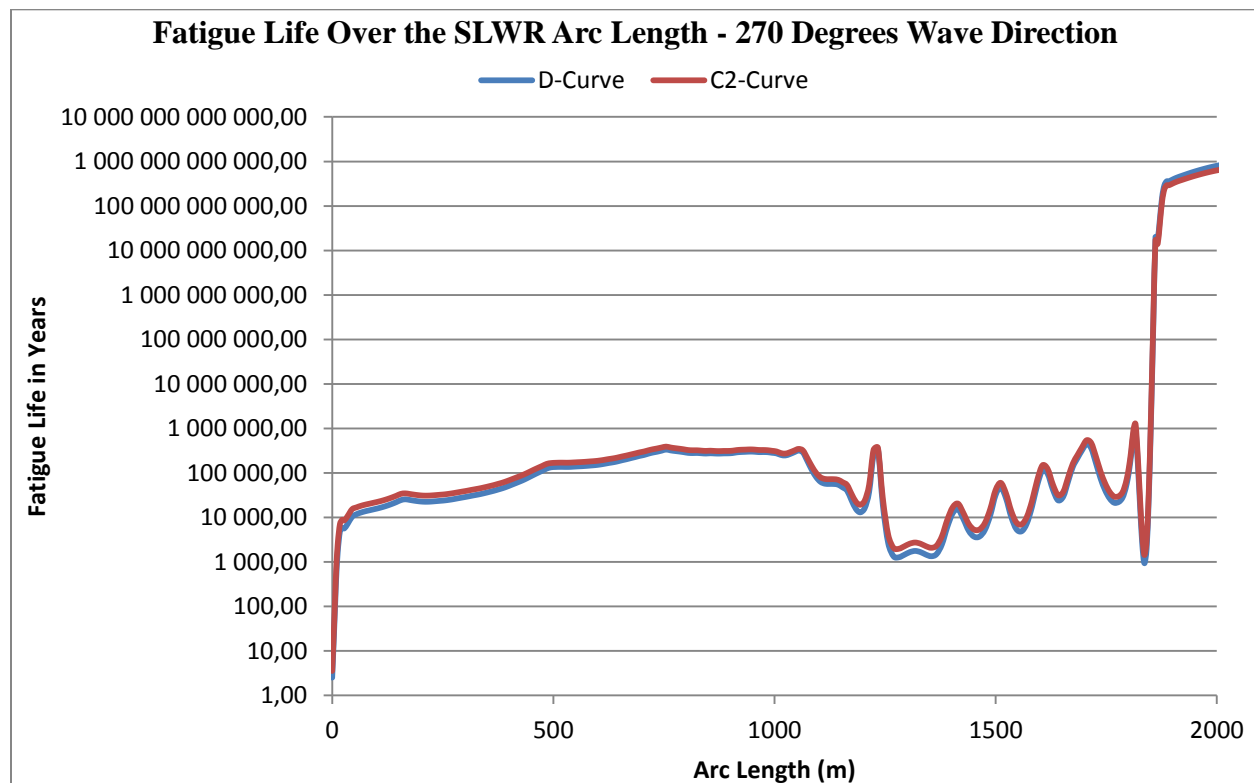


Figure C.10 Wave Induced Fatigue Life – 270 Degrees Wave Direction

C.11 Fatigue Response Results – Wave Heading 300

Table C.11.1 Fatigue Response Summary C2-curve

Worst Damage	
Damage over total exposure	0.00132
Total exposure time (years)	1.0
Life (years)	757
Arc Length (m)	9.0
Theta (deg)	247.5

Table C.11.2 Fatigue Response Summary D-curve

Worst Damage	
Damage over total exposure	0.00205
Total exposure time (years)	1.0
Life (years)	487
Arc Length (m)	9.0
Theta (deg)	247.5

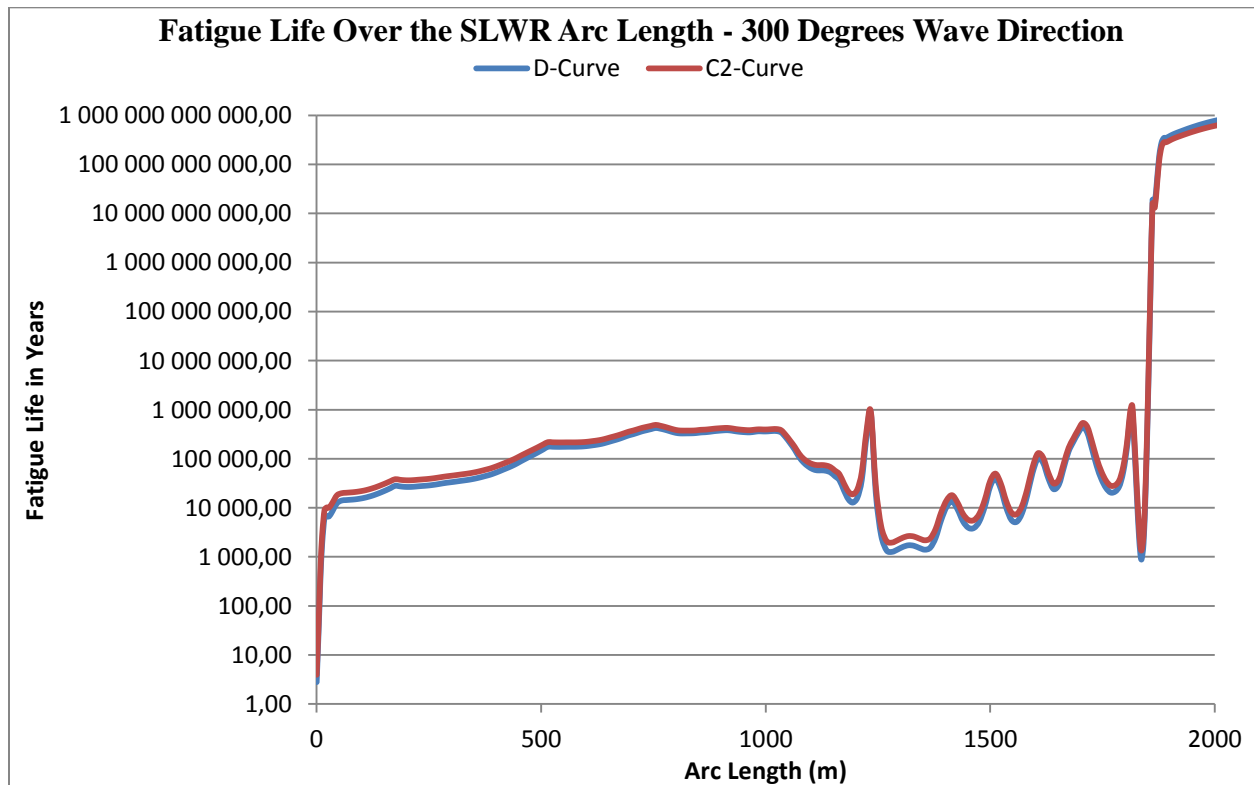


Figure C.11 Wave Induced Fatigue Life – 300 Degrees Wave Direction

C.12 Fatigue Response Results – Wave Heading 330

Table C.12.1 Fatigue Response Summary C2-curve

Worst Damage	
Damage over total exposure	0.00121
Total exposure time (years)	1.0
Life (years)	828
Arc Length (m)	9.0
Theta (deg)	202.5

Table C.12.2 Fatigue Response Summary D-curve

Worst Damage	
Damage over total exposure	0.00188
Total exposure time (years)	1.0
Life (years)	532
Arc Length (m)	9.0
Theta (deg)	202.5

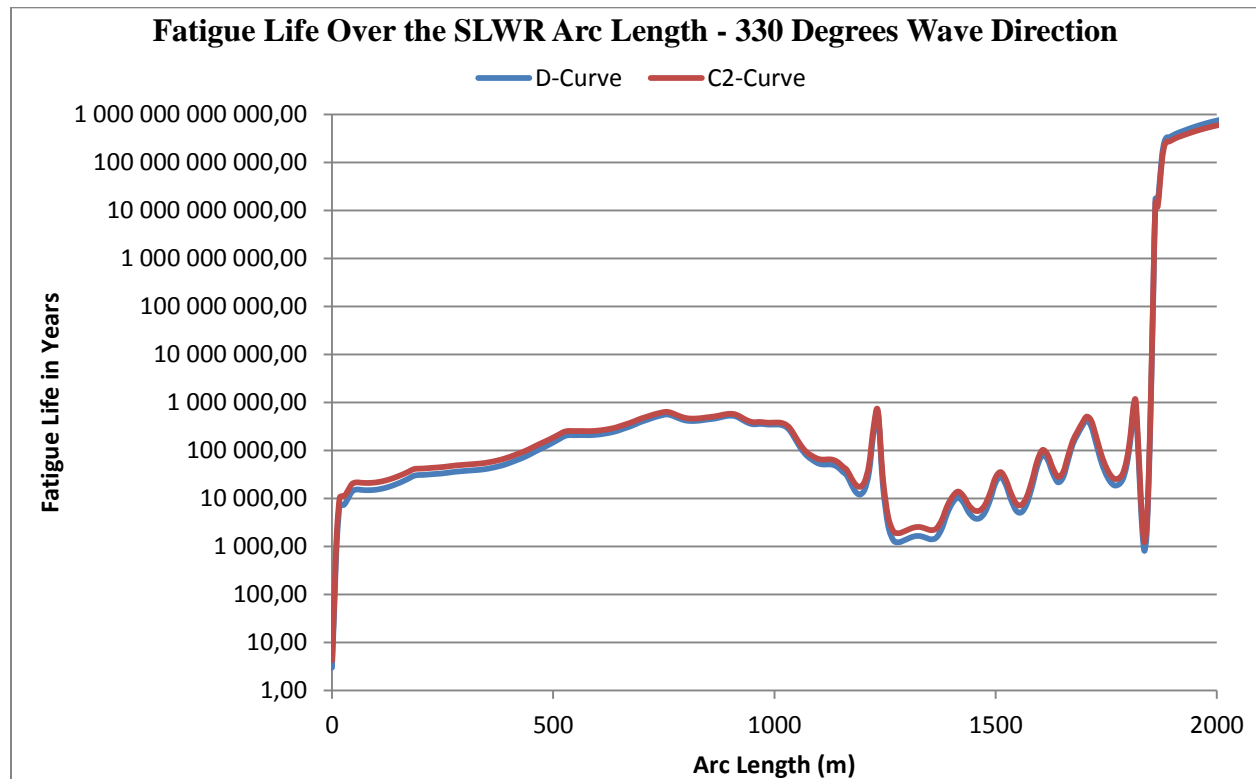


Figure C.12 Wave Induced Fatigue Life – 330 Degrees Wave Direction

C.13 VIV Fatigue Response Results

The following plots showed the raw VIV fatigue damage results resulting from the 14 current profiles, C1 – C14.

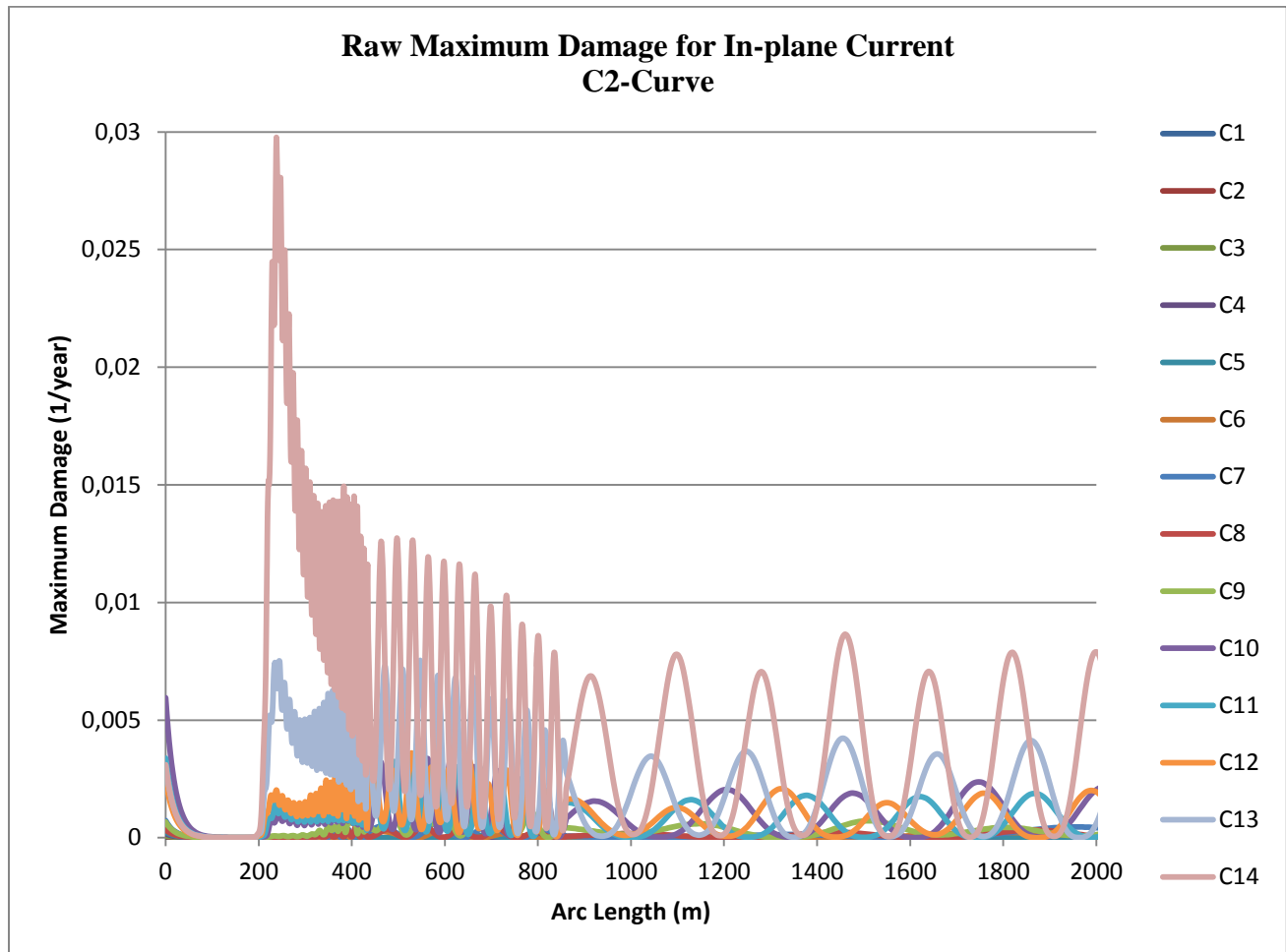


Figure C.13 VIV fatigue damage, in-plane current, C2-curve

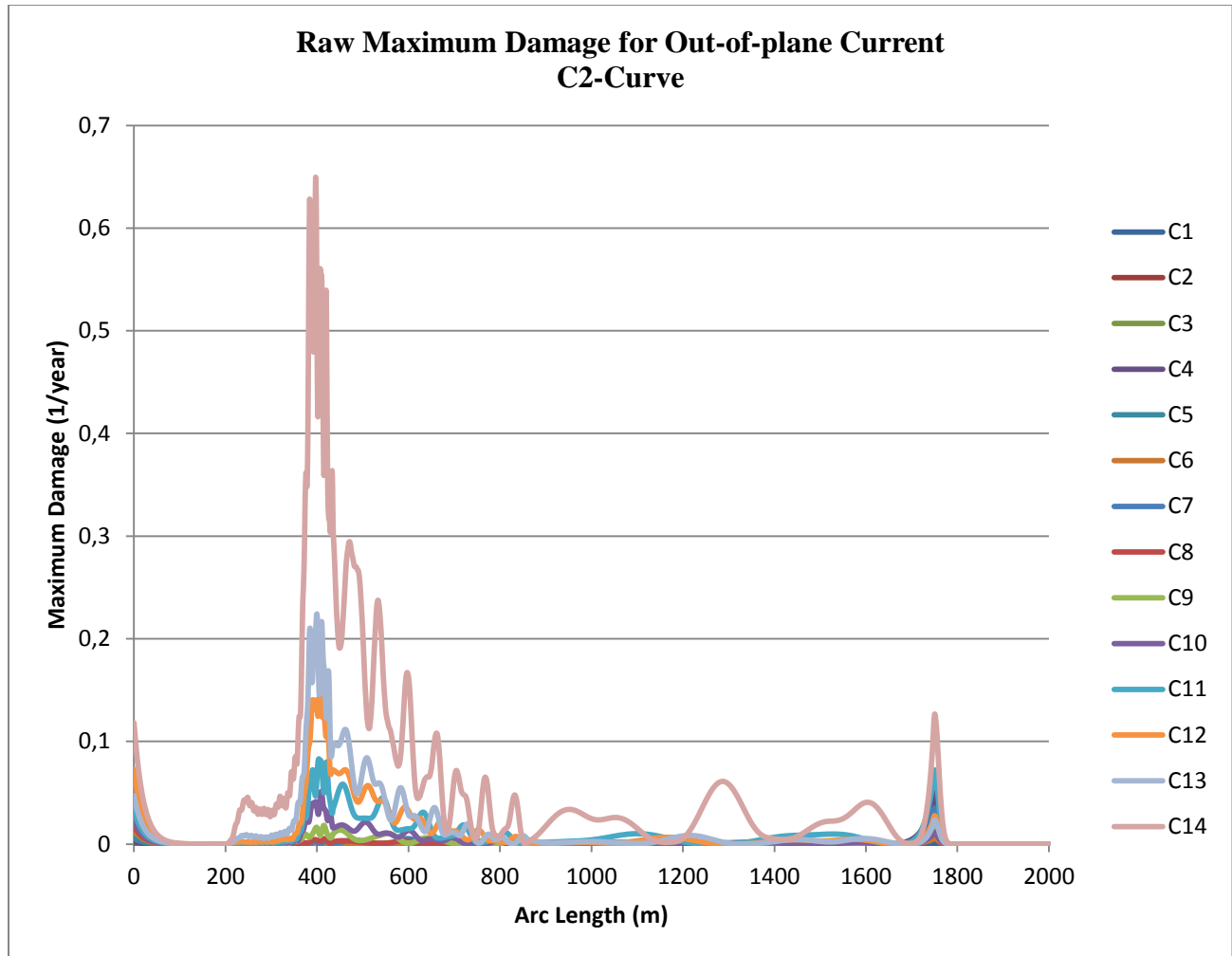


Figure C.14 VIV fatigue damage, out-of-plane current, C2-curve

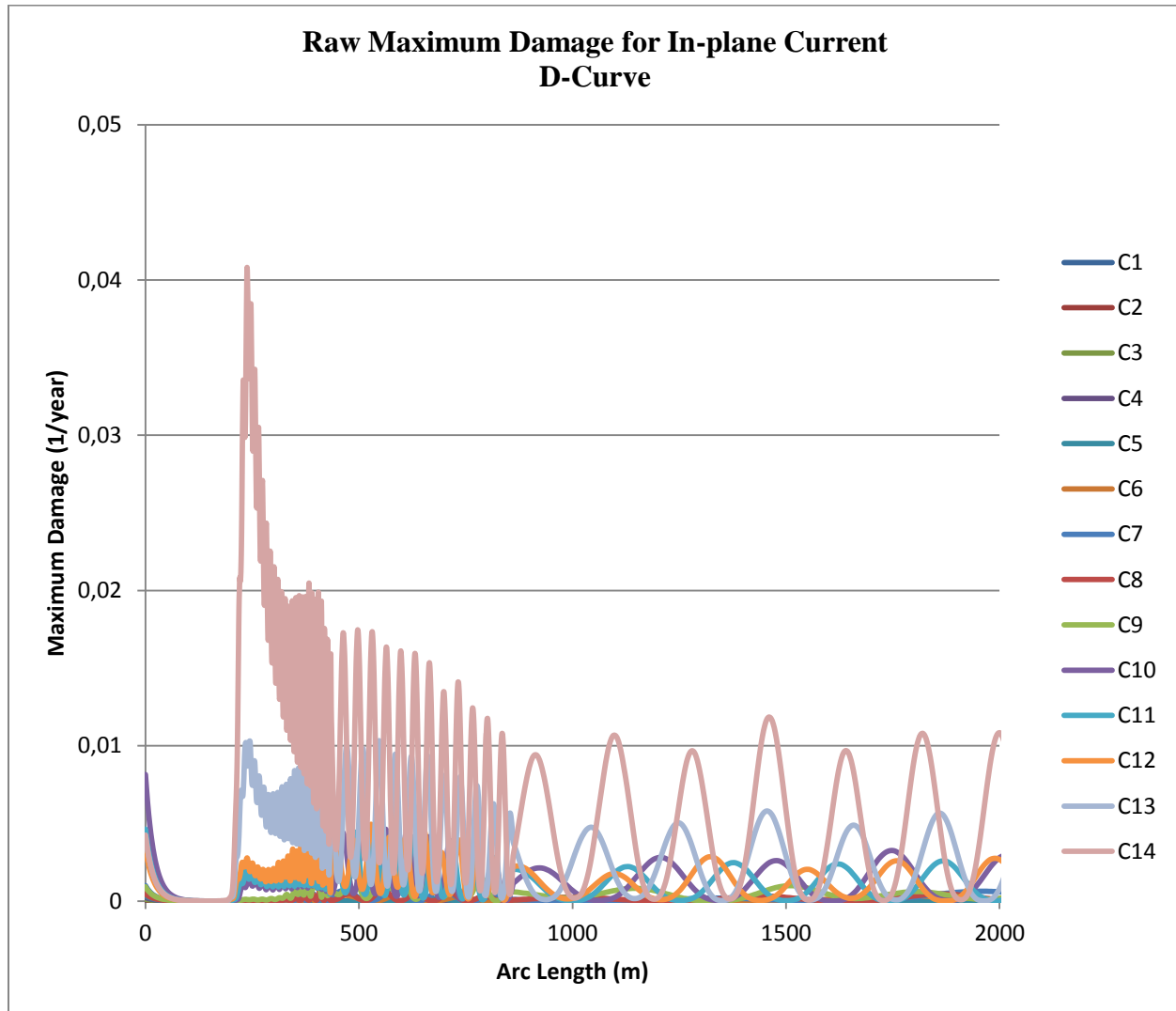


Figure C.15 VIV fatigue damage, in-plane current, D-curve

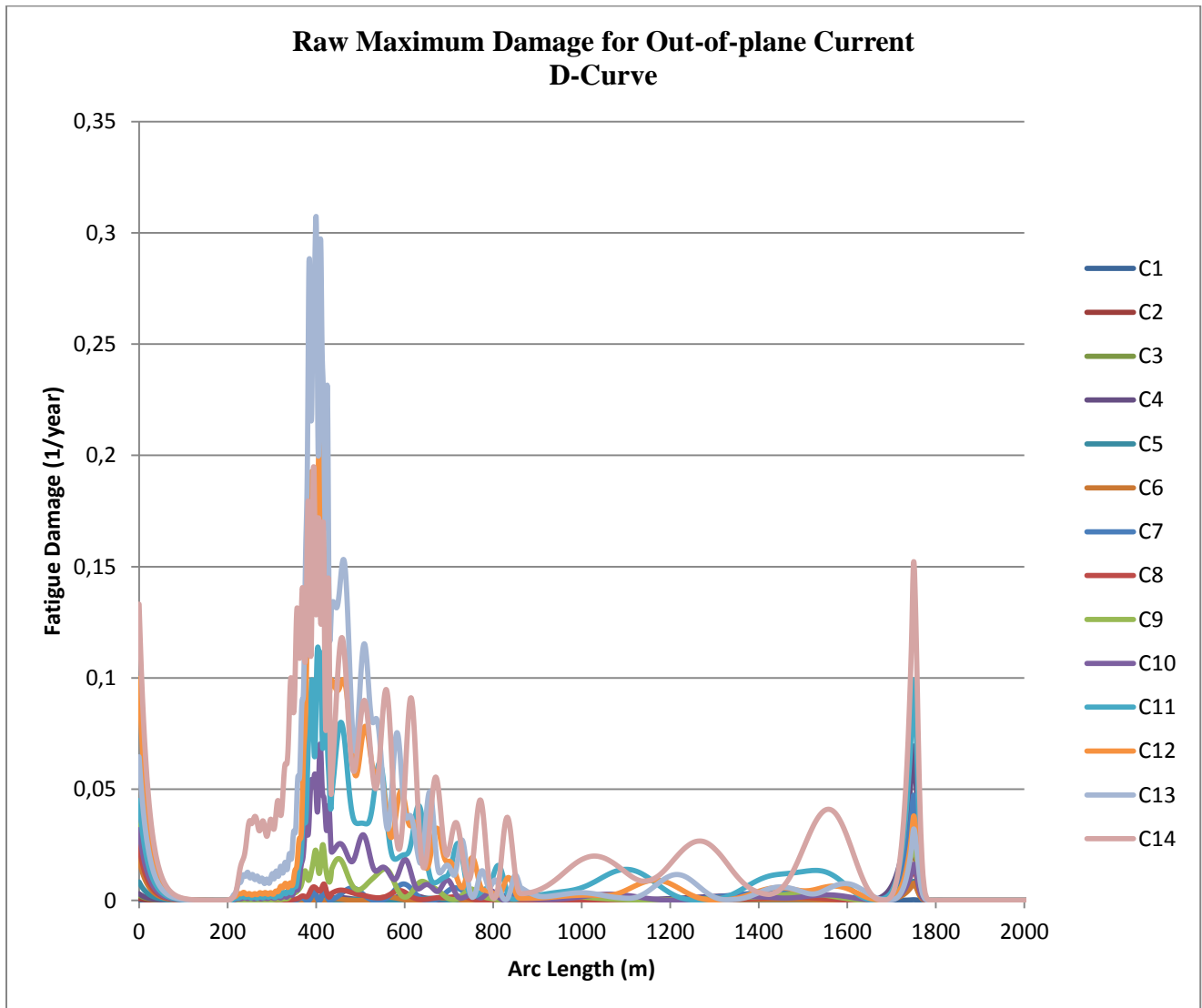


Figure C.16 VIV fatigue damage, out-of-plane current, D-curve

Appendix D – Detailed Sensitivity Results

D.1 Net Buoyancy Sensitivity – Extreme Strength Analysis Results

100-year wave + 10-year current 500 N/m Net Buoyancy	FPSO Position			
	Intact		Accidental	
	Near	Far	Near	Far
Max. Top Angle	18.3	15.2	18.0	16.4
Min. Top Angle	4.5	0.1	4.1	0.2
Max. Effective Top Tension (kN)	1900	2103	1893	2195
Sag Bend				
Max. Effective Tension (kN)	256	967	236	1110
Max. Compression (kN)	64	182	58	203
Max. Bending Moment (kN.m)	449	429	471	437
Max. von Mises Stresses (Mpa)	349	331	364	336
Max. DNV Utilization (LRFD)	0.81	0.82	0.76	0.69
Hog Bend				
Max. Effective Tension (kN)	169	942	152	1088
Max. Compression (kN)	4	151	-	188
Max. Bending Moment (kN.m)	258	387	273	452
Max. von Mises Stresses (Mpa)	242	305	248	346
Max. DNV Utilization (LRFD)	0.56	0.85	0.50	0.70
TDP				
Max. Effective Tension (kN)	118	941	97	1085
Max. Compression (kN)	-	59	-	78
Max. Bending Moment (kN.m)	467	338	471	342
Max. von Mises Stresses (Mpa)	357	272	360	275
Max. DNV Utilization (LRFD)	0.86	0.68	0.77	0.58

100-year wave + 10-year current 600 N/m Net Buoyancy	FPSO Position			
	Intact		Accidental	
	Near	Far	Near	Far
Max. Top Angle	18.5	14.8	18.3	15.9
Min. Top Angle	4.8	0.5	4.4	0.3
Max. Effective Top Tension (kN)	1877	2011	1870	2066
Sag Bend				
Max. Effective Tension (kN)	525	782	233	896
Max. Compression (kN)	56	126	51	141
Max. Bending Moment (kN.m)	435	370	458	381
Max. von Mises Stresses (Mpa)	342	293	356	299
Max. DNV Utilization (LRFD)	0.78	0.72	0.74	0.62
Hog Bend				
Max. Effective Tension (kN)	162	736	148	849
Max. Compression (kN)	-	87	-	120
Max. Bending Moment (kN.m)	284	343	302	389
Max. von Mises Stresses (Mpa)	253	279	261	304
Max. DNV Utilization (LRFD)	0.57	0.74	0.54	0.62
TDP				
Max. Effective Tension (kN)	112	727	95	836
Max. Compression (kN)	-	-	-	2
Max. Bending Moment (kN.m)	423	314	435	321
Max. von Mises Stresses (Mpa)	329	262	337	264
Max. DNV Utilization (LRFD)	0.78	0.62	0.72	0.55

100-year wave + 10-year current 800 N/m Net Buoyancy	FPSO Position			
	Intact		Accidental	
	Near	Far	Near	Far
Max. Top Angle	19.0	14.0	18.8	14.9
Min. Top Angle	5.2	0.1	4.8	0.8
Max. Effective Top Tension (kN)	1831	1914	1825	1943
Sag Bend				
Max. Effective Tension (kN)	483	575	231	648
Max. Compression (kN)	46	62	43	66
Max. Bending Moment (kN.m)	414	311	432	307
Max. von Mises Stresses (Mpa)	328	264	340	262
Max. DNV Utilization (LRFD)	0.75	0.61	0.71	0.53
Hog Bend				
Max. Effective Tension (kN)	157	497	145	563
Max. Compression (kN)	-	-	-	21
Max. Bending Moment (kN.m)	336	301	354	319
Max. von Mises Stresses (Mpa)	277	262	286	268
Max. DNV Utilization (LRFD)	0.64	0.64	0.60	0.54
TDP				
Max. Effective Tension (kN)	114	474	101	534
Max. Compression (kN)	-	-	-	-
Max. Bending Moment (kN.m)	384	260	398	259
Max. von Mises Stresses (Mpa)	305	244	313	243
Max. DNV Utilization (LRFD)	0.71	0.53	0.66	0.47

100-year wave + 10-year current 900 N/m Net Buoyancy	FPSO Position			
	Intact		Accidental	
	Near	Far	Near	Far
Max. Top Angle	19.2	13.7	19.0	14.5
Min. Top Angle	5.30	0.1	5.0	0.4
Max. Effective Top Tension (kN)	1808	1874	1802	1897
Sag Bend				
Max. Effective Tension (kN)	463	521	230	579
Max. Compression (kN)	42	48	40	49
Max. Bending Moment (kN.m)	403	301	421	288
Max. von Mises Stresses (Mpa)	322	261	334	255
Max. DNV Utilization (LRFD)	0.73	0.58	0.69	0.50
Hog Bend				
Max. Effective Tension (kN)	154	431	144	480
Max. Compression (kN)	-	-	-	-
Max. Bending Moment (kN.m)	368	296	384	306
Max. von Mises Stresses (Mpa)	297	261	306	263
Max. DNV Utilization (LRFD)	0.68	0.62	0.65	0.53
TDP				
Max. Effective Tension (kN)	119	399	105	448
Max. Compression (kN)	-	-	-	-
Max. Bending Moment (kN.m)	377	244	390	241
Max. von Mises Stresses (Mpa)	300	238	308	237
Max. DNV Utilization (LRFD)	0.69	0.50	0.65	0.44

D.2 Sag Bend Height Sensitivity – Extreme Strength Analysis Results

100-year wave + 10-year current 200 m Sag Bend Height	FPSO Position			
	Intact		Accidental	
	Near	Far	Near	Far
Max. Top Angle	19.5	14.9	19.2	16.1
Min. Top Angle	5.0	0.6	4.6	0.2
Max. Effective Top Tension (kN)	1658	1837	1651	1895
Sag Bend				
Max. Effective Tension (kN)	223	692	207	793
Max. Compression (kN)	51	115	47	126
Max. Bending Moment (kN.m)	479	388	504	394
Max. von Mises Stresses (Mpa)	370	305	386	308
Max. DNV Utilization (LRFD)	0.85	0.76	0.81	0.66
Hog Bend				
Max. Effective Tension (kN)	147	614	134	721
Max. Compression (kN)	-	92	-	109
Max. Bending Moment (kN.m)	357	392	376	407
Max. von Mises Stresses (Mpa)	289	308	301	317
Max. DNV Utilization (LRFD)	0.67	0.79	0.63	0.67
TDP				
Max. Effective Tension (kN)	93	570	86	679
Max. Compression (kN)	-	-	-	-
Max. Bending Moment (kN.m)	428	302	442	304
Max. von Mises Stresses (Mpa)	332	259	341	259
Max. DNV Utilization (LRFD)	0.77	0.60	0.72	0.53

100-year wave + 10-year current 300 m Sag Bend Height	FPSO Position			
	Intact		Accidental	
	Near	Far	Near	Far
Max. Top Angle	20.3	15.5	20.1	17.2
Min. Top Angle	5.1	0.4	4.6	0.3
Max. Effective Top Tension (kN)	1445	1747	1438	1847
Sag Bend				
Max. Effective Tension (kN)	199	776	182	918
Max. Compression (kN)	56	163	50	179
Max. Bending Moment (kN.m)	561	465	583	471
Max. von Mises Stresses (Mpa)	422	354	437	359
Max. DNV Utilization (LRFD)	0.98	0.89	0.91	0.76
Hog Bend				
Max. Effective Tension (kN)	134	701	120	846
Max. Compression (kN)	9	150	1	168
Max. Bending Moment (kN.m)	419	476	441	490
Max. von Mises Stresses (Mpa)	329	362	343	371
Max. DNV Utilization (LRFD)	0.77	0.93	0.72	0.79
TDP				
Max. Effective Tension (kN)	81	617	73	762
Max. Compression (kN)	-	-	-	-
Max. Bending Moment (kN.m)	481	328	495	327
Max. von Mises Stresses (Mpa)	366	269	376	268
Max. DNV Utilization (LRFD)	0.85	0.65	0.79	0.56

100-year wave + 10-year current 400 m Sag Bend Height	FPSO Position			
	Intact		Accidental	
	Near	Far	Near	Far
Max. Top Angle	21.1	16.3	20.9	18.3
Min. Top Angle	5.1	0.5	4.6	0.1
Max. Effective Top Tension (kN)	1258	1754	1251	1919
Sag Bend				
Max. Effective Tension (kN)	182	939	164	1132
Max. Compression (kN)	66	218	59	232
Max. Bending Moment (kN.m)	650	552	675	554
Max. von Mises Stresses (Mpa)	480	414	497	416
Max. DNV Utilization (LRFD)	1.12	1.05	1.04	0.87
Hog Bend				
Max. Effective Tension (kN)	125	859	110	1055
Max. Compression (kN)	33	209	24	225
Max. Bending Moment (kN.m)	501	564	525	575
Max. von Mises Stresses (Mpa)	382	422	398	430
Max. DNV Utilization (LRFD)	0.91	1.09	0.84	0.90
TDP				
Max. Effective Tension (kN)	69	729	60	925
Max. Compression (kN)	-	-	-	-
Max. Bending Moment (kN.m)	539	321	559	259
Max. von Mises Stresses (Mpa)	404	266	418	244
Max. DNV Utilization (LRFD)	0.94	0.63	0.88	0.47

D.3 Buoyant Section Length Sensitivity – Extreme Strength Analysis Results

100-year wave + 10-year current 360 m Buoyant Section Length	FPSO Position			
	Intact		Accidental	
	Near	Far	Near	Far
Max. Top Angle	18.6	15.1	18.3	16.3
Min. Top Angle	4.7	0.2	4.3	0.04
Max. Effective Top Tension (kN)	1841	2005	1834	2072
Sag Bend				
Max. Effective Tension (kN)	237	808	219	929
Max. Compression (kN)	49	123	45	141
Max. Bending Moment (kN.m)	450	386	475	398
Max. von Mises Stresses (Mpa)	351	302	367	310
Max. DNV Utilization (LRFD)	0.80	0.76	0.74	0.66
Hog Bend				
Max. Effective Tension (kN)	155	766	141	896
Max. Compression (kN)	-	104	-	125
Max. Bending Moment (kN.m)	333	405	353	425
Max. von Mises Stresses (Mpa)	274	315	285	327
Max. DNV Utilization (LRFD)	0.64	0.81	0.60	0.70
TDP				
Max. Effective Tension (kN)	109	759	97	891
Max. Compression (kN)	-	-	-	12
Max. Bending Moment (kN.m)	426	323	438	325
Max. von Mises Stresses (Mpa)	331	266	339	266
Max. DNV Utilization (LRFD)	0.77	0.65	0.71	0.56

100-year wave + 10-year current 396 m Buoyant Section Length	FPSO Position			
	Intact		Accidental	
	Near	Far	Near	Far
Max. Top Angle	18.7	14.7	18.4	15.7
Min. Top Angle	4.8	0.6	4.5	0.002
Max. Effective Top Tension (kN)	1853	1974	1846	2018
Sag Bend				
Max. Effective Tension (kN)	244	716	227	809
Max. Compression (kN)	49	97	46	109
Max. Bending Moment (kN.m)	433	350	456	358
Max. von Mises Stresses (Mpa)	340	280	354	285
Max. DNV Utilization (LRFD)	0.78	0.69	0.71	0.61
Hog Bend				
Max. Effective Tension (kN)	157	650	144	750
Max. Compression (kN)	-	68	-	85
Max. Bending Moment (kN.m)	317	355	335	371
Max. von Mises Stresses (Mpa)	267	284	275	294
Max. DNV Utilization (LRFD)	0.61	0.72	0.58	0.62
TDP				
Max. Effective Tension (kN)	107	632	97	739
Max. Compression (kN)	-	-	-	-
Max. Bending Moment (kN.m)	412	298	424	300
Max. von Mises Stresses (Mpa)	322	256	330	257
Max. DNV Utilization (LRFD)	0.75	0.60	0.67	0.53

100-year wave + 10-year current 444 m Buoyant Section Length	FPSO Position			
	Intact		Accidental	
	Near	Far	Near	Far
Max. Top Angle	18.8	14.1	18.6	15.1
Min. Top Angle	5.1	0.2	4.7	0.5
Max. Effective Top Tension (kN)	1854	1945	1848	1976
Sag Bend				
Max. Effective Tension (kN)	251	627	236	696
Max. Compression (kN)	50	78	47	84
Max. Bending Moment (kN.m)	415	317	435	322
Max. von Mises Stresses (Mpa)	329	265	341	267
Max. DNV Utilization (LRFD)	0.75	0.63	0.68	0.56
Hog Bend				
Max. Effective Tension (kN)	160	545	148	620
Max. Compression (kN)	-	34	-	46
Max. Bending Moment (kN.m)	301	313	319	324
Max. von Mises Stresses (Mpa)	261	264	268	269
Max. DNV Utilization (LRFD)	0.59	0.65	0.54	0.56
TDP				
Max. Effective Tension (kN)	103	508	95	587
Max. Compression (kN)	-	-	-	-
Max. Bending Moment (kN.m)	390	271	402	273
Max. von Mises Stresses (Mpa)	308	247	316	247
Max. DNV Utilization (LRFD)	0.72	0.55	0.63	0.49

100-year wave + 10-year current 480 m Buoyant Section Length	FPSO Position			
	Intact		Accidental	
	Near	Far	Near	Far
Max. Top Angle	19.0	13.8	18.7	14.6
Min. Top Angle	5.2	0.2	4.9	0.6
Max. Effective Top Tension (kN)	1859	1933	1853	1957
Sag Bend				
Max. Effective Tension (kN)	257	582	242	637
Max. Compression (kN)	52	70	49	73
Max. Bending Moment (kN.m)	401	296	417	299
Max. von Mises Stresses (Mpa)	320	257	331	258
Max. DNV Utilization (LRFD)	0.73	0.60	0.65	0.53
Hog Bend				
Max. Effective Tension (kN)	162	486	151	545
Max. Compression (kN)	-	13	-	22
Max. Bending Moment (kN.m)	292	285	308	294
Max. von Mises Stresses (Mpa)	257	253	264	257
Max. DNV Utilization (LRFD)	0.57	0.60	0.54	0.52
TDP				
Max. Effective Tension (kN)	101	436	94	500
Max. Compression (kN)	-	-	-	-
Max. Bending Moment (kN.m)	379	259	391	256
Max. von Mises Stresses (Mpa)	301	243	309	242
Max. DNV Utilization (LRFD)	0.70	0.53	0.62	0.47

D.4 Hang-off Angle Sensitivity – Extreme Strength Analysis Results

100-year wave + 10-year current Hang-off Angle = 6 Degrees	FPSO Position			
	Intact		Accidental	
	Near	Far	Near	Far
Max. Top Angle	17.8	11.1	17.6	11.8
Min. Top Angle	3.4	0.2	3.1	0.5
Max. Effective Top Tension (kN)	1781	1825	1776	1842
Sag Bend				
Max. Effective Tension (kN)	182	435	171	476
Max. Compression (kN)	37	64	35	68
Max. Bending Moment (kN.m)	534	339	558	336
Max. von Mises Stresses (Mpa)	405	275	421	274
Max. DNV Utilization (LRFD)	0.93	0.66	0.88	0.58
Hog Bend				
Max. Effective Tension (kN)	110	345	102	388
Max. Compression (kN)	-	9	-	18
Max. Bending Moment (kN.m)	396	300	419	309
Max. von Mises Stresses (Mpa)	312	261	327	263
Max. DNV Utilization (LRFD)	0.73	0.62	0.69	0.54
TDP				
Max. Effective Tension (kN)	77	309	71	355
Max. Compression (kN)	-	-	-	-
Max. Bending Moment (kN.m)	462	293	477	288
Max. von Mises Stresses (MPa)	354	256	364	254
Max. DNV Utilization (LRFD)	0.82	0.57	0.77	0.51

100-year wave + 10-year current Hang-off Angle = 7 Degrees	FPSO Position			
	Intact		Accidental	
	Near	Far	Near	Far
Max. Top Angle	18.2	12.8	18.0	13.7
Min. Top Angle	4.1	0.5	3.8	0.2
Max. Effective Top Tension (kN)	1814	1884	1809	1909
Sag Bend				
Max. Effective Tension (kN)	214	541	201	600
Max. Compression (kN)	43	72	40	78
Max. Bending Moment (kN.m)	475	329	497	332
Max. von Mises Stresses (MPa)	367	270	381	272
Max. DNV Utilization (LRFD)	0.84	0.65	0.79	0.57
Hog Bend				
Max. Effective Tension (kN)	134	458	123	521
Max. Compression (kN)	-	27	-	38
Max. Bending Moment (kN.m)	347	315	367	325
Max. von Mises Stresses (MPa)	281	265	293	269
Max. DNV Utilization (LRFD)	0.65	0.65	0.62	0.56
TDP				
Max. Effective Tension (kN)	90	423	82	490
Max. Compression (kN)	-	-	-	-
Max. Bending Moment (kN.m)	428	284	441	284
Max. von Mises Stresses (MPa)	332	252	341	252
Max. DNV Utilization (LRFD)	0.77	0.57	0.72	0.50

100-year wave + 10-year current Hang-off Angle = 9 Degrees	FPSO Position			
	Intact		Accidental	
	Near	Far	Near	Far
Max. Top Angle	19.1	16.4	18.8	17.5
Min. Top Angle	5.5	0.3	5.1	0.1
Max. Effective Top Tension (kN)	1889	2040	1881	2095
Sag Bend				
Max. Effective Tension (kN)	283	816	264	921
Max. Compression (kN)	57	95	53	106
Max. Bending Moment (kN.m)	386	334	404	342
Max. von Mises Stresses (MPa)	311	272	322	275
Max. DNV Utilization (LRFD)	0.71	0.67	0.67	0.59
Hog Bend				
Max. Effective Tension (kN)	186	751	171	864
Max. Compression (kN)	-	65	-	81
Max. Bending Moment (kN.m)	278	345	293	359
Max. von Mises Stresses (MPa)	254	278	258	286
Max. DNV Utilization (LRFD)	0.55	0.71	0.52	0.61
TDP				
Max. Effective Tension (kN)	122	729	111	847
Max. Compression (kN)	-	-	-	-
Max. Bending Moment (kN.m)	377	286	388	290
Max. von Mises Stresses (MPa)	300	251	307	253
Max. DNV Utilization (LRFD)	0.70	0.58	0.65	0.51

100-year wave + 10-year current Hang-off Angle = 10 Degrees	FPSO Position			
	Intact		Accidental	
	Near	Far	Near	Far
Max. Top Angle	19.6	18.1	19.3	19.4
Min. Top Angle	6.2	0.3	5.7	0.4
Max. Effective Top Tension (kN)	1930	2146	1921	2227
Sag Bend				
Max. Effective Tension (kN)	321	983	299	1116
Max. Compression (kN)	65	111	59	126
Max. Bending Moment (kN.m)	351	341	368	350
Max. von Mises Stresses (MPa)	289	274	300	280
Max. DNV Utilization (LRFD)	0.66	0.69	0.62	0.60
Hog Bend				
Max. Effective Tension (kN)	216	932	197	1074
Max. Compression (kN)	-	85	-	104
Max. Bending Moment (kN.m)	271	360	266	374
Max. von Mises Stresses (MPa)	249	287	249	296
Max. DNV Utilization (LRFD)	0.56	0.73	0.48	0.63
TDP				
Max. Effective Tension (kN)	143	914	127	1062
Max. Compression (kN)	-	-	-	-
Max. Bending Moment (kN.m)	358	289	368	290
Max. von Mises Stresses (MPa)	288	252	295	252
Max. DNV Utilization (LRFD)	0.68	0.60	0.62	0.51